



Search for supersymmetry in final states with missing transverse momentum and charm-tagged jets using 139 fb^{-1} of proton–proton collisions at $\sqrt{s} = 13 \text{ TeV}$ with the ATLAS detector

The ATLAS Collaboration

The paper presents a search for supersymmetric particles produced in proton–proton collisions at $\sqrt{s} = 13 \text{ TeV}$ and decaying into final states with missing transverse momentum and jets originating from charm quarks. The data were taken with the ATLAS detector at the Large Hadron Collider at CERN from 2015 to 2018 and correspond to an integrated luminosity of 139 fb^{-1} . No significant excess of events over the expected Standard Model background expectation is observed in optimized signal regions, and limits are set on the production cross-sections of the supersymmetric particles. Pair production of charm squarks or top squarks, each decaying into a charm quark and the lightest supersymmetric particle $\tilde{\chi}_1^0$, is excluded at 95% confidence level for squarks with masses up to 900 GeV for scenarios where the mass of $\tilde{\chi}_1^0$ is below 50 GeV. Additionally, the production of leptoquarks with masses up to 900 GeV is excluded for the scenario where up-type leptoquarks decay into a charm quark and a neutrino. Model-independent limits on cross-sections and event yields for processes beyond the Standard Model are also reported.

Contents

1	Introduction	3
2	ATLAS detector	4
3	Data and simulated event samples	5
4	Event reconstruction	6
5	Event selection	8
	5.1 Signal regions	8
	5.2 Background estimation and the control regions	11
	5.3 Validation of background estimates	12
6	Systematic uncertainties	15
7	Results and interpretation	19
8	Conclusion	27

1 Introduction

Supersymmetric (SUSY) extensions of the Standard Model (SM) of particle physics predict new particles which are partners of SM particles [1–6] – the partners of SM fermions being bosons and those of SM bosons being fermions – and provide solutions to the hierarchy problem [7–10]. R -parity-conserving SUSY models [11] are considered in this paper and predict that the supersymmetric partners of quarks (squarks) will be produced in pairs at the Large Hadron Collider (LHC) and that the lightest SUSY particle (LSP) is stable. The lightest neutralino, $\tilde{\chi}_1^0$, is considered to be the LSP and is a dark-matter candidate [12, 13].

The search described in this paper targets SUSY models where top or charm squarks (\tilde{t}_1/\tilde{c}_1) are the lightest squarks, with masses less than about one TeV [14]. For top squarks considered in this search, flavour-violating effects allow the top squark to decay into a charm quark and an LSP, as shown in Figure 1(a). This results in a final state with two charm quarks and missing transverse momentum from the LSPs, which escape detection. The extent of flavour-violating effects is model dependent, but when there is significant mixing between the top squark and the charm squark [15], the branching fraction of $\tilde{t}_1 \rightarrow c\tilde{\chi}_1^0$ can exceed the branching fraction of $\tilde{t} \rightarrow t^*\tilde{\chi}_1^0$, where t^* can be either an on-shell or off-shell top quark.

In supersymmetric models with minimal flavour-violating effects, charm squarks could be considerably lighter than other squarks. This motivates searches for pair production of charm squarks, with each charm squark decaying into a charm quark and an LSP as shown in Figure 1(b). Notably, the model of charm squark pair production in Figure 1(b) shares the same experimental signature and production cross-section as for the top squark pairs in Figure 1(a). The experimental signature includes jets that contain charm hadrons but no bottom hadrons and momentum imbalance caused by the two LSPs. The search discussed in this paper was optimized for the case where the branching fraction of the decay of top or charm squark into a charm quark plus the LSP is unity. However, the results of the search are also interpreted in the scenario of top squark production with a varying branching fraction of the top squark decay into a charm quark plus the LSP ranging from 0.1 to 1, with the alternative decay being to a top quark plus the LSP.

Leptoquark (LQ) models [16–24] with up-type scalar LQs (LQ^u) or vector LQs (vLQ) predict their pair production and subsequent decay into $c\nu c\nu$, with the same experimental signature as in top and charm squark production models (see Figure 1(c)). The following models are considered: U_1 vLQ models that couple to second-generation quarks and third-generation leptons (vLQ_{23}^u , where the subscript indicates the quark and lepton generations) in both the minimal and Yang–Mills coupling scenarios [25,

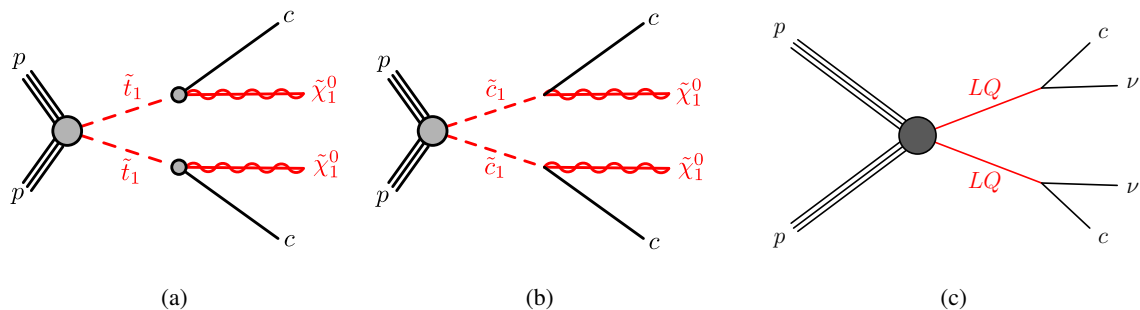


Figure 1: Representative diagrams for pair production of (a) top squarks (\tilde{t}_1) and (b) charm squarks (\tilde{c}_1), with subsequent decay into charm quarks and neutralinos ($\tilde{\chi}_1^0$), and (c) pair production of leptoquarks decaying into charm quarks and neutrinos.

26], assuming a branching fraction (\mathcal{B}) of $\mathcal{B}(\nu\text{LQ}_{23}^u \rightarrow c\nu_\tau) = 0.5$ in both cases with the alternative decay being $\nu\text{LQ}_{23}^u \rightarrow s\tau$; and models where scalar LQs couple to second-generation quarks and first- or second-generation leptons [27–29], allowing a range of $\mathcal{B}(\text{LQ}^u \rightarrow c\nu_{e/\mu})$ values (here the alternative decay is $\text{LQ}^u \rightarrow se/\mu$).

This search for top squark, charm squark, and leptoquark pair production uses pp collisions from the LHC at a centre-of-mass energy of $\sqrt{s} = 13$ TeV recorded by the ATLAS experiment from 2015 to 2018. A previous search by ATLAS [30], based on the identification of jets containing charm hadrons but no bottom hadrons (c -tagging), used 36.1 fb^{-1} of collisions and was able to probe top and charm squark masses up to 850 GeV. In addition to a larger dataset, the search herein also benefits from improvements in c -tagging and from an advanced technique, Recursive Jigsaw Reconstruction [31], which provides sensitivity to models with small mass splittings between the top squark and the LSP. Other ATLAS results also have sensitivity to the models considered in this paper: a search using final states with an energetic jet (but no c -tagging) and large missing transverse momentum [32] was particularly sensitive to models with small mass differences between the top/charm squark and the LSP, while a search for single squark production that did not utilize c -tagging [33] had good sensitivity to models with large top/charm squark masses, and a more recent search for top squark pair production focused on squarks decaying into either a top quark or charm quark plus an LSP [34]. The most recent search performed by the CMS Collaboration [35] used 137 fb^{-1} of $\sqrt{s} = 13$ TeV pp collisions from the LHC, but only considered mass differences between the top squark and the LSP of less than 80 GeV, while the present ATLAS search explores mass differences ranging from 20 GeV to about 1 TeV. Finally, for the considered leptoquark models, this paper is the first to report results from the full Run 2 dataset of an LHC experiment.

2 ATLAS detector

The ATLAS detector [36] at the LHC covers nearly the entire solid angle around the collision point.¹ It consists of an inner tracking detector surrounded by a thin superconducting solenoid, electromagnetic and hadronic calorimeters, and a muon spectrometer incorporating three large superconducting air-core toroidal magnets.

The inner-detector system (ID) is immersed in a 2 T axial magnetic field and provides charged-particle tracking in the range $|\eta| < 2.5$. The high-granularity silicon pixel detector covers the vertex region and typically provides four measurements per track, the first hit generally being in the insertable B-layer (IBL) installed before Run 2 [37, 38]. It is followed by the SemiConductor Tracker (SCT), which usually provides eight measurements per track. These silicon detectors are complemented by the transition radiation tracker (TRT), which enables radially extended track reconstruction up to $|\eta| = 2.0$. The TRT also provides electron identification information based on the fraction of hits (typically 30 in total) above a higher energy-deposit threshold corresponding to transition radiation.

The calorimeter system covers the pseudorapidity range $|\eta| < 4.9$. Within the region $|\eta| < 3.2$, electromagnetic calorimetry is provided by barrel and endcap high-granularity lead/liquid-argon (LAr)

¹ ATLAS uses a right-handed coordinate system with its origin at the nominal interaction point (IP) in the centre of the detector and the z -axis along the beam pipe. The x -axis points from the IP to the centre of the LHC ring, and the y -axis points upwards. Polar coordinates (r, ϕ) are used in the transverse plane, ϕ being the azimuthal angle around the z -axis. The pseudorapidity is defined in terms of the polar angle θ as $\eta = -\ln \tan(\theta/2)$ and is equal to the rapidity $y = \frac{1}{2} \ln \left(\frac{E+p_z}{E-p_z} \right)$ in the relativistic limit. Angular distance is measured in units of $\Delta R \equiv \sqrt{(\Delta y)^2 + (\Delta\phi)^2}$.

calorimeters, with an additional thin LAr presampler covering $|\eta| < 1.8$ to correct for energy loss in material upstream of the calorimeters. Hadronic calorimetry is provided by the steel/scintillator-tile calorimeter, segmented into three barrel structures within $|\eta| < 1.7$, and two copper/LAr hadronic endcap calorimeters. The solid angle coverage is completed with forward copper/LAr and tungsten/LAr calorimeter modules optimised for electromagnetic and hadronic energy measurements respectively.

The muon spectrometer (MS) comprises separate trigger and high-precision tracking chambers measuring the deflection of muons in a magnetic field generated by the superconducting air-core toroidal magnets. The field integral of the toroids ranges between 2.0 and 6.0 T m across most of the detector. Three layers of precision chambers, each consisting of layers of monitored drift tubes, cover the region $|\eta| < 2.7$, complemented by cathode-strip chambers in the forward region, where the background is highest. The muon trigger system covers the range $|\eta| < 2.4$ with resistive-plate chambers in the barrel, and thin-gap chambers in the endcap regions.

The luminosity is measured mainly by the LUCID-2 [39] detector that records Cherenkov light produced in the quartz windows of photomultipliers located close to the beampipe.

Events are selected by the first-level trigger system implemented in custom hardware, followed by selections made by algorithms implemented in software in the high-level trigger [40]. The first-level trigger accepts events from the 40 MHz bunch crossings at a rate below 100 kHz, which the high-level trigger further reduces in order to record complete events to disk at about 1 kHz.

A software suite [41] is used in data simulation, in the reconstruction and analysis of real and simulated data, in detector operations, and in the trigger and data acquisition systems of the experiment.

3 Data and simulated event samples

The data used in this analysis were recorded with a fully operational detector from stable-proton-beam collisions, and are clear of a significant amount of cosmic-ray or beam-induced background [42]. The total integrated luminosity of this dataset is $139.0 \pm 2.4 \text{ fb}^{-1}$ [43], determined using the LUCID-2 detector [44] for the primary luminosity measurements, complemented by measurements from the inner detector and calorimeters. The LHC accelerates and collides protons in bunches and there are multiple pp collisions in every bunch crossing in addition to the much less frequent hard-scattering collisions of interest. The bunch crossings happen every 25 ns. The average number of additional proton–proton interactions per bunch crossing (pileup) grew from 13 in 2015 to a value of about 38 in 2017.

Missing transverse momentum triggers were used to select the data [45] for this analysis. The triggers had thresholds of 70 GeV in 2015 and early 2016, 100 GeV in late 2016 and 2017, and 110 GeV in 2018. These triggers reach an efficiency plateau for offline missing transverse momenta greater than 200 GeV.

The predictions for signal and background contributions are obtained with Monte Carlo (MC) simulated event samples. To match the LHC beam conditions, these simulated event samples also contain pileup interactions. The simulated events were processed through the ATLAS detector simulation [46] and then subjected to the same reconstruction algorithms as the data. All samples were processed with the full GEANT4 [47] detector model with the exception of the samples with leptoquarks or direct top or charm squark production which were processed with ATLFast-II detector simulations [48]. Finally, the simulated samples were corrected to improve the accuracy of the pileup modelling, jet momenta, lepton efficiency and momenta, trigger efficiencies, missing transverse momentum, and c -tagging efficiency.

Table 1: Overview of the simulated background samples. The simulated vector bosons, V , are massive W and Z bosons. The NNPDF3.0_{NLO} [51] parton distribution functions (PDF) set is used.

Background process	Matrix element generator	PDF accuracy	Parton showering and hadronization	Underlying event tune	Cross-section calculation accuracy
$pp \rightarrow V$ +jets	SHERPA 2.2.11 [49]	NNLO	SHERPA	Default	NNLO [52]
$pp \rightarrow t\bar{t}V$ +jets	AMC@NLO 2.3.3 [53]	NLO	PYTHIA 8.210 [54]	A14 [55]	NLO [53]
$pp \rightarrow t\bar{t}$ +jets	POWHEG BOX v2 [56]	NNLO	PYTHIA 8.230	A14	NNLO+NNLL [57–62]
$pp \rightarrow t$ +jets / tW +jets	POWHEG BOX v2	NNLO	PYTHIA 8.230	A14	NNLO+NNLL [63–65]
$pp \rightarrow VV$ +jets	SHERPA 2.2.1–2.2.2 [66]	NNLO	SHERPA	Default	NLO

Standard Model background samples were produced with various event generators as shown in Table 1. All samples, except the ones that use the SHERPA event generator [49], were processed with EVTGEN 1.7.0 [50] for the b - and c -hadron decays. The cross-sections, which were used to normalize the samples, were calculated separately with higher-order corrections in the strong coupling (α_s) for all samples except for the diboson production ($pp \rightarrow VV$ +jets) sample, where the cross-section calculated by the SHERPA event generator was retained. For the SHERPA sample of single vector bosons produced in association with jets (V +jets), virtual electroweak loop-terms were included at next-to-leading-order (NLO) accuracy.

The SUSY event samples were generated with MADGRAPH5_AMC@NLO 2.8.1 [53] at leading order (LO) in the strong coupling constant (α_s) with up to two additional partons using the NNPDF3.0_{NLO} [51] parton distribution function (PDF) set and were showered and hadronized with PYTHIA 8.244 [54] using the A14 set of tuned parameters (tune) in PYTHIA [55]. Samples with a small mass difference between the top squark and $\tilde{\chi}_1^0$ (up to 140 GeV) were generated with MADGRAPH5_AMC@NLO 2.9.5 and then interfaced with PYTHIA 8.306. These samples were also processed with EVTGEN 1.7.0.

The top squark and charm squark signal cross-sections were calculated from pair production of scalar coloured particles and with the gluino assumed to be massive enough to not significantly contribute to the production process. Consequently, each production cross-section depends only on the squark mass. These cross-sections are computed at approximate next-to-next-to-leading-order (NNLO) accuracy in α_s with resummation of next-to-next-to-leading logarithmic (NNLL) soft gluon terms [67–70].

The samples with pair-produced scalar LQs were generated with matrix elements calculated at NLO accuracy in α_s with MADGRAPH5_AMC@NLO 2.6.0 [53], using the method described in Ref. [27], in which NLO matrix elements [28, 29] are interfaced to PYTHIA 8.230. The total cross-sections of scalar LQ pair production were computed at approximate NNLO accuracy in α_s with resummation of NNLL soft gluon terms [67–70]. The cross-sections do not include lepton t -channel contributions, which are neglected in Ref. [27] and may lead to corrections at the percent level [71]. For vector-LQ pair production, the matrix elements were calculated at LO in α_s following the model described in Ref. [25], and events were generated using MADGRAPH5_AMC@NLO 2.9.5 in conjunction with PYTHIA 8.306. Parton luminosities were provided by the five-flavour scheme NNPDF3.0_{NLO} PDF set and the underlying event was modelled with the A14 tune in PYTHIA. These samples were also processed with EVTGEN 1.7.0.

4 Event reconstruction

Events are required to have a primary vertex reconstructed from at least two tracks with transverse momentum $p_T > 0.5$ GeV. If more than one such vertex is found, the one with the largest sum of squares

of transverse momenta of associated tracks is selected as the hard-scattering collision [72]. The other vertices are considered as pileup.

Hadronic jet candidates are reconstructed using the anti- k_t jet algorithm [73, 74] with radius parameter $R = 0.4$, using particle-flow objects (PFOs) [75] as inputs. PFOs are charged-particle tracks matched to the hard-scatter vertex with the requirement $|z_0 \sin(\theta)| < 2.0$ mm (where z_0 is the longitudinal impact parameter) and calorimeter energy clusters surviving an energy subtraction algorithm that removes the energy contributions deposited by good quality tracks from any vertex. Jet energy scale corrections, derived from MC simulation and data, are used to calibrate the average energies of jet candidates to the scale of their constituent particles [76]. Jets with $|\eta| < 4.5$ are used to calculate the missing transverse momentum [77], while jets with $p_T > 20$ GeV and $|\eta| < 2.8$ are considered to be “signal” jets. Jets containing a large particle momentum contribution from pileup vertices, as measured by the jet vertex tagger (JVT) discriminant [78], are rejected if they have $p_T < 60$ GeV, $|\eta| < 2.5$ and a discriminant value of $JVT < 0.5$.

Jets can be identified as c -tagged or b -tagged jets if they lie within the inner-detector acceptance of $|\eta| < 2.5$. To identify jets containing c -hadrons, the charm-tagging algorithm $DL1r_c$, optimized for a similar search [34], is used. The $DL1r_c$ algorithm is based on the ATLAS $DL1r$ algorithm [79], which uses a selection of inputs including information about the impact parameters of ID tracks, the presence of displaced secondary vertices, and the reconstructed flight paths of b - and c -hadrons inside the jet. The algorithm provides three probabilities for a jet to either contain b -hadrons, c -hadrons, or light-flavor hadrons. These three probabilities are combined in a similar way to the b -tagging algorithm, but with fine-tuned parameters specifically optimized for identifying jets containing c -hadrons but not b -hadrons; the f_b parameter was set to 0.28. The $DL1r$ b -tagging algorithm is used to identify b -jets which are no longer considered as potential c -jet candidates. The $DL1r$ algorithm has 77% identification efficiency for b -jets and 20% and 0.9% misidentification probabilities for c -jets and light-flavor jets, respectively, evaluated in a sample of simulated SM $t\bar{t}$ events. The c -tagging algorithm (referred to as “ c -tagging with b -veto”) is tuned to have an efficiency of 20% by requiring that the final $DL1r_c$ discriminant be greater than 1.315. This corresponds to rejection factors of 29 for b -jets and 57 for light-flavor jets; and a τ -lepton misidentification efficiency of 15%. These efficiencies and rejections factors are determined with a sample of simulated $t\bar{t}$ events. Both the simulated c -jet identification efficiency and misidentification probabilities are corrected to match those measured in data. The approach employed is similar to that for b -tagging [80–82]. Between p_T ranges of 20 GeV and 250 GeV, the scale factors are compatible with unity for all jet-flavor corrections. For c -jets, the systematic uncertainties range from 17% for $p_T < 65$ GeV to a few percent for higher- p_T jets (up to 3 TeV), while for b -jets and light-flavor jets, the uncertainties are 5–7% and approximately 13%, respectively, for all p_T ranges below 3 TeV. For b - and c -jets with $p_T > 3$ TeV, the uncertainties on the scale factors are up to 30%.

Electron candidates are constructed from energy deposits in the EM calorimeter matched to an ID track. “Baseline” electron candidates, which are used to veto events with electrons, must pass a loose likelihood-based identification selection [83] and have $p_T > 4.5$ GeV and $|\eta| < 2.47$. The longitudinal impact parameter of the ID track associated with a “baseline” electron is required to satisfy $|z_0 \sin(\theta)| < 0.5$ mm. Electrons used for regions rich in the dominant SM background processes with prompt electrons (i.e. W +jets and Z +jets) must meet further selection criteria: $p_T > 10$ GeV, “Loose” isolation [83], $|d_0/\sigma(d_0)| < 5$ where d_0 is the transverse impact parameter and $\sigma(d_0)$ is its uncertainty, and the “Tight” likelihood-based identification selection [83]. Electrons satisfying these criteria are referred to as “signal” electrons.

Muon candidates are found by combining track segments from the inner detector and muon spectrometer or by extrapolating from the forward sections of the muon spectrometer, in the region $2.5 < |\eta| < 2.7$. “Baseline” muon candidates, which are used to veto events with muons, are required to pass “Medium”

identification [84] and have $p_T > 4$ GeV, $|\eta| < 2.7$, and $|z_0 \sin(\theta)| < 0.5$ mm. Muons passing the more stringent “Loose_VarRad” isolation [84], $|d_0/\sigma(d_0)| < 3$, and $p_T > 10$ GeV requirements are referred to as “signal” muons.

Hadronically decaying τ -leptons are reconstructed from jets with $p_T > 10$ GeV and either $|\eta| < 1.37$ or $1.52 < |\eta| < 2.5$ [85]. In addition, τ -lepton candidates must have $p_T > 20$ GeV, one or three charged-particle tracks, and tracks with a total electric charge of ± 1 times the electron charge. The τ -leptons are also required to meet the “Loose” criterion of the neural-network-based identification algorithm [86].

To prevent double-counting of electrons as jets, jets within $\Delta R = 0.2$ of an electron are not considered further unless the jet is b -tagged; b -tagged jets are removed if the overlapping electron has $p_T > 100$ GeV, otherwise the electron is removed. Muons are not counted if they are within $\Delta R = (0.04 + 10 \text{ GeV}/p_T(\text{jet}))$ of a jet. This criterion is applied to remove muons from decays of b - and c -hadrons but retain high- p_T muons resulting from decays of high- p_T massive particles, which tend to be less isolated than muons from decays of low- p_T massive particles. Electrons that share an inner-detector track with a muon are discarded. If a τ -lepton candidate is found to overlap ($\Delta R < 0.2$) with a muon or electron, the τ -lepton is removed. Jets within $\Delta R = 0.4$ of a τ -lepton are removed. This removal of overlapping objects is only performed for baseline objects.

The missing transverse momentum \vec{p}_T^{miss} , with magnitude E_T^{miss} [87], is calculated as the negative vector sum of the transverse momenta of jets, τ -leptons, electrons, and muons. Photons are counted as jets since they are not considered in this search. To account for the underlying event, the missing transverse momentum computation also considers tracks with $p_T > 0.5$ GeV that are associated with the primary vertex but not with any reconstructed particle or jet.

The significance of missing transverse momentum, denoted by E_T^{miss} Sig., is the ratio of E_T^{miss} to its variance [88]. The variance is calculated using the p_T resolution of each component used to evaluate the E_T^{miss} . The correlation between the components is also included.

5 Event selection

The search uses simulated data to design signal regions that have sensitivity to the SUSY models of interest. Control regions that have high purity in particular background processes are used to estimate major background contributions; their normalizations are determined by the data and are extrapolated to the signal regions using simulation. The control regions are designed to not overlap with the signal regions, to have selection criteria similar to those of the signal regions so as to reduce uncertainties from the extrapolation, and to have only a small contamination from signal processes. In addition to the signal and control regions, validation regions are used to validate the background modelling before examining the recorded data in the signal regions (unblinding). Detailed descriptions of the statistical data analysis and how the SM backgrounds are constrained with a fit are provided in Section 7.

5.1 Signal regions

To maximize the discovery potential, the search uses two sets of signal regions targeting two drastically different kinematic regions: *High-Mass* and *Compressed*. The signal regions were designed using simulated event samples to maximize the expected sensitivity. The High-Mass signal regions are sensitive

to leptoquark models and SUSY models with large leptoquark or top squark masses ($\gtrsim 600$ GeV) and a large difference between the top squark and LSP masses ($\gtrsim 200$ GeV); here E_T^{miss} -based variables are relied upon to separate signal events from background events. The Compressed signal regions are sensitive to SUSY models with both smaller top squark masses and compressed spectra, $\Delta m(\tilde{t}_1, \tilde{\chi}_1^0) \lesssim 175$ GeV; here the presence of high-momentum jets originating from initial-state radiation (ISR) and Recursive Jigsaw Reconstruction (RJR) [31] are used to suppress the SM background. The High-Mass and Compressed regions do not overlap because the High-Mass regions require the leading jet to be a c -tagged jet while the Compressed regions require the leading jet not to be c -tagged.

The signal models targeted in this search are expected to produce events that have significant E_T^{miss} – even in the Compressed region for which additional jet activity boosts the neutralinos resulting in large E_T^{miss} – so all events are required to have $E_T^{\text{miss}} > 250$ GeV. The signal processes do not produce any leptons, so events containing electrons, muons, or τ -leptons are vetoed. All regions, unless otherwise indicated, include jets with $p_T > 20$ GeV and require at least one jet with $p_T > 250$ GeV. For High-Mass signal regions, all jet-related variables are computed using jets with $p_T > 40$ GeV. At least two jets must be present, and at least one must be identified as a c -tagged jet. To reject backgrounds originating from top-quark-pair ($t\bar{t}$) decays, events with b -tagged jets are discarded. Finally, the minimum azimuthal angle separation ($\Delta\phi$) between the (up to) four leading jets and the \vec{p}_T^{miss} is required to be greater than 0.4 to reject multijet backgrounds, reducing them to negligible levels such that they need not be considered further in this search.

Three non-overlapping High-Mass signal regions, named SR-HM1, SR-HM2 and SR-HM3, are defined as shown in Table 2. The SUSY scenario with $\mathcal{B}(\tilde{t}_1/\tilde{c}_1 \rightarrow c + \tilde{\chi}_1^0) = 1$ and $m(\tilde{t}_1, \tilde{\chi}_1^0) = (1000, 1)$ GeV is used to optimize the selection for SR-HM1, while the scenario with $m(\tilde{t}_1, \tilde{\chi}_1^0) = (700, 400)$ GeV is used to optimize the selection for SR-HM2 and SR-HM3. All signal models are expected to produce two c -tagged jets, so all three regions require the presence of at least two c -tagged jets. Additionally, the signal models which are used to optimize the High-Mass signal regions are expected to have highly energetic c -tagged jets, motivating the requirement that the leading jet be c -tagged and that the subleading jet have a p_T ($p_T(j_2)$) of at least 150 GeV. Standard Model background contributions with two c -tagged jets originating from real charm quarks are expected to be produced from $g \rightarrow c\bar{c}$, where g is a gluon, and m_{cc} , the invariant mass of the two highest- p_T c -tagged jets, is expected to have a falling spectrum. Thus, SR-HM1, SR-HM2, and SR-HM-3 require m_{cc} to be at least 200 GeV. Different m_{cc} requirements are made in SR-HM2 and SR-HM3 to target signal samples with $\Delta m(\tilde{t}_1, \tilde{\chi}_1^0) \sim 300$ GeV and ~ 400 GeV, respectively. An upper bound on m_{cc} was added to SR-HM3 to reject V +jets backgrounds where m_{cc} falls less steeply than in the signal samples above $m_{cc} \sim 600$ GeV. The minimum transverse mass $m_T^{\text{min}}(c)$, where $m_T(c) = \sqrt{2p_T(c) \times E_T^{\text{miss}} \times (1 - \cos \Delta\phi(c, \vec{p}_T^{\text{miss}}))}$ is calculated for each c -tagged jet, is required to be at least 250 GeV to reject $W(\rightarrow \tau\nu) + \text{jets}$ backgrounds containing hadronically decaying τ -leptons misidentified as c -tagged jets. Finally, various E_T^{miss} Sig. requirements are imposed to target signal models which are expected to have different kinematics. In addition to SR-HM1, SR-HM2, and SR-HM3, a signal region SR-HM-Disc with less stringent requirements is defined and is only used to set model-independent cross-section limits.

Four Compressed signal regions, named SR-Comp1, SR-Comp2, SR-Comp3 and SR-Comp-1c, are defined as shown in Table 3. All Compressed signal regions are orthogonal to the High-Mass signal regions as the leading jet is required to not be c -tagged. The most compressed SUSY scenarios, with $\Delta m(\tilde{t}_1, \tilde{\chi}_1^0) \approx 20\text{--}50$ GeV, are targeted with SR-Comp1 and SR-Comp-1c. SUSY scenarios with $\Delta m(\tilde{t}_1, \tilde{\chi}_1^0) \approx 80$ GeV are targeted with SR-Comp2, and a looser, more general signal region, SR-Comp3,

Table 2: Requirements of the SR-HM1–3 High-Mass regions, which are aimed at signal models with high top squark mass ($\gtrsim 600$ GeV), and SR-HM-Disc which is aimed at a broad range of models.

Variable	SR-HM1	SR-HM2	SR-HM3	SR-HM-Disc
Number of c -tagged jets	≥ 2			
Leading jet is c -tagged	yes			
$m_T^{\min}(c)$ [GeV]	> 300			
$p_T(j_2)$ [GeV]	> 200	> 150		
m_{cc} [GeV]	> 200	200–400	400–600	> 200
E_T^{miss} Sig.	> 22	15–22		> 15

Table 3: Requirements of the Compressed signal regions that target signal models with top-squark–neutralino mass differences between 20 GeV and 175 GeV.

Variable	SR-Comp1	SR-Comp2	SR-Comp3	SR-Comp-1c
Number of c -tagged jets	≥ 2			$= 1$
Leading jet is c -tagged	no			
$m_T^{\min}(c)$ [GeV]	–	> 80	> 120	< 250
m_{cc} [GeV]	–	–	> 100	–
p_T^{CM} [GeV]	–	–	–	< 10
m_V [GeV]	–	–	–	< 80
$\Delta\phi(\vec{p}_T^{\text{miss}}, j_1)$	–	–	–	> 2
$N_{c\text{-jets}}^S$	≥ 2			$= 1$
p_T^{ISR} [GeV]	> 550	> 500	> 400	> 700
R_{ISR}	> 0.85	0.75–0.85	> 0.65	0.9–1.0

is designed to target a wide range of larger mass splittings $50 \text{ GeV} \lesssim \Delta m(\tilde{t}_1, \tilde{\chi}_1^0) \lesssim 175 \text{ GeV}$. At least two c -tagged jets are required for SR-Comp1, while only one is required for SR-Comp-1c to increase signal contributions for the low- p_T regime where the c -tagging efficiency decreases. SR-Comp-1c also has a requirement of $\Delta\phi(\vec{p}_T^{\text{miss}}, j_1) > 2$ on the azimuthal angle separation between the leading jet and the \vec{p}_T^{miss} . In SR-Comp3, selections on $m_T^{\min}(c)$ and m_{cc} improve background rejection, with the latter serving to reduce background contributions from $g \rightarrow c\bar{c}$. There is some overlap between the Compressed signal regions: SR-Comp3 overlaps with SR-Comp1 and SR-Comp2, but SR-Comp1, SR-Comp2, and SR-Comp-1c are all orthogonal to one another, and SR-Comp-1c is orthogonal to SR-Comp3. Recursive Jigsaw Reconstruction [89] is used in the Compressed signal regions to enhance background rejection. In the presence of an ISR system, which consists of one or more jets produced by initial-state radiation, the $\tilde{t}_1\tilde{t}_1$ or $\tilde{c}_1\tilde{c}_1$ system is boosted in the transverse plane. Kinematic variables are then defined appropriately for the assignment of objects to either the ISR system or the sparticle (squarks plus LSPs) system. This method is equivalent to grouping the event objects according to the axis of maximum back-to-back p_T in the event’s centre-of-mass (CM) frame, where the p_T of all objects sums vectorially to zero. The technique provides a

suite of variables which are leveraged in the Compressed signal regions and include R_{ISR} , which is the projection of the invisible system's p_T direction vector onto the ISR system's p_T direction vector. The ISR and sparticle systems tend to be approximately back-to-back in compressed SUSY events, resulting in R_{ISR} values close to unity, while SM backgrounds tend to populate a wider range of R_{ISR} values. The vector sum of the jets' transverse momenta in the ISR frame, p_T^{ISR} , is also used to reject background. For SM backgrounds, p_T^{ISR} has a smoothly falling distribution, while for compressed SUSY signal models, a peak at higher p_T^{ISR} is seen, with the location of the peak typically being related to the mass of the parent SUSY particle. The number of c -tagged jets assigned to the sparticle (S) frame of the ISR decay tree, $N_{c\text{-jets}}^{\text{S}}$, is also utilized as a discriminating variable. To suppress the increased SM contributions, SR-Comp-1c requires more stringent selections on R_{ISR} and p_T^{ISR} , and additional selections are also imposed on p_T^{CM} , the transverse momentum of the CM frame as evaluated in the laboratory frame, and m_V , the invariant mass of objects assigned to the visible (V) system.

Model-independent cross-section limits are set in the signal regions with the least stringent requirements (SR-HM1, SR-Comp3, and SR-HM-Disc) to search for any “beyond the Standard Model” (BSM) contributions. SR-HM-Disc has requirements similar to those in the other SR-HM regions, but it has a less stringent requirement on m_{cc} ($m_{cc} > 200$ GeV) and lacks the upper bound on E_T^{miss} Sig. applied in SR-HM2 and SR-HM3 (see Table 2).

5.2 Background estimation and the control regions

The dominant backgrounds in all the signal regions are from processes with W or Z bosons produced in association with jets, with the bosons decaying as $W \rightarrow \ell\nu$ or $Z \rightarrow \nu\nu$ and producing real missing transverse momentum. The Z +jets background has similar contributions from $Z + c\bar{c}$, $Z + cj$, and $Z + jj$ (where j indicates a non-charm quark) in all signal regions except SR-Comp-1c, where the $Z + jj$ background dominates. The W +jets background has larger contributions from the $W + cj$ and $W + jj$ components than from $W + c\bar{c}$. To reduce the systematic uncertainties, these backgrounds are estimated by extrapolating production-rate correction factors from the control regions (CRs) to the signal regions using the simulated samples. The extrapolation is performed in lepton multiplicity as illustrated in Figure 2 while other requirements in the CRs are made to be as close as possible to those in the signal regions. The normalization of the Z +jets and W +jets backgrounds is performed *in situ* with the two-lepton (CRZ) and one-lepton (CRW) control regions, respectively. Three groups of CRs are designed for each background contribution: one set of CRs for the High-Mass signal regions, one set for the Compressed signal regions with two c -tagged jets, and one set for the Compressed signal region with one c -tagged jet. Contamination from signal processes was checked and found to be negligible in the defined CRs. Background processes that contribute less significantly are not normalized using control regions but using calculated cross-sections and include processes involving top quarks and multiple vector bosons. These processes are grouped together and referred to as “Other” processes in the remainder of this document.

The data for the Z +jets control regions (CRZ) were collected with the lowest unprescaled single-electron and single-muon triggers. These triggers have nearly constant efficiency for leptons with a p_T ($p_T(\ell_1)$) greater than 27 GeV. To ensure a high-purity sample of Z +jets events, the invariant mass of the two signal leptons is required to be consistent with the mass of the Z boson ($76 \text{ GeV} < m_{\ell\ell} < 106 \text{ GeV}$). Further details of the CRZ selection are shown in Table 4.

For all the Z +jets control regions, E_T^{miss} and all the other variables that use it (including E_T^{miss} Sig.) treat the leptons as invisible by subtracting their contribution from the \vec{p}_T^{miss} computation; these variables are

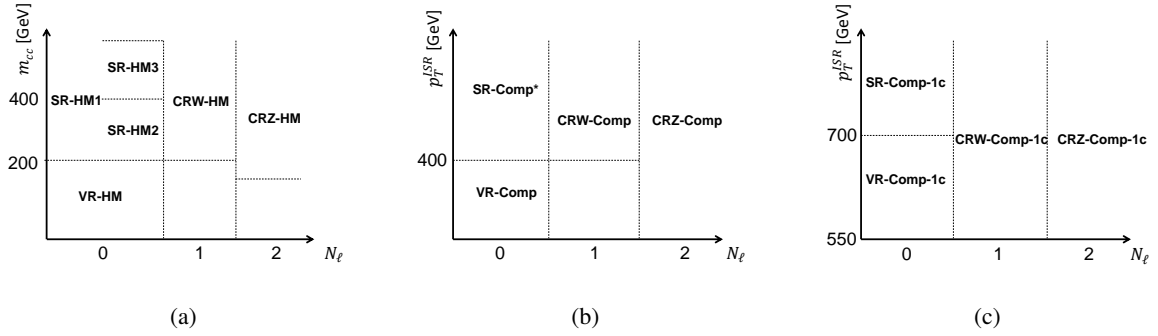


Figure 2: Phase-space partitioning between the signal, control, and validation regions for the (a) High-Mass signal regions, (b) Compressed signal regions SR-Comp1, SR-Comp2 and SR-Comp3, and (c) SR-Comp-1c. Control regions differ from the signal and validation regions by the electron and muon multiplicities (exactly one electron or muon in the W +jets control regions and two electrons or muons in the Z +jets regions) while the validation regions veto events with leptons as in the signal regions. The asterisk in “SR-Comp*” is a wildcard character to denote all the Compressed signal regions which require two c -tagged jets.

indicated with a prime ('). The treatment of the two leptons as invisible particles emulates the dominant contribution from $Z \rightarrow \nu\nu$ decays. To avoid significant extrapolation uncertainties between signal and control regions related to jet flavour composition, the requirements on the number of c -tagged jets ($= 1$ or ≥ 2) and on $m_T^{\min'}$ (c) are kept as close as possible to those in the Compressed signal regions while also ensuring that the CRs provide sufficiently small statistical uncertainty in the Z +jets production rate. Distributions of selected kinematic observables are shown in Figure 3. These distributions illustrate the accuracy of the simulated samples' modelling of the data.

The W +jets control regions (CRW) require exactly one signal electron or muon. To keep the kinematic selection in the CRWs and the corresponding signal regions similar, all the CRWs require events to pass the E_T^{miss} trigger and to have $E_T^{\text{miss}} > 250$ GeV. To ensure a high purity of W +jets background and to avoid contamination from $t\bar{t}$ processes, CRW-Comp includes a veto on events that include a τ -lepton. CRW-Comp has a higher contamination from $t\bar{t}$ than is seen in CRW-HM because of the former's lower $m_T^{\min}(c)$ requirement, which is made to match the requirements in SR-Comp. CRW-Comp-1c contains events that have different kinematics due to its one- c -tag and high- p_T -ISR requirements, and thus does not require additional $t\bar{t}$ rejection from a τ -lepton veto. A detailed description of all the CRW selections is shown in Table 5. Figure 4 shows the distributions of the main kinematic variables used for extrapolation from the CRWs to the Compressed signal regions.

5.3 Validation of background estimates

The validation regions are used to test the accuracy of the procedure used to extrapolate the background from the control region to the signal regions before unblinding data in the signal regions. The parameter used in the extrapolation between the control and signal regions is the electron and muon multiplicity. Therefore, the validation regions veto events with leptons as do the signal regions. The validation regions are designed to have a background composition that consists of the dominant background processes expected in the signal regions, i.e. Z +jets and W +jets. The validation regions are orthogonal to the signal regions and control regions and have sufficient event yields to test the extrapolation procedure with reasonable accuracy.

Table 4: Requirements of the Z+jets control regions for SR-HM1, SR-HM2, and SR-HM3 (CRZ-HM), SR-Comp1, SR-Comp2, and SR-Comp3 (CRZ-Comp), and SR-Comp-1c (CRZ-Comp-1c). Variables that are calculated using E_T^{miss} (including E_T^{miss} Sig.) use an E_T^{miss} variant that includes contributions from electrons/muons that are treated as invisible, and are indicated by a prime (').

Variable	CRZ-HM	CRZ-Comp	CRZ-Comp-1c
Used for	SR-HM	SR-Comp	SR-Comp-1c
$p_T(j_1)$	> 250 GeV		> 350 GeV
Number of c -tagged jets	≥ 2		= 1
Leading jet is c -tagged	yes	no	
Number of signal muons/electrons	= 2		
Passed single-electron/muon triggers	yes		
$p_T(\ell_1)$ [GeV]	> 30		
$m_{\ell\ell}$ [GeV]	76–106		
E_T^{miss} [GeV]	< 200		
$E_T^{\text{miss}'}$ [GeV]	> 200		
m_{cc} [GeV]	> 150	–	
$m_T^{\text{min}'}(c)$ [GeV]	> 150	–	< 250
$E_T^{\text{miss}'}$ Sig.	> 10	–	
$N_{c\text{-jets}}^{S'}$	–	≥ 1	= 1
R'_{ISR}	–	> 0.75	0.9–1.0
$p_T^{\text{ISR}'}$ [GeV]	–		> 550
$\Delta\phi(\vec{p}_T^{\text{miss}'}, j_1)$	–		> 2

The validation regions are also designed to avoid a large contamination from signal scenarios, with less than 20% contamination seen for the models not excluded by the previous ATLAS search.

To validate the extrapolation of the backgrounds from the control regions CRW-HM and CRZ-HM to the High-Mass signal regions SR-HM1, SR-HM2 and SR-HM3, a single validation region VR-HM is used, with an expected Z+jets and W+jets contribution of 45% and 26%, respectively. The requirements for VR-HM are the same as in the signal region, except for a reversal of the m_{cc} requirement, an absence of E_T^{miss} Sig. and $p_T(j_2)$ requirements, and a less stringent requirement of $m_T^{\text{min}}(c) > 200$ GeV (as compared to $m_T^{\text{min}}(c) > 300$ GeV in the signal regions).

The normalization procedure for Compressed regions that require at least two charm-tagged jets, i.e. SR-Comp1, SR-Comp2, and SR-Comp3, is validated in one region, VR-Comp. This region is orthogonal to the signal regions because it has a reversed p_T^{ISR} requirement ($p_T^{\text{ISR}} < 400$ GeV). The other requirements, including the veto on events with leading c -tagged jets that makes the Compressed regions orthogonal to the High-Mass regions, are kept the same as in the signal regions, with the following four exceptions. The

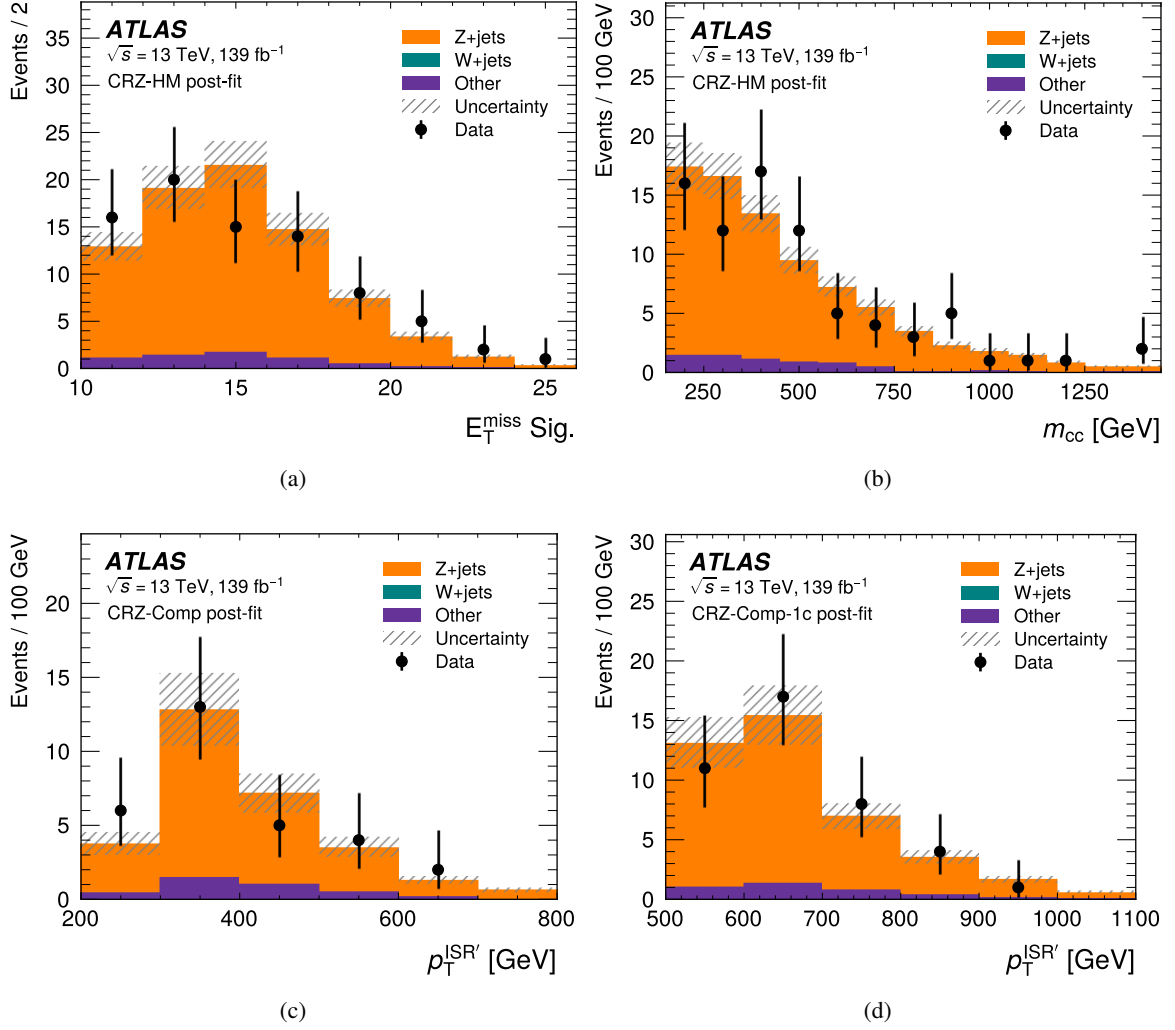


Figure 3: Distributions showing the level of agreement between data (points) and the SM expectation (stacked histograms, after simultaneously fitting the Z +jets and W +jets backgrounds) in the Z +jets control regions for some variables which have different selection criteria in the signal regions: (a) E_T^{miss} Sig. in CRZ-HM, (b) m_{cc} in CRZ-HM, (c) $p_T^{\text{ISR}'}$ in CRZ-Comp, and (d) $p_T^{\text{ISR}'}$ in CRZ-Comp-1c. The hatched uncertainty band around the total SM expectation includes theory-based and detector-related systematic uncertainties and MC statistical uncertainties. Processes with top quarks and multiple vector bosons are included in “Other”. The W +jets background contribution is negligible and not visible in the plots. The right-most bin in each histogram does not include the overflow entry but the x -axis range is chosen to include all observed data.

c -tagged jet multiplicity in the sparticle frame, $N_{c\text{-jets}}^S$, is loosened to be greater than or equal to one (rather than two in the signal regions). The requirement on R_{ISR} is also less stringent in VR-Comp ($R_{\text{ISR}} > 0.65$) than in SR-Comp1 ($R_{\text{ISR}} > 0.85$) and SR-Comp2 ($0.75 < R_{\text{ISR}} < 0.85$) but is the same as in SR-Comp3. Additionally, $m_T^{\text{min}}(c)$ is required to be greater than 80 GeV in VR-Comp, whereas there is no requirement on $m_T^{\text{min}}(c)$ in SR-Comp1. SR-Comp2 also requires a minimum of 80 GeV, and SR-Comp3 requires $m_T^{\text{min}}(c) > 120$ GeV. Finally, no requirement is made on m_{cc} in VR-Comp, as is the case in SR-Comp1 and SR-Comp2, but which differs from the $m_{cc} > 100$ GeV requirement in SR-Comp3.

Table 5: Requirements of the W +jets control regions for SR-HM1, SR-HM2, and SR-HM3 (CRW-HM), SR-Comp1, SR-Comp2, and SR-Comp3 (CRW-Comp), and SR-Comp-1c (CRW-Comp-1c).

Variable	CRW-HM	CRW-Comp	CRW-Comp-1c
Used for	SR-HM	SR-Comp	SR-Comp-1c
$p_T(j_1)$ [GeV]	> 250		> 350
Number of c -tagged jets	≥ 2		= 1
Number of signal muons/electrons	= 1		
Passed E_T^{miss} trigger	yes		
E_T^{miss} [GeV]	> 250		
m_{cc} [GeV]	> 200	–	
$m_T^{\text{min}}(c)$ [GeV]	> 200	> 120	< 250
E_T^{miss} Sig.	> 14	–	
Leading jet is c -tagged	yes	no	
$N_{c\text{-jets}}^S$	–	≥ 1	= 1
p_T^{ISR} [GeV]	–	> 400	> 550
R_{ISR}	–	> 0.65	0.9–1.0
τ veto	–	yes	–
$\Delta\phi(\vec{p}_T^{\text{miss}}, j_1)$	–		> 2

The one- c -tag validation region is identical to SR-Comp-1c with the exception of the defining reversal of the p_T^{ISR} requirement relative to the signal region and the widening of the R_{ISR} window from $0.9 < R_{\text{ISR}} < 1.0$ in SR-Comp-1c to $0.85 < R_{\text{ISR}} < 1.05$. The full set of selections for all validation regions is shown in Table 6, while distributions of the main kinematic variables that differ between the validation regions and the signal regions are shown in Figure 5.

6 Systematic uncertainties

The effect of systematic uncertainties is taken into account for the limited accuracy of the background and signal predictions. To properly treat correlations of uncertainties across the signal and control regions, the uncertainties are separated by source. There are uncertainties for the simulated detector response, integrated luminosity [43], number of simulated events, predicted cross-sections, parton distribution functions, underlying event and minimum-bias pp collisions, parton hadronization models, limited accuracy of matrix element and parton shower calculations, and experimental effects. Below is a discussion of the most relevant sources of uncertainty affecting the search.

The uncertainty in the measured c -tagging efficiency is one of the dominant sources of uncertainty because all the signal and control regions require events with one or more c -tagged jets. The simulated event

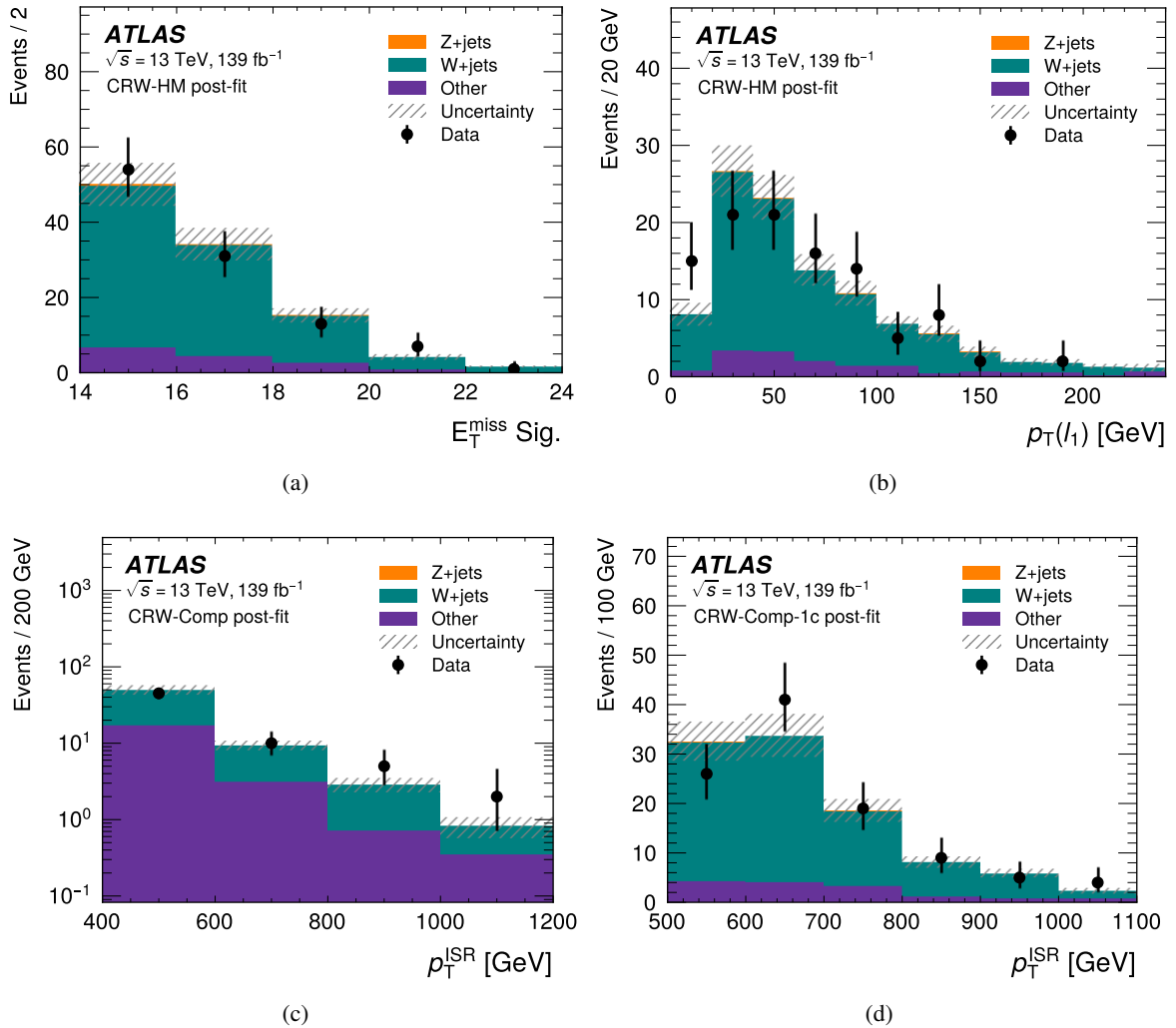


Figure 4: Distributions showing the level of agreement between the data (points) and the SM expectation (stacked histograms, after simultaneously fitting the Z+jets and W+jets backgrounds) in the W+jets control regions for some variables which have different selection criteria in the signal regions: (a) E_T^{miss} Sig. in CRW-HM, (b) p_T of leading lepton in CRW-HM, (c) p_T^{ISR} in CRW-Comp, and (d) p_T^{ISR} in CRW-Comp-1c. The hatched uncertainty band around the total SM expectation includes theory-based and detector-related systematic uncertainties and MC statistical uncertainties. Processes with top quarks and multiple vector bosons are included in “Other”. The Z+jets background contribution is negligible and not visible in the plots. The right-most bin in each histogram does not include the overflow entry but the x -axis range is chosen to include all observed data.

samples are reweighted so that the predicted and measured identification efficiencies of c -tagged jets are identical and so the uncertainties are propagated. The uncertainty in the c -tagging efficiency also depends on the jet p_T and whether the tagged jet is initiated by a b -quark, c -quark, or light quark [80–82].

The uncertainties in the predicted jet energies are driven by the accuracy of the measured jet energies and resolution [76]. There is an uncertainty in the contribution from jets that originate from the overlapping pp interactions but are mistakenly counted as coming from the hard scatter [78]. This includes the efficiency of identifying jets originating from secondary pp interactions and the accuracy of simulated minimum-bias

Table 6: Requirements of the validation regions.

Variable	VR-HM	VR-Comp	VR-Comp-1c
Validates backgrounds in	SR-HM	SR-Comp	SR-Comp-1c
Number of c -tagged jets	≥ 2		$= 1$
Passed E_T^{miss} trigger	yes		
E_T^{miss} [GeV]	> 250		
m_{cc} [GeV]	> 200	–	
$m_T^{\text{min}}(c)$ [GeV]	> 200	> 80	> 100
Leading jet is c -tagged	yes	no	
$N_{c\text{-jets}}^S$	–	≥ 1	$= 1$
p_T^{ISR} [GeV]	–	< 400	
R_{ISR}	–	> 0.65	$0.85\text{--}1.05$
τ veto	yes		
$\Delta\phi(\vec{p}_T^{\text{miss}}, j_1)$	–		> 2
p_T^{CM} [GeV]	–		< 10
m_V [GeV]	–		< 80

interactions.

The theoretical uncertainties for the W +jets and Z +jets backgrounds are estimated with SHERPA. Uncertainties due to inaccuracies in the matrix element calculation and parton showering are estimated by varying the generator’s parameters. The envelope of the associated predicted distributions is taken as the uncertainty. The matrix element matching scale is varied between 15 GeV and 30 GeV. Its nominal value is 20 GeV. The renormalization and factorization scales are varied by factors of 0.5 and 2 independently. The impact of the PDF uncertainties is taken into account in addition to the generator uncertainties.

The secondary backgrounds such as top-quark pairs produced in association with jets [90] and vector-boson pairs produced in association with jets, labeled as “Other” in the figures and tables, have a minor effect on the total background estimate. A normalization uncertainty of 25% is assigned and treated as fully correlated across regions. This uncertainty estimate, is meant to cover cross-section normalization and modeling uncertainties and does not contribute significantly to the total uncertainty. Treating the uncertainty uncorrelated between regions was found to increase the total expected background contribution by at most one standard deviation in SR-Comp2 and SR-Comp3 with a negligible effect on the final result.

Additionally, for signal predictions (i.e. SUSY and LQ), theoretical uncertainties are taken as an envelope of the results obtained when varying the factorization and renormalization scales independently by factors of 0.5 and 2. The Var3c parameter (which corresponds to the strong coupling parameter, α_s , used for ISR) of the A14 underlying-event tune is also varied. The contribution from these uncertainties is largest in the compressed regions, where it reaches 20%.

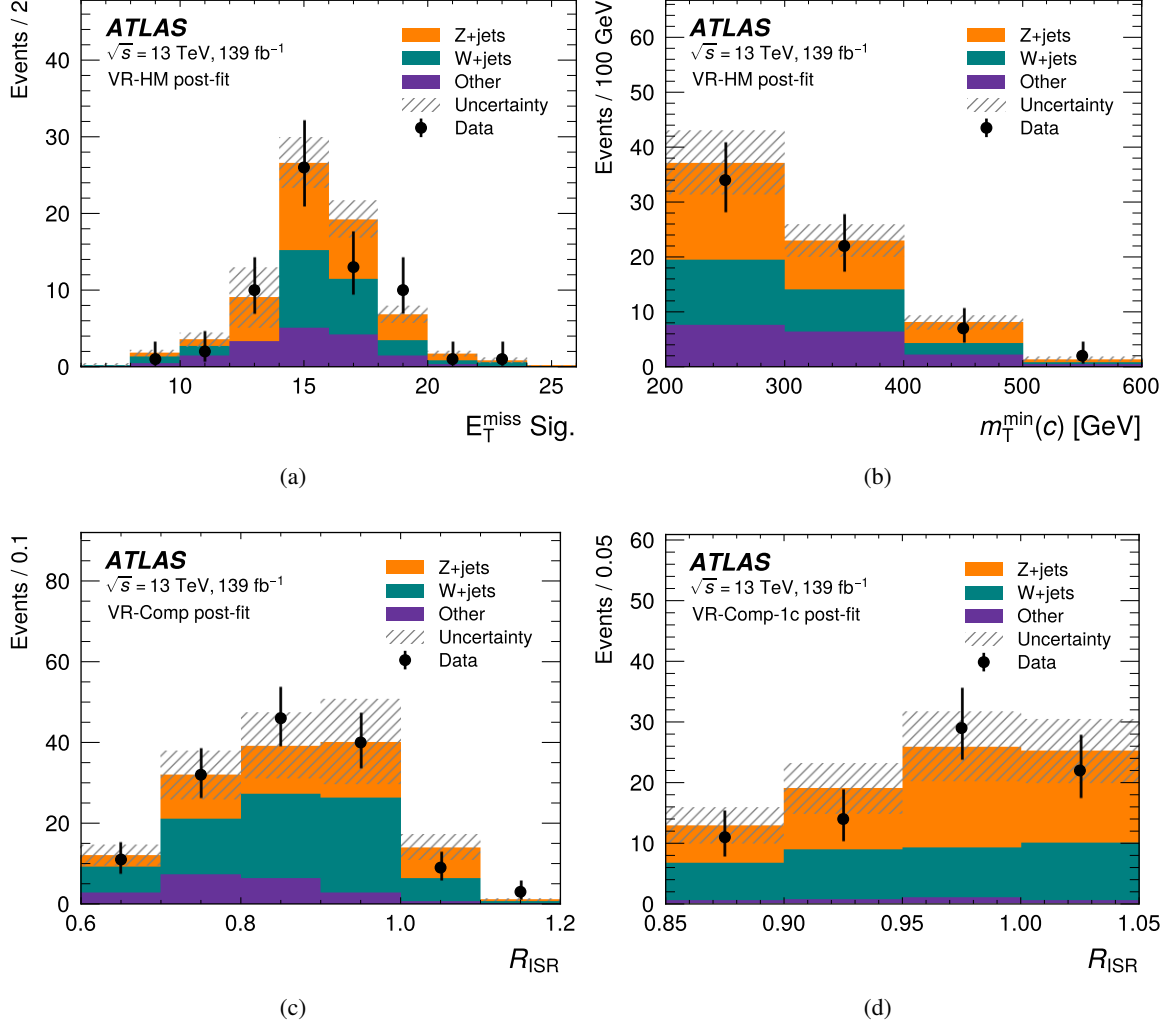


Figure 5: Distributions, in various validation regions, showing the level of agreement between the data (points) and the SM expectation (stacked histograms, after simultaneously fitting the Z+jets and W+jets backgrounds) for variables which have different selection criteria in the signal regions: (a) $E_T^{\text{miss}} \text{ Sig.}$ in VR-HM, (b) $m_T^{\text{min}}(c)$ in VR-HM, (c) R_{ISR} in VR-Comp, and (d) R_{ISR} in VR-Comp-1c. The hatched uncertainty band around the total SM expectation includes theory-based and detector-related systematic uncertainties and MC statistical uncertainties. Processes with top quarks and multiple vector bosons are included in “Other”. The right-most bin in each histogram does not include the overflow entry but the x -axis range is chosen to include all observed data.

7 Results and interpretation

A statistical analysis of the data is performed with a simultaneous likelihood fit [91] that includes the effects of systematic uncertainties on the number of fitted signal and background events through nuisance parameters that change the expected contributions in the control and signal (or validation) regions in a correlated manner. The likelihood probability is calculated by combining Poisson probabilities for the signal, validation, and control regions with a Gaussian probability distribution for each systematic uncertainty. The fit is performed simultaneously across all signal (or validation) and control regions, extracting free-floating normalization factors for the W +jets and Z +jets background contributions, with three normalization factors for each (i.e. for High-Mass, Compressed, and one- c -tag regions).

A “background-only” fit is performed for the High-Mass (CRZ-HM, CRW-HM), Compressed (CRZ-Comp, CRW-Comp), and one- c -tag (CRZ-Comp-1c, CRW-Comp-1c) regions using the likelihood in the control regions and extrapolating the normalization of Z +jets and W +jets contributions into the validation or signal regions (thus not considering the data yield in the signal and validation regions). The fitting strategy reduces systematic uncertainties in the signal regions because the control regions are chosen to minimize the extrapolation uncertainties. Thus the effect on the W +jets and Z +jets background estimates due to systematic uncertainties is similar in the control and signal regions and partially cancels out. This strategy is especially effective in the High-Mass regions, where the total uncertainty of the SM backgrounds is reduced from 30%–37% to 13%–17%. The systematic uncertainties that contribute the most to the total post-fit uncertainty are related to c -tagging and V +jets theoretical uncertainties. Theoretical systematic uncertainties are dominated by the variations of the scales, with contributions to the total uncertainty ranging from 14% to 36%, while the largest contributions from c -tagging-related systematic uncertainties to the total uncertainty of the background estimate in the signal regions range from 8% to 14%.

No significant excesses over the expected SM backgrounds in the validation and signal regions are observed when considering all statistical and systematic (experimental and theory) uncertainties, as shown in Tables 7 and 8 and Figure 6. The extracted normalization factors for the W +jets and Z +jets backgrounds are shown in Table 9 and are generally consistent with unity given their associated uncertainties, with the normalization factors for W +jets background being larger across all control regions. Selected kinematic distributions in the signal regions are shown in Figure 7.

The exclusion fit is performed for each signal model individually, using the signal and control regions. For SUSY models, the two statistical combinations considered use the three High-Mass signal regions with non-overlapping Compressed signal regions: the first combines SR-HM1, SR-HM2, SR-HM3, SR-Comp1, SR-Comp2, and SR-Comp-1c, while the second combines SR-HM1, SR-HM2, SR-HM3, SR-Comp3, and SR-Comp-1c. For both combinations, all six control regions are used to estimate the background contributions. To maximize the exclusion power of the two configurations, the combination with the lowest expected CL_S [93] value is chosen for the final result. The expected sensitivity is calculated by generating pseudo-experiments that assume an absence of BSM signals. Exclusion limits are set at 95% confidence level (CL) and are shown for the considered SUSY models in Figure 8. The expected exclusion limits from this search exceed those from the previous ATLAS search that used c -tagging [30] (grey-filled contour and dashed line in Figure 8), while being complementary to an ATLAS search for single squark production that did not utilize c -tagging [33] (green-filled contour and dashed line in ??) for $m_{\tilde{t}_1/\tilde{c}_1} \lesssim 920$ GeV and $m(\tilde{\chi}_1^0) \gtrsim 400$ GeV, and is also complementary to an ATLAS single-jet search [32] (cyan-filled contour and dashed line in ??) for $\Delta m(\tilde{t}_1, \tilde{\chi}_1^0) \gtrsim 30$ GeV.

Table 7: Post-fit event yields for the High-Mass control, validation, and signal regions. The Z+jets and W+jets backgrounds are normalized by fits within the control regions. Processes with top quarks and multiple vector bosons are included in “Other”. Pre-fit event yields for a representative signal point for each of the signal regions are also shown.

	CRW-HM	CRZ-HM	VR-HM
Z+jets	0.66 ± 0.12	74 ± 9	31 ± 5
W+jets	90 ± 11	0.030 ± 0.009	22 ± 4
Other	15 ± 4	6.6 ± 1.8	17 ± 5
Total SM	106 ± 10	81 ± 9	70 ± 8
Observed	106	81	65

	SR-HM1	SR-HM2	SR-HM3	SR-HM-Disc
Z+jets	5.2 ± 1.3	12.3 ± 3.4	14.7 ± 2.7	58 ± 9
W+jets	3.2 ± 0.7	9.8 ± 1.7	12.5 ± 2.1	43 ± 6
Other	0.88 ± 0.33	1.6 ± 0.6	2.2 ± 0.7	9.0 ± 2.5
Total SM	9.3 ± 1.6	24 ± 4	29 ± 4	110 ± 12
Observed	13	31	27	133
$m(\tilde{t}_1, \tilde{\chi}_1^0) = (1000, 1) \text{ GeV}$	6.6 ± 1.0	12.7 ± 2.1		12.7 ± 2.1
$m(\tilde{t}_1, \tilde{\chi}_1^0) = (750, 450) \text{ GeV}$		17.3 ± 2.6	12.6 ± 2.1	41 ± 7

Exclusion limits are also presented in Figure 9 for an alternative interpretation in which top squarks are pair produced and each decays into a neutralino and either a top or a charm quark, with $\mathcal{B}(\tilde{t}_1 \rightarrow c + \tilde{\chi}_1^0)$ being varied between 0.1 and 1. Due to the b -jet veto imposed, none of the signal and control regions are sensitive to the decay pathway producing a top quark; nonetheless these decay modes are included in the simulated signal samples. Two cases are studied: the mass of the neutralino is fixed to either 1 GeV or 200 GeV. The strongest limits are set when the top squark decays only via the $c + \tilde{\chi}_1^0$ channel, as expected, with top squark masses up to approximately 900 GeV being excluded at 95% CL in both cases. The scenario in which $m(\tilde{\chi}_1^0) = 1 \text{ GeV}$ presents a boosted decay topology over the entire range of top squark masses considered, and as such, the major constraining power comes from the High-Mass signal regions. A monotonic decrease in sensitivity is observed with decreasing branching fraction to $c + \tilde{\chi}_1^0$. For $m(\tilde{\chi}_1^0) = 200 \text{ GeV}$ neutralinos, the Compressed signal regions gradually become more sensitive as the top squark mass decreases, causing the change in behaviour near $m(\tilde{t}_1) = 500 \text{ GeV}$.

Additional limits are set in terms of LQ models after performing a combined fit of the LQ signals using only the High-Mass regions because of similarities in kinematics in the scenario where the LSP is massless. In the case of scalar-LQ models, events were reweighted to span the full range of branching fractions of the LQ decay into $c\nu$. Expected and observed exclusion limits on the $\mathcal{B}(\text{LQ}^u \rightarrow c\nu_e)$ and $\mathcal{B}(\text{LQ}^u \rightarrow c\nu_\mu)$ at 95% CL are presented in Figure 10 as a function of the leptoquark mass, with the observed upper limit on the production cross-section shown on the z -axis. Leptoquarks with masses up to approximately 900 GeV are excluded.

Vector-LQ models are excluded at 95% CL up to masses of 950 GeV in the minimal coupling scenario, and 1150 GeV for the Yang–Mills case, for an assumed branching fraction of $\mathcal{B}(\nu\text{LQ}_{23}^u \rightarrow c\nu_\tau) = 0.5$. Upper

Table 8: Post-fit event yields for the Compressed control, validation, and signal regions. The Z+jets and W+jets backgrounds are normalized by fits within the control regions. Processes with top quarks and multiple vector bosons are included in “Other”. Pre-fit event yields for a representative signal point in each signal region are also shown.

	CRW-Comp	CRZ-Comp	CRW-Comp-1c	CRZ-Comp-1c	VR-Comp	VR-Comp-1c
Z+jets	0.33 ± 0.12	26 ± 6	0.65 ± 0.18	38 ± 7	48 ± 12	48 ± 13
W+jets	41 ± 10	–	89 ± 11	–	71 ± 25	32 ± 11
Other	22 ± 6	3.9 ± 1.2	15 ± 4	4.0 ± 1.1	21 ± 6	2.8 ± 0.8
Total SM	63 ± 8	30 ± 5	105 ± 10	42 ± 6	139 ± 27	83 ± 17
Observed	63	30	105	42	141	76

	SR-Comp1	SR-Comp2	SR-Comp3	SR-Comp-1c
Z+jets	0.9 ± 0.4	1.6 ± 0.9	3.1 ± 0.9	4.3 ± 1.2
W+jets	2.2 ± 1.0	1.3 ± 0.7	0.9 ± 0.6	2.8 ± 0.9
Other	0.56 ± 0.19	0.62 ± 0.20	1.04 ± 0.34	0.68 ± 0.29
Total SM	3.7 ± 1.2	3.5 ± 1.2	5.0 ± 1.2	7.9 ± 1.7
Observed	3	6	8	12
$m(\tilde{t}_1, \tilde{\chi}_1^0) = (600, 550)$ GeV	6.1 ± 1.3			
$m(\tilde{t}_1, \tilde{\chi}_1^0) = (550, 470)$ GeV		6.0 ± 0.8		
$m(\tilde{t}_1, \tilde{\chi}_1^0) = (550, 375)$ GeV			7.9 ± 2.1	
$m(\tilde{t}_1, \tilde{\chi}_1^0) = (450, 430)$ GeV				11.2 ± 1.7

Table 9: Summary of the extracted normalization factors when considering only the likelihood in the control regions for the High-Mass (HM) regions, the Compressed regions that require two c -tagged jets (Comp), and the Compressed regions requiring exactly one c -tagged jet (Comp-1c). Uncertainties include both the statistical and systematic components but do not include the extrapolation into the signal region, which can reduce the total uncertainty. The W+jets normalization factors have larger uncertainties because of the larger effect of theoretical uncertainties.

Region	Normalization factor
HM Z+jets	1.0 ± 0.4
Comp Z+jets	1.0 ± 0.4
Comp-1c Z+jets	1.1 ± 0.4
HM W+jets	1.4 ± 0.6
Comp W+jets	1.3 ± 0.7
Comp-1c W+jets	1.6 ± 0.7

limits on the production cross-section for both the minimal and Yang–Mills coupling scenarios are shown in Figure 11, with the theoretical cross-section at LO and the $\pm 1\sigma$ interval (encompassing the effects of PDF, α_s , renormalization and factorization scale variations) shown in blue.

A model-independent fit is performed for signal regions with the least stringent requirements: SR-HM1, SR-Comp3, and SR-HM-Disc. For the model-independent interpretation, the SM background estimates are fit to the observed yields in both the CRs and SRs, testing for the potential presence of any BSM events in the SRs. The observed cross-section limit, $\langle \epsilon \sigma \rangle_{\text{obs}}^{95}$, is calculated by dividing the observed limit on the

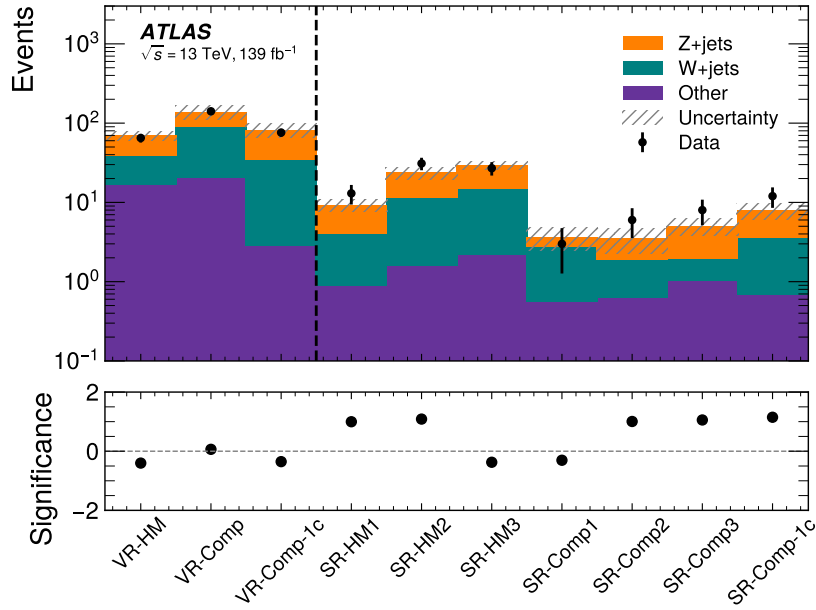


Figure 6: Comparison of event yields for the data (points) and SM expectation (stacked histograms) in all signal and validation regions after the background-only fits. The hatched uncertainty band around the SM prediction represents the total uncertainty, i.e. combining the detector-related and theory-based systematic uncertainties and the MC statistical uncertainties. The significance of the difference between the data and the SM background prediction, calculated with the profile-likelihood method described in Ref. [92] and using the total uncertainty, is shown in the bottom panel. Processes with top quarks and multiple vector bosons are included in “Other”.

signal strength, S_{obs}^{95} , by the integrated luminosity. These limits on the number of BSM events are shown in Table 10 and can be reinterpreted for a generic BSM model by calculating the identification efficiency and detector acceptance for the model of interest.

Table 10: Model-independent upper limits on the BSM event yields and cross-sections. The $\langle \epsilon\sigma \rangle_{\text{obs}}^{95}$ is the observed upper limit on the visible BSM cross-section at 95% CL, and S_{obs}^{95} is the observed upper limit on the number of BSM events. Similarly, S_{exp}^{95} is the expected upper limit on the number of BSM events but it is computed assuming that the observed number of events is identical to the number of background events. The discovery p -value ($p_{\text{obs}}(S = 0)$), which tests the compatibility of the observed data with the background-only (zero signal yield) hypothesis relative to fluctuations of the background, is shown in the last column.

Signal Region	$\langle \epsilon\sigma \rangle_{\text{obs}}^{95}$ [fb]	S_{obs}^{95}	S_{exp}^{95}	$p_{\text{obs}}(S = 0)$
SR-HM1	0.09	12.8	$9.7^{+4.2}_{-2.9}$	0.19
SR-HM-Disc	0.36	50.7	34^{+13}_{-9}	0.09
SR-Comp3	0.07	9.2	$6.5^{+3.2}_{-2.0}$	0.15
SR-Comp-1c	0.08	11.6	$8.0^{+3.8}_{-2.4}$	0.13

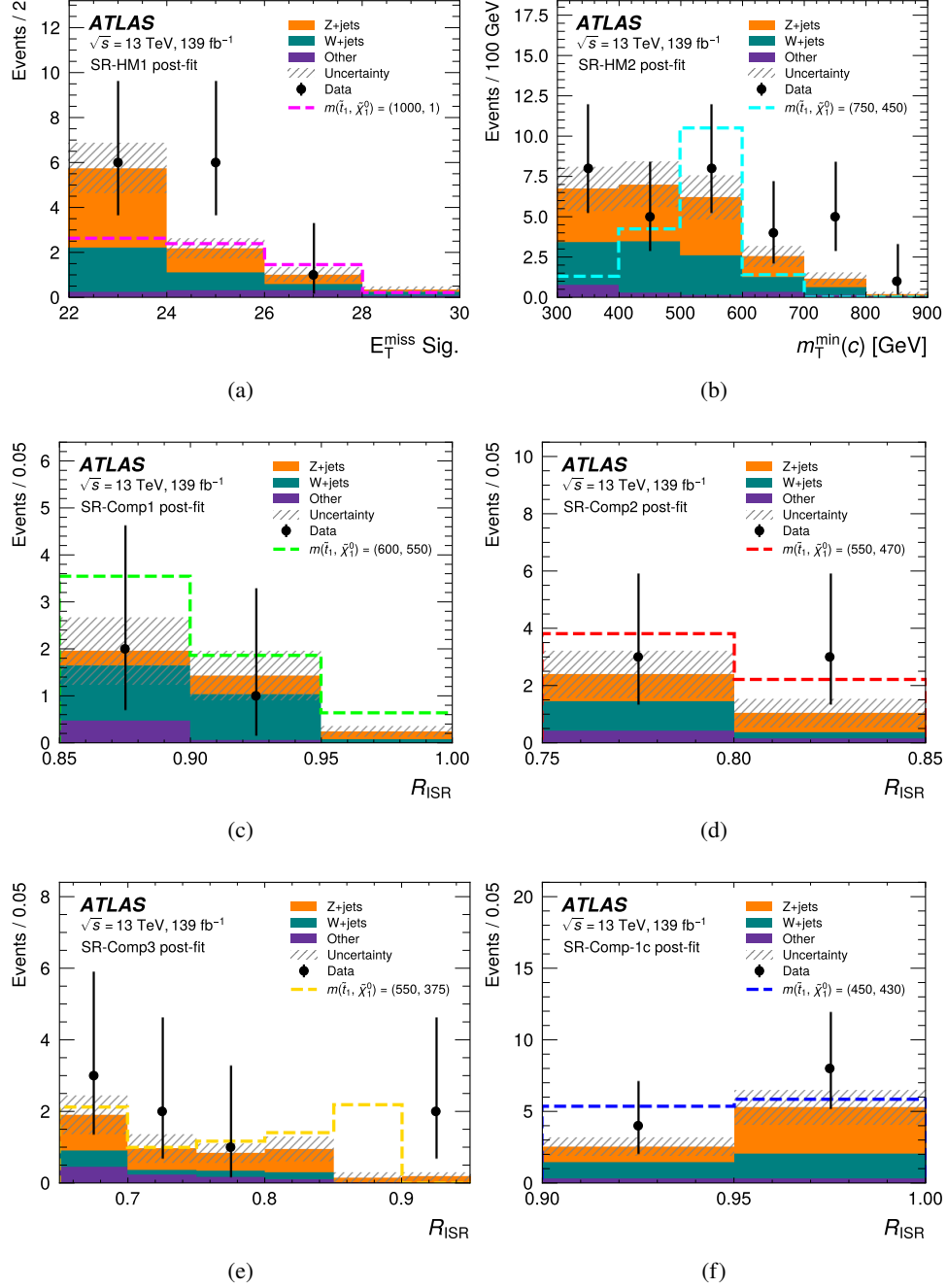


Figure 7: Distributions for the signal regions showing the data (points) and the expected backgrounds (stacked histograms), after simultaneously fitting all the control regions. The histograms are binned in the key variables for each signal region: (a) $E_T^{\text{miss}} \text{ Sig.}$ for SR-HM1, (b) $m_T^{\text{min}(c)}$ for SR-HM2, (c) R_{ISR} for SR-Comp1, (d) R_{ISR} for SR-Comp2, (e) R_{ISR} for SR-Comp3, and (f) R_{ISR} for SR-Comp-1c. The hatched band is the total systematic uncertainty for the expected backgrounds. Distributions of representative $\tilde{t}_1 \bar{\tilde{t}}_1$ signals for different mass assumptions (or similar) are shown as dashed lines using pre-fit signal contributions. Processes with top quarks and multiple vector bosons are included in “Other”. The right-most bin in each histogram does not include the overflow entry but the x -axis range is chosen to include all observed data.

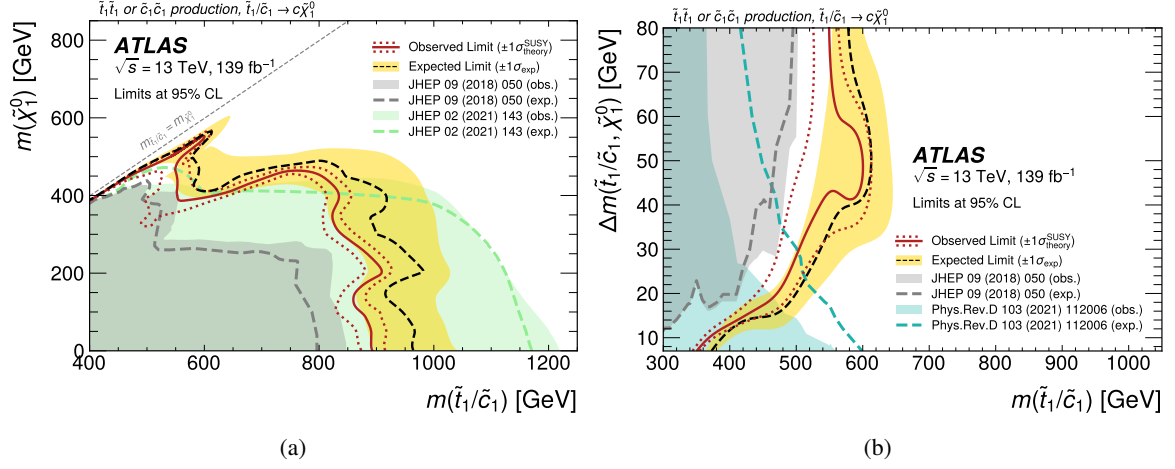


Figure 8: Exclusion limits at 95% CL for pair production of top squarks decaying into charm quarks and neutralinos. The expected limit is shown as a dashed line while the $\pm 1\sigma$ interval is shown as a yellow band. The observed limit is shown as a red line and the effect of varying the signal cross-section by $\pm 1\sigma$ of its predicted theoretical uncertainty is shown as red dashed lines. The contours are shown as two-dimensional projections for masses of squarks and neutralinos (a) and their differences (b). The exclusion contour from the previous ATLAS result that used charm tagging (Ref. [30]) is shown as a grey-dashed line (expected) and grey-filled contour (observed). For (a), the single-squark-production exclusion contour from the ATLAS squarks and gluinos search that did not utilize charm tagging (Ref. [33]) is shown as a green-dashed line (expected) and green-filled contour (observed), while for (b), the contour from the ATLAS single-jet search (Ref. [32]) is shown as a cyan-dashed line (expected) and cyan-filled contour (observed).

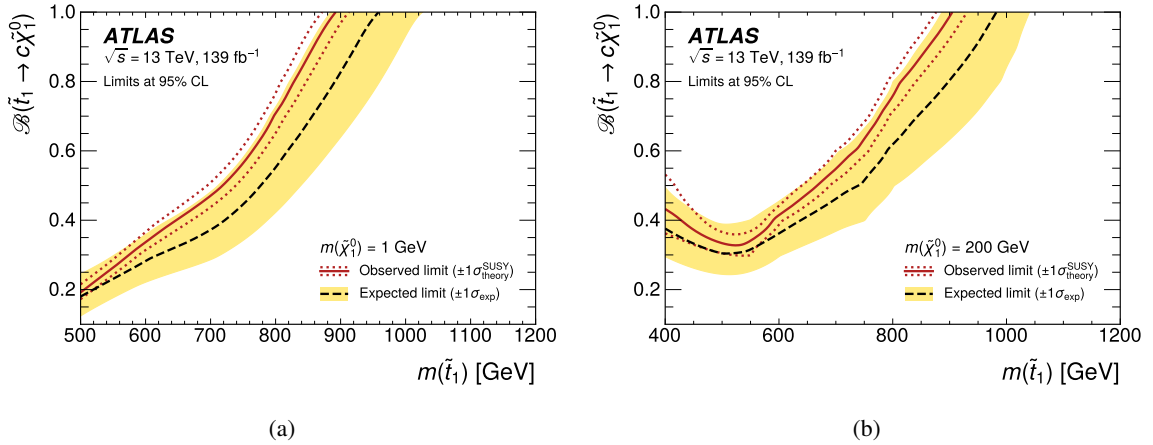


Figure 9: The expected and observed exclusion contours for pair production of top squarks decaying into top or charm quarks and neutralinos. The contours are shown as two-dimensional projections in the plane of the squark mass and assumed branching fraction, whose value is varied between 0 (all decays to $t + \tilde{\chi}_1^0$) and 1 (all decays to $c + \tilde{\chi}_1^0$). The mass of the neutralino is fixed to either (a) 1 GeV or (b) 200 GeV. The cross-section limits for the contours are calculated by combining the signal regions as discussed earlier in the paper. The branching fractions above and masses below the lines (high branching fraction and low mass, and thus high production cross-section) are excluded. The expected limit is shown as a dashed line, while the $\pm 1\sigma$ interval is shown as a yellow band. The observed limit is shown as a red line and the effect of varying the signal cross-section by $\pm 1\sigma$ of its predicted theoretical uncertainty is shown as red dashed lines.

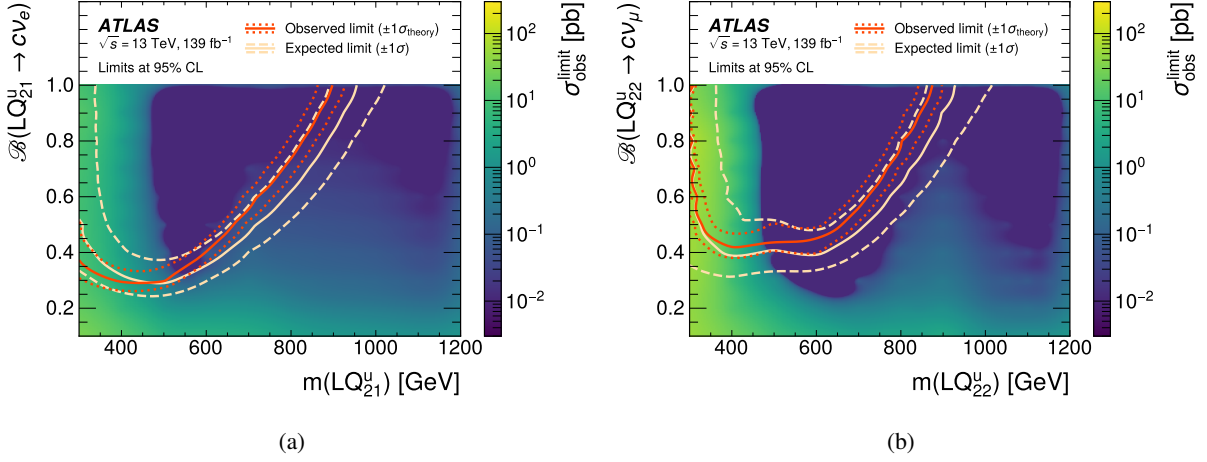


Figure 10: Expected (white) and observed (red) exclusion limits at 95% CL for up-type scalar LQs coupled to (a) first- and (b) second-generation leptons. The observed upper limit on the production cross-section is plotted on the z -axis as a function of (a) $\mathcal{B}(\text{LQ}^u \rightarrow c\nu_e)$ with the alternative decay being $\text{LQ}^u \rightarrow s + e$ and (b) $\mathcal{B}(\text{LQ}^u \rightarrow c\nu_\mu)$ with the alternative decay being $\text{LQ}^u \rightarrow s + \mu$ (y -axis) and the leptoquark masses (x -axis). The branching fractions above and masses below the lines (high branching fraction and low mass, and thus high production cross-section) are excluded. The $\pm 1\sigma$ interval of the expected limit is shown as dashed white lines while the effect of varying the signal cross-section by $\pm 1\sigma$ of its predicted theoretical uncertainty is shown as red dashed lines.

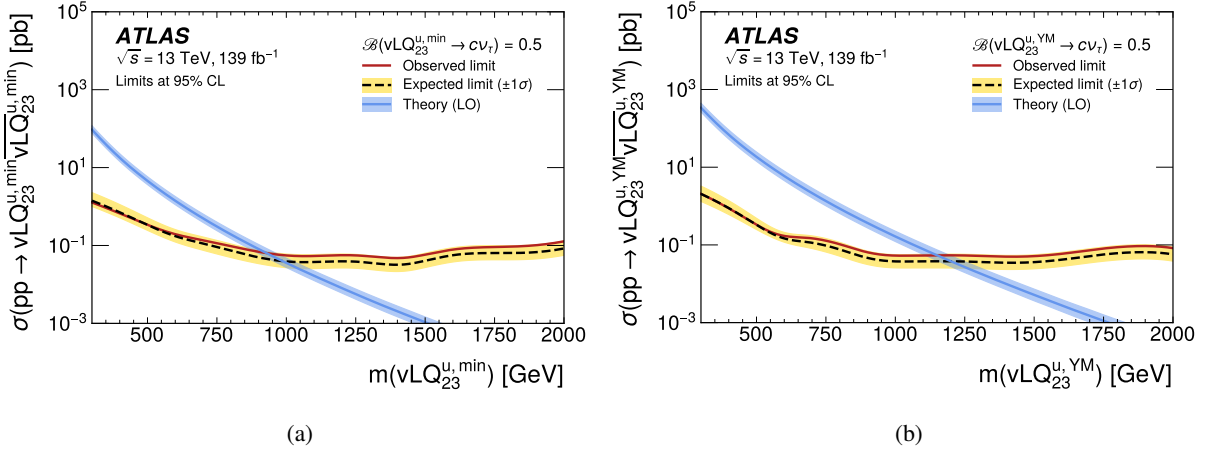


Figure 11: Expected (dashed) and observed (solid) cross-section upper limits as a function of leptoquark mass for $U(1)$ vector-LQ models in the (a) minimal and (b) Yang–Mills coupling scenarios with $\beta_{23} = 1$, corresponding to a branching fraction $\mathcal{B}(\nu\text{LQ}_{23}^u \rightarrow c\nu_\tau) = 0.5$. The $\pm 1\sigma$ interval of the expected limit is shown as a yellow band. The theoretical prediction and its $\pm 1\sigma$ interval band are shown in blue.

8 Conclusion

This paper presents a search targeting BSM models contributing to final states with missing transverse momentum and charm-tagged jets, based on a 139 fb^{-1} dataset of proton–proton collisions at $\sqrt{s} = 13 \text{ TeV}$ recorded by the ATLAS experiment at the LHC. The observed experimental data are found to agree with the SM background estimate. The results are interpreted as upper limits at 95% CL on the production cross-section of selected SUSY and leptoquark models and as model-independent upper limits on the production cross-section for BSM particles. Top/charm squark masses are excluded up to $\sim 900 \text{ GeV}$, assuming each squark decays into a charm quark and an LSP. This is a $\sim 100 \text{ GeV}$ improvement on the previous ATLAS search that used c -tagging. The increase in sensitivity is driven by the larger experimental dataset, the sophisticated design of the signal regions (which includes different strategies for large and small mass splittings between the top squark and the LSP), and improvements in c -tagging. The search also excludes, for the first time at the LHC, scalar leptoquarks with a mass below 900 GeV that decay into a charm quark and either a first- or second-generation neutrino. Finally, vector-leptoquark models in the minimal and Yang–Mills coupling scenarios are excluded at 95% CL up to masses of 950 GeV and 1150 GeV , respectively, assuming a branching fraction of $\mathcal{B}(\nu\text{LQ}_{23}^u \rightarrow c\nu_\tau) = 0.5$.

Acknowledgements

We thank CERN for the very successful operation of the LHC and its injectors, as well as the support staff at CERN and at our institutions worldwide without whom ATLAS could not be operated efficiently.

The crucial computing support from all WLCG partners is acknowledged gratefully, in particular from CERN, the ATLAS Tier-1 facilities at TRIUMF/SFU (Canada), NDGF (Denmark, Norway, Sweden), CC-IN2P3 (France), KIT/GridKA (Germany), INFN-CNAF (Italy), NL-T1 (Netherlands), PIC (Spain), RAL (UK) and BNL (USA), the Tier-2 facilities worldwide and large non-WLCG resource providers. Major contributors of computing resources are listed in Ref. [94].

We gratefully acknowledge the support of ANPCyT, Argentina; YerPhI, Armenia; ARC, Australia; BMWFW and FWF, Austria; ANAS, Azerbaijan; CNPq and FAPESP, Brazil; NSERC, NRC and CFI, Canada; CERN; ANID, Chile; CAS, MOST and NSFC, China; Minciencias, Colombia; MEYS CR, Czech Republic; DNRF and DNSRC, Denmark; IN2P3-CNRS and CEA-DRF/IRFU, France; SRNSFG, Georgia; BMBF, HGF and MPG, Germany; GSRI, Greece; RGC and Hong Kong SAR, China; ISF and Benozio Center, Israel; INFN, Italy; MEXT and JSPS, Japan; CNRST, Morocco; NWO, Netherlands; RCN, Norway; MNiSW, Poland; FCT, Portugal; MNE/IFA, Romania; MESTD, Serbia; MSSR, Slovakia; ARIS and MVZI, Slovenia; DSI/NRF, South Africa; MICIU/AEI, Spain; SRC and Wallenberg Foundation, Sweden; SERI, SNSF and Cantons of Bern and Geneva, Switzerland; NSTC, Taipei; TENMAK, Türkiye; STFC/UKRI, United Kingdom; DOE and NSF, United States of America.

Individual groups and members have received support from BCKDF, CANARIE, CRC and DRAC, Canada; CERN-CZ, FORTE and PRIMUS, Czech Republic; COST, ERC, ERDF, Horizon 2020, ICSC-NextGenerationEU and Marie Skłodowska-Curie Actions, European Union; Investissements d’Avenir Labex, Investissements d’Avenir Idex and ANR, France; DFG and AvH Foundation, Germany; Herakleitos, Thales and Aristeia programmes co-financed by EU-ESF and the Greek NSRF, Greece; BSF-NSF and MINERVA, Israel; Norwegian Financial Mechanism 2014–2021, Norway; NCN and NAWA, Poland; La Caixa Banking Foundation, CERCA Programme Generalitat de Catalunya and PROMETEO and GenT

Programmes Generalitat Valenciana, Spain; Göran Gustafssons Stiftelse, Sweden; The Royal Society and Leverhulme Trust, United Kingdom.

In addition, individual members wish to acknowledge support from CERN: European Organization for Nuclear Research (CERN PJAS); Chile: Agencia Nacional de Investigación y Desarrollo (FONDECYT 1190886, FONDECYT 1230812, FONDECYT 1230987); China: Chinese Ministry of Science and Technology (MOST-2023YFA1605700), National Natural Science Foundation of China (NSFC - 12175119, NSFC 12275265, NSFC-12075060); Czech Republic: Czech Science Foundation (GACR - 24-11373S), Ministry of Education Youth and Sports (FORTE CZ.02.01.01/00/22_008/0004632), PRIMUS Research Programme (PRIMUS/21/SCI/017); EU: H2020 European Research Council (ERC - 101002463); European Union: European Research Council (ERC - 948254, ERC 101089007), Horizon 2020 Framework Programme (MUCCA - CHIST-ERA-19-XAI-00), European Union, Future Artificial Intelligence Research (FAIR-NextGenerationEU PE00000013), Italian Center for High Performance Computing, Big Data and Quantum Computing (ICSC, NextGenerationEU); France: Agence Nationale de la Recherche (ANR-20-CE31-0013, ANR-21-CE31-0013, ANR-21-CE31-0022, ANR-22-EDIR-0002), Investissements d'Avenir Labex (ANR-11-LABX-0012); Germany: Baden-Württemberg Stiftung (BW Stiftung-Postdoc Eliteprogramme), Deutsche Forschungsgemeinschaft (DFG - 469666862, DFG - CR 312/5-2); Italy: Istituto Nazionale di Fisica Nucleare (ICSC, NextGenerationEU), Ministero dell'Università e della Ricerca (PRIN - 20223N7F8K - PNRR M4.C2.1.1); Japan: Japan Society for the Promotion of Science (JSPS KAKENHI JP21H05085, JSPS KAKENHI JP22H01227, JSPS KAKENHI JP22H04944, JSPS KAKENHI JP22KK0227); Netherlands: Netherlands Organisation for Scientific Research (NWO Veni 2020 - VI.Veni.202.179); Norway: Research Council of Norway (RCN-314472); Poland: Ministry of Science and Higher Education (IDUB AGH, POB8, D4 no 9722), Polish National Agency for Academic Exchange (PPN/PPO/2020/1/00002/U/00001), Polish National Science Centre (NCN 2021/42/E/ST2/00350, NCN OPUS nr 2022/47/B/ST2/03059, NCN UMO-2019/34/E/ST2/00393, UMO-2020/37/B/ST2/01043, UMO-2021/40/C/ST2/00187, UMO-2022/47/O/ST2/00148, UMO-2023/49/B/ST2/04085); Slovenia: Slovenian Research Agency (ARIS grant J1-3010); Spain: Generalitat Valenciana (Artemisa, FEDER, IDIFEDER/2018/048), Ministry of Science and Innovation (MCIN & NextGenEU PCI2022-135018-2, MICIN & FEDER PID2021-125273NB, RYC2019-028510-I, RYC2020-030254-I, RYC2021-031273-I, RYC2022-038164-I), PROMETEO and GenT Programmes Generalitat Valenciana (CIDEAGENT/2019/023, CIDEAGENT/2019/027); Sweden: Swedish Research Council (Swedish Research Council 2023-04654, VR 2018-00482, VR 2022-03845, VR 2022-04683, VR 2023-03403, VR grant 2021-03651), Knut and Alice Wallenberg Foundation (KAW 2018.0157, KAW 2018.0458, KAW 2019.0447, KAW 2022.0358); Switzerland: Swiss National Science Foundation (SNSF - PCEFP2_194658); United Kingdom: Leverhulme Trust (Leverhulme Trust RPG-2020-004), Royal Society (NIF-R1-231091); United States of America: U.S. Department of Energy (ECA DE-AC02-76SF00515), Neubauer Family Foundation.

References

- [1] Y. Golfand and E. Likhtman, *Extension of the Algebra of Poincare Group Generators and Violation of P Invariance*, JETP Lett. **13** (1971) 323, [Pisma Zh. Eksp. Teor. Fiz. **13** (1971) 452].
- [2] D. Volkov and V. Akulov, *Is the neutrino a goldstone particle?* *Phys. Lett. B* **46** (1973) 109.
- [3] J. Wess and B. Zumino, *Supergauge transformations in four dimensions*, *Nucl. Phys. B* **70** (1974) 39.

- [4] J. Wess and B. Zumino, *Supergauge invariant extension of quantum electrodynamics*, [Nucl. Phys. B **78** \(1974\) 1](#).
- [5] S. Ferrara and B. Zumino, *Supergauge invariant Yang-Mills theories*, [Nucl. Phys. B **79** \(1974\) 413](#).
- [6] A. Salam and J. Strathdee, *Super-symmetry and non-Abelian gauges*, [Phys. Lett. B **51** \(1974\) 353](#).
- [7] N. Sakai, *Naturalness in supersymmetric GUTS*, [Z. Phys. C **11** \(1981\) 153](#).
- [8] S. Dimopoulos, S. Raby, and F. Wilczek, *Supersymmetry and the scale of unification*, [Phys. Rev. D **24** \(1981\) 1681](#).
- [9] L. E. Ibáñez and G. G. Ross, *Low-energy predictions in supersymmetric grand unified theories*, [Phys. Lett. B **105** \(1981\) 439](#).
- [10] S. Dimopoulos and H. Georgi, *Softly broken supersymmetry and SU(5)*, [Nucl. Phys. B **193** \(1981\) 150](#).
- [11] G. R. Farrar and P. Fayet, *Phenomenology of the production, decay, and detection of new hadronic states associated with supersymmetry*, [Phys. Lett. B **76** \(1978\) 575](#).
- [12] H. Goldberg, *Constraint on the Photino Mass from Cosmology*, [Phys. Rev. Lett. **50** \(1983\) 1419](#), Erratum: [Phys. Rev. Lett. **103** \(2009\) 099905](#).
- [13] J. Ellis, J. Hagelin, D. V. Nanopoulos, K. A. Olive, and M. Srednicki, *Supersymmetric relics from the big bang*, [Nucl. Phys. B **238** \(1984\) 453](#).
- [14] R. Mahbubani, M. Papucci, G. Perez, J. T. Ruderman, and A. Weiler, *Light Nondegenerate Squarks at the LHC*, [Phys. Rev. Lett. **110** \(2013\) 151804](#), arXiv: [1212.3328 \[hep-ph\]](#).
- [15] R. Gröber, M. Mühlleitner, E. Popenza, and A. Wlotzka, *Light stop decays into $Wb\tilde{\chi}_1^0$ near the kinematic threshold*, [Phys. Lett. B **747** \(2015\) 144](#), arXiv: [1502.05935 \[hep-ph\]](#).
- [16] S. Dimopoulos and L. Susskind, *Mass without scalars*, [Nucl. Phys. B **155** \(1979\) 237](#).
- [17] S. Dimopoulos, *Technicoloured signatures*, [Nucl. Phys. B **168** \(1980\) 69](#).
- [18] E. Eichten and K. Lane, *Dynamical breaking of weak interaction symmetries*, [Phys. Lett. B **90** \(1980\) 125](#).
- [19] V. Angelopoulos et al., *Search for new quarks suggested by the superstring*, [Nucl. Phys. B **292** \(1987\) 59](#).
- [20] W. Buchmüller and D. Wyler, *Constraints on SU(5)-type leptoquarks*, [Phys. Lett. B **177** \(1986\) 377](#).
- [21] J. C. Pati and A. Salam, *Lepton number as the fourth "color"*, [Phys. Rev. D **10** \(1 1974\) 275](#).
- [22] H. Georgi and S. L. Glashow, *Unity of All Elementary-Particle Forces*, [Phys. Rev. Lett. **32** \(8 1974\) 438](#).
- [23] B. Diaz, M. Schmaltz, and Y.-M. Zhong, *The leptoquark Hunter's guide: Pair production*, [JHEP **10** \(2017\) 097](#), arXiv: [1706.05033 \[hep-ph\]](#).
- [24] A. Belyaev, C. Leroy, R. Mehdiyev, and A. Pukhov, *Leptoquark single and pair production at LHC with CalcHEP/CompHEP in the complete model*, [JHEP **09** \(2005\) 005](#).
- [25] A. Belyaev, C. Leroy, R. Mehdiyev, and A. Pukhov, *Leptoquark single and pair production at LHC with CalcHEP/CompHEP in the complete model*, [JHEP **09** \(2005\) 005](#), arXiv: [hep-ph/0502067](#).

- [26] J. Blumlein, E. Boos, and A. Kryukov, *Leptoquark pair production in hadronic interactions*, *Z. Phys. C* **76** (1997) 137, arXiv: [hep-ph/9610408](#).
- [27] T. Mandal, S. Mitra, and S. Seth, *Pair Production of Scalar Leptoquarks at the LHC to NLO Parton Shower Accuracy*, *Phys. Rev. D* **93** (2016) 035018, arXiv: [1506.07369 \[hep-ph\]](#).
- [28] M. Krämer, T. Plehn, M. Spira, and P. M. Zerwas, *Pair production of scalar leptoquarks at the CERN LHC*, *Phys. Rev. D* **71** (2005) 057503, arXiv: [hep-ph/0411038](#).
- [29] M. Krämer, T. Plehn, M. Spira, and P. M. Zerwas, *Pair production of scalar leptoquarks at the Fermilab Tevatron*, *Phys. Rev. Lett.* **79** (1997) 341, arXiv: [hep-ph/9704322](#).
- [30] ATLAS Collaboration, *Search for supersymmetry in final states with charm jets and missing transverse momentum in 13 TeV pp collisions with the ATLAS detector*, *JHEP* **09** (2018) 050, arXiv: [1805.01649 \[hep-ex\]](#).
- [31] P. Jackson and C. Rogan, *Recursive Jigsaw Reconstruction: HEP event analysis in the presence of kinematic and combinatoric ambiguities*, *Phys. Rev. D* **96** (2017) 112007, arXiv: [1705.10733 \[hep-ph\]](#).
- [32] ATLAS Collaboration, *Search for new phenomena in events with an energetic jet and missing transverse momentum in pp collisions at $\sqrt{s} = 13$ TeV with the ATLAS detector*, *Phys. Rev. D* **103** (2021) 112006, arXiv: [2102.10874 \[hep-ex\]](#).
- [33] ATLAS Collaboration, *Search for squarks and gluinos in final states with jets and missing transverse momentum using 139 fb^{-1} of $\sqrt{s} = 13$ TeV pp collision data with the ATLAS detector*, *JHEP* **02** (2021) 143, arXiv: [2010.14293 \[hep-ex\]](#).
- [34] ATLAS Collaboration, *A search for top-squark pair production, in final states containing a top quark, a charm quark and missing transverse momentum, using the 139 fb^{-1} of pp collision data collected by the ATLAS detector*, *JHEP* **07** (2024) 250, arXiv: [2402.12137 \[hep-ex\]](#).
- [35] CMS Collaboration, *Search for top squark production in fully hadronic final states in proton–proton collisions at $\sqrt{s} = 13$ TeV*, *Phys. Rev. D* **104** (2021) 052001, arXiv: [2103.01290 \[hep-ex\]](#).
- [36] ATLAS Collaboration, *The ATLAS Experiment at the CERN Large Hadron Collider*, *JINST* **3** (2008) S08003.
- [37] ATLAS Collaboration, *ATLAS Insertable B-Layer: Technical Design Report*, ATLAS-TDR-19; CERN-LHCC-2010-013, 2010, URL: <https://cds.cern.ch/record/1291633>, Addendum: ATLAS-TDR-19-ADD-1; CERN-LHCC-2012-009, 2012, URL: <https://cds.cern.ch/record/1451888>.
- [38] B. Abbott et al., *Production and integration of the ATLAS Insertable B-Layer*, *JINST* **13** (2018) T05008, arXiv: [1803.00844 \[physics.ins-det\]](#).
- [39] G. Avoni et al., *The new LUCID-2 detector for luminosity measurement and monitoring in ATLAS*, *JINST* **13** (2018) P07017.
- [40] ATLAS Collaboration, *Performance of the ATLAS trigger system in 2015*, *Eur. Phys. J. C* **77** (2017) 317, arXiv: [1611.09661 \[hep-ex\]](#).
- [41] ATLAS Collaboration, *Software and computing for Run 3 of the ATLAS experiment at the LHC*, (2024), arXiv: [2404.06335 \[hep-ex\]](#).

- [42] ATLAS Collaboration, *ATLAS data quality operations and performance for 2015–2018 data-taking*, *JINST* **15** (2020) P04003, arXiv: 1911.04632 [physics.ins-det].
- [43] ATLAS Collaboration, *Luminosity determination in pp collisions at $\sqrt{s} = 13$ TeV using the ATLAS detector at the LHC*, ATLAS-CONF-2019-021, 2019, URL: <https://cds.cern.ch/record/2677054>.
- [44] G. Avoni et al., *The new LUCID-2 detector for luminosity measurement and monitoring in ATLAS*, *JINST* **13** (2018) P07017.
- [45] ATLAS Collaboration, *Performance of the missing transverse momentum triggers for the ATLAS detector during Run-2 data taking*, *JHEP* **08** (2020) 080, arXiv: 2005.09554 [hep-ex].
- [46] ATLAS Collaboration, *The ATLAS Simulation Infrastructure*, *Eur. Phys. J. C* **70** (2010) 823, arXiv: 1005.4568 [physics.ins-det].
- [47] S. Agostinelli et al., *GEANT4 – a simulation toolkit*, *Nucl. Instrum. Meth. A* **506** (2003) 250.
- [48] ATLAS Collaboration, *The new Fast Calorimeter Simulation in ATLAS*, ATL-SOFT-PUB-2018-002, 2018, URL: <https://cds.cern.ch/record/2630434>.
- [49] T. Gleisberg et al., *Event generation with SHERPA 1.1*, *JHEP* **02** (2009) 007, arXiv: 0811.4622 [hep-ph].
- [50] D. J. Lange, *The EvtGen particle decay simulation package*, *Nucl. Instrum. Meth. A* **462** (2001) 152.
- [51] NNPDF Collaboration, R. D. Ball, et al., *Parton distributions for the LHC run II*, *JHEP* **04** (2015) 040, arXiv: 1410.8849 [hep-ph].
- [52] ATLAS Collaboration, *Modelling and computational improvements to the simulation of single vector-boson plus jet processes for the ATLAS experiment*, *JHEP* **08** (2022) 089, arXiv: 2112.09588 [hep-ex].
- [53] J. Alwall et al., *The automated computation of tree-level and next-to-leading order differential cross sections, and their matching to parton shower simulations*, *JHEP* **07** (2014) 079, arXiv: 1405.0301 [hep-ph].
- [54] T. Sjöstrand et al., *An introduction to PYTHIA 8.2*, *Comput. Phys. Commun.* **191** (2015) 159, arXiv: 1410.3012 [hep-ph].
- [55] ATLAS Collaboration, *ATLAS Pythia 8 tunes to 7 TeV data*, ATL-PHYS-PUB-2014-021, 2014, URL: <https://cds.cern.ch/record/1966419>.
- [56] S. Alioli, P. Nason, C. Oleari, and E. Re, *A general framework for implementing NLO calculations in shower Monte Carlo programs: the POWHEG BOX*, *JHEP* **06** (2010) 043, arXiv: 1002.2581 [hep-ph].
- [57] M. Czakon, P. Fiedler, and A. Mitov, *Total Top-Quark Pair-Production Cross Section at Hadron Colliders Through $\mathcal{O}(\alpha_s^4)$* , *Phys. Rev. Lett.* **110** (2013) 252004, arXiv: 1303.6254 [hep-ph].
- [58] M. Czakon and A. Mitov, *NNLO corrections to top pair production at hadron colliders: the quark-gluon reaction*, *JHEP* **01** (2013) 080, arXiv: 1210.6832 [hep-ph].
- [59] M. Czakon and A. Mitov, *NNLO corrections to top-pair production at hadron colliders: the all-fermionic scattering channels*, *JHEP* **12** (2012) 054, arXiv: 1207.0236 [hep-ph].

- [60] P. Bärnreuther, M. Czakon, and A. Mitov, *Percent-Level-Precision Physics at the Tevatron: Next-to-Next-to-Leading Order QCD Corrections to $q\bar{q} \rightarrow t\bar{t} + X$* , *Phys. Rev. Lett.* **109** (2012) 132001, arXiv: 1204.5201 [hep-ph].
- [61] M. Cacciari, M. Czakon, M. Mangano, A. Mitov, and P. Nason, *Top-pair production at hadron colliders with next-to-next-to-leading logarithmic soft-gluon resummation*, *Phys. Lett. B* **710** (2012) 612, arXiv: 1111.5869 [hep-ph].
- [62] M. Czakon and A. Mitov, *Top++: A program for the calculation of the top-pair cross-section at hadron colliders*, *Comput. Phys. Commun.* **185** (2014) 2930, arXiv: 1112.5675 [hep-ph].
- [63] N. Kidonakis, *Next-to-next-to-leading-order collinear and soft gluon corrections for t-channel single top quark production*, *Phys. Rev. D* **83** (2011) 091503, arXiv: 1103.2792 [hep-ph].
- [64] N. Kidonakis, *Two-loop soft anomalous dimensions for single top quark associated production with a W^- or H^-* , *Phys. Rev. D* **82** (2010) 054018, arXiv: 1005.4451 [hep-ph].
- [65] N. Kidonakis, *Next-to-next-to-leading logarithm resummation for s-channel single top quark production*, *Phys. Rev. D* **81** (2010) 054028, arXiv: 1001.5034 [hep-ph].
- [66] E. Bothmann et al., *Event generation with Sherpa 2.2*, *SciPost Phys.* **7** (2019) 034, arXiv: 1905.09127 [hep-ph].
- [67] W. Beenakker, C. Borschensky, M. Krämer, A. Kulesza, and E. Laenen, *NNLL-fast: predictions for coloured supersymmetric particle production at the LHC with threshold and Coulomb resummation*, *JHEP* **12** (2016) 133, arXiv: 1607.07741 [hep-ph].
- [68] W. Beenakker, M. Krämer, T. Plehn, M. Spira, and P. M. Zerwas, *Stop production at hadron colliders*, *Nucl. Phys. B* **515** (1998) 3, arXiv: hep-ph/9710451.
- [69] W. Beenakker et al., *Supersymmetric top and bottom squark production at hadron colliders*, *JHEP* **08** (2010) 098, arXiv: 1006.4771 [hep-ph].
- [70] W. Beenakker et al., *NNLL resummation for stop pair-production at the LHC*, *JHEP* **05** (2016) 153, arXiv: 1601.02954 [hep-ph].
- [71] C. Borschensky, B. Fuks, A. Kulesza, and D. Schwartländer, *Scalar leptoquark pair production at hadron colliders*, *Phys. Rev. D* **101** (2020) 115017, arXiv: 2002.08971 [hep-ph].
- [72] ATLAS Collaboration, *Vertex Reconstruction Performance of the ATLAS Detector at $\sqrt{s} = 13$ TeV*, ATL-PHYS-PUB-2015-026, 2015, URL: <https://cds.cern.ch/record/2037717>.
- [73] M. Cacciari, G. P. Salam, and G. Soyez, *The anti- k_t jet clustering algorithm*, *JHEP* **04** (2008) 063, arXiv: 0802.1189 [hep-ph].
- [74] M. Cacciari, G. P. Salam, and G. Soyez, *FastJet user manual*, *Eur. Phys. J. C* **72** (2012) 1896, arXiv: 1111.6097 [hep-ph].
- [75] ATLAS Collaboration, *Jet reconstruction and performance using particle flow with the ATLAS Detector*, *Eur. Phys. J. C* **77** (2017) 466, arXiv: 1703.10485 [hep-ex].

- [76] ATLAS Collaboration, *Jet energy scale and resolution measured in proton–proton collisions at $\sqrt{s} = 13$ TeV with the ATLAS detector*, *Eur. Phys. J. C* **81** (2021) 689, arXiv: 2007.02645 [hep-ex].
- [77] ATLAS Collaboration, *E_T^{miss} performance in the ATLAS detector using 2015–2016 LHC pp collisions*, ATLAS-CONF-2018-023, 2018, URL: <https://cds.cern.ch/record/2625233>.
- [78] ATLAS Collaboration, *Performance of pile-up mitigation techniques for jets in pp collisions at $\sqrt{s} = 8$ TeV using the ATLAS detector*, *Eur. Phys. J. C* **76** (2016) 581, arXiv: 1510.03823 [hep-ex].
- [79] ATLAS Collaboration, *ATLAS flavour-tagging algorithms for the LHC Run 2 pp collision dataset*, *Eur. Phys. J. C* **83** (2023) 681, arXiv: 2211.16345 [physics.data-an].
- [80] ATLAS Collaboration, *Measurement of the c -jet mistagging efficiency in $t\bar{t}$ events using pp collision data at $\sqrt{s} = 13$ TeV collected with the ATLAS detector*, *Eur. Phys. J. C* **82** (2022) 95, arXiv: 2109.10627 [hep-ex].
- [81] ATLAS Collaboration, *ATLAS b -jet identification performance and efficiency measurement with $t\bar{t}$ events in pp collisions at $\sqrt{s} = 13$ TeV*, *Eur. Phys. J. C* **79** (2019) 970, arXiv: 1907.05120 [hep-ex].
- [82] ATLAS Collaboration, *Calibration of the light-flavour jet mistagging efficiency of the b -tagging algorithms with Z +jets events using 139fb^{-1} of ATLAS proton–proton collision data at $\sqrt{s} = 13$ TeV*, *Eur. Phys. J. C* **83** (2023) 728, arXiv: 2301.06319 [hep-ex].
- [83] ATLAS Collaboration, *Electron and photon performance measurements with the ATLAS detector using the 2015–2017 LHC proton–proton collision data*, *JINST* **14** (2019) P12006, arXiv: 1908.00005 [hep-ex].
- [84] ATLAS Collaboration, *Muon reconstruction and identification efficiency in ATLAS using the full Run 2 pp collision data set at $\sqrt{s} = 13$ TeV*, *Eur. Phys. J. C* **81** (2021) 578, arXiv: 2012.00578 [hep-ex].
- [85] ATLAS Collaboration, *Reconstruction, Energy Calibration, and Identification of Hadronically Decaying Tau Leptons in the ATLAS Experiment for Run-2 of the LHC*, ATL-PHYS-PUB-2015-045, 2015, URL: <https://cds.cern.ch/record/2064383>.
- [86] ATLAS Collaboration, *Identification of hadronic tau lepton decays using neural networks in the ATLAS experiment*, ATL-PHYS-PUB-2019-033, 2019, URL: <https://cds.cern.ch/record/2688062>.
- [87] ATLAS Collaboration, *The performance of missing transverse momentum reconstruction and its significance with the ATLAS detector using 140fb^{-1} of $\sqrt{s} = 13$ TeV pp collisions*, (2024), arXiv: 2402.05858 [hep-ex].
- [88] ATLAS Collaboration, *Object-based missing transverse momentum significance in the ATLAS Detector*, ATLAS-CONF-2018-038, 2018, URL: <https://cds.cern.ch/record/2630948>.
- [89] ATLAS Collaboration, *Searches for new phenomena in events with two leptons, jets, and missing transverse momentum in 139fb^{-1} of $\sqrt{s} = 13$ TeV pp collisions with the ATLAS detector*, *Eur. Phys. J. C* **83** (2023) 515, arXiv: 2204.13072 [hep-ex].

- [90] ATLAS Collaboration, *Measurements of inclusive and differential fiducial cross-sections of $t\bar{t}$ production with additional heavy-flavour jets in proton–proton collisions at $\sqrt{s} = 13$ TeV with the ATLAS detector*, [JHEP **04** \(2019\) 046](#), arXiv: [1811.12113 \[hep-ex\]](#).
- [91] G. Cowan, K. Cranmer, E. Gross, and O. Vitells, *Asymptotic formulae for likelihood-based tests of new physics*, [Eur. Phys. J. C **71** \(2011\) 1554](#), arXiv: [1007.1727 \[physics.data-an\]](#), Erratum: [Eur. Phys. J. C **73** \(2013\) 2501](#).
- [92] R. D. Cousins, J. T. Linnemann, and J. Tucker, *Evaluation of three methods for calculating statistical significance when incorporating a systematic uncertainty into a test of the background-only hypothesis for a Poisson process*, [Nucl. Instrum. Meth. A **595** \(2008\) 480](#), arXiv: [physics/0702156 \[physics.data-an\]](#).
- [93] A. L. Read, *Presentation of search results: the CL_S technique*, [J. Phys. G **28** \(2002\) 2693](#).
- [94] ATLAS Collaboration, *ATLAS Computing Acknowledgements*, ATL-SOFT-PUB-2023-001, 2023, URL: <https://cds.cern.ch/record/2869272>.

The ATLAS Collaboration

G. Aad ¹⁰⁴, E. Aakvaag ¹⁷, B. Abbott ¹²³, S. Abdelhameed ^{119a}, K. Abeling ⁵⁶, N.J. Abicht ⁵⁰, S.H. Abidi ³⁰, M. Aboeela ⁴⁵, A. Aboulhorma ^{36e}, H. Abramowicz ¹⁵⁵, H. Abreu ¹⁵⁴, Y. Abulaiti ¹²⁰, B.S. Acharya ^{70a,70b,1}, A. Ackermann ^{64a}, C. Adam Bourdarios ⁴, L. Adamczyk ^{87a}, S.V. Addepalli ²⁷, M.J. Addison ¹⁰³, J. Adelman ¹¹⁸, A. Adiguzel ^{22c}, T. Adye ¹³⁷, A.A. Affolder ¹³⁹, Y. Afik ⁴⁰, M.N. Agaras ¹³, J. Agarwala ^{74a,74b}, A. Aggarwal ¹⁰², C. Agheorghiesei ^{28c}, F. Ahmadov ^{39,z}, W.S. Ahmed ¹⁰⁶, S. Ahuja ⁹⁷, X. Ai ^{63e}, G. Aielli ^{77a,77b}, A. Aikot ¹⁶⁶, M. Ait Tamlihat ^{36e}, B. Aitbenkikh ^{36a}, M. Akbiyik ¹⁰², T.P.A. Åkesson ¹⁰⁰, A.V. Akimov ³⁸, D. Akiyama ¹⁷¹, N.N. Akolkar ²⁵, S. Aktas ^{22a}, K. Al Houry ⁴², G.L. Alberghi ^{24b}, J. Albert ¹⁶⁸, P. Albicocco ⁵⁴, G.L. Albouy ⁶¹, S. Alderweireldt ⁵³, Z.L. Alegria ¹²⁴, M. Aleksa ³⁷, I.N. Aleksandrov ³⁹, C. Alexa ^{28b}, T. Alexopoulos ¹⁰, F. Alfonsi ^{24b}, M. Algren ⁵⁷, M. Alhroob ¹⁷⁰, B. Ali ¹³⁵, H.M.J. Ali ⁹³, S. Ali ³², S.W. Alibocus ⁹⁴, M. Aliev ^{34c}, G. Alimonti ^{72a}, W. Alkahi ⁵⁶, C. Allaire ⁶⁷, B.M.M. Allbrooke ¹⁵⁰, J.F. Allen ⁵³, C.A. Allendes Flores ^{140f}, P.P. Allport ²¹, A. Aloisio ^{73a,73b}, F. Alonso ⁹², C. Alpigiani ¹⁴², Z.M.K. Alsolami ⁹³, M. Alvarez Estevez ¹⁰¹, A. Alvarez Fernandez ¹⁰², M. Alves Cardoso ⁵⁷, M.G. Alvigi ^{73a,73b}, M. Aly ¹⁰³, Y. Amaral Coutinho ^{84b}, A. Ambler ¹⁰⁶, C. Amelung ³⁷, M. Amerl ¹⁰³, C.G. Ames ¹¹¹, D. Amidei ¹⁰⁸, K.J. Amirie ¹⁵⁸, S.P. Amor Dos Santos ^{133a}, K.R. Amos ¹⁶⁶, S. An ⁸⁵, V. Ananiev ¹²⁸, C. Anastopoulos ¹⁴³, T. Andeen ¹¹, J.K. Anders ³⁷, A.C. Anderson ⁶⁰, S.Y. Andreato ^{48a,48b}, A. Andreatza ^{72a,72b}, S. Angelidakis ⁹, A. Angerami ⁴², A.V. Anisenkov ³⁸, A. Annovi ^{75a}, C. Antel ⁵⁷, E. Antipov ¹⁴⁹, M. Antonelli ⁵⁴, F. Anulli ^{76a}, M. Aoki ⁸⁵, T. Aoki ¹⁵⁷, M.A. Aparo ¹⁵⁰, L. Aperio Bella ⁴⁹, C. Appelt ¹⁹, A. Apyan ²⁷, S.J. Arbiol Val ⁸⁸, C. Arcangeletti ⁵⁴, A.T.H. Arce ⁵², E. Arena ⁹⁴, J-F. Arguin ¹¹⁰, S. Argyropoulos ⁵⁵, J.-H. Arling ⁴⁹, O. Arnaez ⁴, H. Arnold ¹⁴⁹, G. Artoni ^{76a,76b}, H. Asada ¹¹³, K. Asai ¹²¹, S. Asai ¹⁵⁷, N.A. Asbah ³⁷, R.A. Ashby Pickering ¹⁷⁰, K. Assamagan ³⁰, R. Astalos ^{29a}, K.S.V. Astrand ¹⁰⁰, S. Atashi ¹⁶², R.J. Atkin ^{34a}, M. Atkinson ¹⁶⁵, H. Atmani ^{36f}, P.A. Atmasiddha ¹³¹, K. Augsten ¹³⁵, S. Auricchio ^{73a,73b}, A.D. Auriol ²¹, V.A. Austrup ¹⁰³, G. Avolio ³⁷, K. Axiotis ⁵⁷, G. Azuelos ^{110,ae}, D. Babal ^{29b}, H. Bachacou ¹³⁸, K. Bachas ^{156,p}, A. Bachi ³⁵, F. Backman ^{48a,48b}, A. Badea ⁴⁰, T.M. Baer ¹⁰⁸, P. Bagnaia ^{76a,76b}, M. Bahmani ¹⁹, D. Bahner ⁵⁵, K. Bai ¹²⁶, J.T. Baines ¹³⁷, L. Baines ⁹⁶, O.K. Baker ¹⁷⁵, E. Bakos ¹⁶, D. Bakshi Gupta ⁸, L.E. Balabram Filho ^{84b}, V. Balakrishnan ¹²³, R. Balasubramanian ¹¹⁷, E.M. Baldin ³⁸, P. Balek ^{87a}, E. Ballabene ^{24b,24a}, F. Balli ¹³⁸, L.M. Baltes ^{64a}, W.K. Balunas ³³, J. Balz ¹⁰², I. Bamwidhi ^{119b}, E. Banas ⁸⁸, M. Bandieramonte ¹³², A. Bandyopadhyay ²⁵, S. Bansal ²⁵, L. Barak ¹⁵⁵, M. Barakat ⁴⁹, E.L. Barberio ¹⁰⁷, D. Barberis ^{58b,58a}, M. Barbero ¹⁰⁴, M.Z. Barel ¹¹⁷, K.N. Barends ^{34a}, T. Barillari ¹¹², M-S. Barisits ³⁷, T. Barklow ¹⁴⁷, P. Baron ¹²⁵, D.A. Baron Moreno ¹⁰³, A. Baroncelli ^{63a}, A.J. Barr ¹²⁹, J.D. Barr ⁹⁸, F. Barreiro ¹⁰¹, J. Barreiro Guimarães da Costa ¹⁴, U. Barron ¹⁵⁵, M.G. Barros Teixeira ^{133a}, S. Barsov ³⁸, F. Bartels ^{64a}, R. Bartoldus ¹⁴⁷, A.E. Barton ⁹³, P. Bartos ^{29a}, A. Basan ¹⁰², M. Baselga ⁵⁰, A. Bassalat ^{67,b}, M.J. Basso ^{159a}, S. Bataju ⁴⁵, R. Bate ¹⁶⁷, R.L. Bates ⁶⁰, S. Batlamous ¹⁰¹, B. Batool ¹⁴⁵, M. Battaglia ¹³⁹, D. Battulga ¹⁹, M. Baucé ^{76a,76b}, M. Bauer ⁸⁰, P. Bauer ²⁵, L.T. Bazzano Hurrell ³¹, J.B. Beacham ⁵², T. Beau ¹³⁰, J.Y. Beaucamp ⁹², P.H. Beauchemin ¹⁶¹, P. Bechtel ²⁵, H.P. Beck ^{20,o}, K. Becker ¹⁷⁰, A.J. Beddall ⁸³, V.A. Bednyakov ³⁹, C.P. Bee ¹⁴⁹, L.J. Beemster ¹⁶, T.A. Beermann ³⁷, M. Begalli ^{84d}, M. Begel ³⁰, A. Behera ¹⁴⁹, J.K. Behr ⁴⁹, J.F. Beirer ³⁷, F. Beisiegel ²⁵, M. Belfkir ^{119b}, G. Bella ¹⁵⁵, L. Bellagamba ^{24b}, A. Bellerive ³⁵, P. Bellos ²¹, K. Beloborodov ³⁸, D. Benchechroun ^{36a}, F. Bendebba ^{36a}, Y. Benhammou ¹⁵⁵,

K.C. Benkendorfer ⁶², L. Beresford ⁴⁹, M. Beretta ⁵⁴, E. Bergeaas Kuutmann ¹⁶⁴, N. Berger ⁴,
 B. Bergmann ¹³⁵, J. Beringer ^{18a}, G. Bernardi ⁵, C. Bernius ¹⁴⁷, F.U. Bernlochner ²⁵,
 F. Bernon ^{37,104}, A. Berrocal Guardia ¹³, T. Berry ⁹⁷, P. Berta ¹³⁶, A. Berthold ⁵¹, S. Bethke ¹¹²,
 A. Betti ^{76a,76b}, A.J. Bevan ⁹⁶, N.K. Bhalla ⁵⁵, S. Bhatta ¹⁴⁹, D.S. Bhattacharya ¹⁶⁹,
 P. Bhattarai ¹⁴⁷, K.D. Bhide ⁵⁵, V.S. Bhopatkar ¹²⁴, R.M. Bianchi ¹³², G. Bianco ^{24b,24a},
 O. Biebel ¹¹¹, R. Bielski ¹²⁶, M. Biglietti ^{78a}, C.S. Billingsley ⁴⁵, M. Bindi ⁵⁶, A. Bingul ^{22b},
 C. Bini ^{76a,76b}, A. Biondini ⁹⁴, G.A. Bird ³³, M. Birman ¹⁷², M. Biros ¹³⁶, S. Biryukov ¹⁵⁰,
 T. Bisanz ⁵⁰, E. Bisceglie ^{44b,44a}, J.P. Biswal ¹³⁷, D. Biswas ¹⁴⁵, I. Bloch ⁴⁹, A. Blue ⁶⁰,
 U. Blumenschein ⁹⁶, J. Blumenthal ¹⁰², V.S. Bobrovnikov ³⁸, M. Boehler ⁵⁵, B. Boehm ¹⁶⁹,
 D. Bogavac ³⁷, A.G. Bogdanchikov ³⁸, C. Bohm ^{48a}, V. Boisvert ⁹⁷, P. Bokan ³⁷, T. Bold ^{87a},
 M. Bomben ⁵, M. Bona ⁹⁶, M. Boonekamp ¹³⁸, C.D. Booth ⁹⁷, A.G. Borbély ⁶⁰,
 I.S. Bordulev ³⁸, H.M. Borecka-Bielska ¹¹⁰, G. Borissov ⁹³, D. Bortoletto ¹²⁹, D. Boscherini ^{24b},
 M. Bosman ¹³, J.D. Bossio Sola ³⁷, K. Bouaouda ^{36a}, N. Bouchhar ¹⁶⁶, L. Boudet ⁴,
 J. Boudreau ¹³², E.V. Bouhova-Thacker ⁹³, D. Boumediene ⁴¹, R. Bouquet ^{58b,58a}, A. Boveia ¹²²,
 J. Boyd ³⁷, D. Boye ³⁰, I.R. Boyko ³⁹, L. Bozianu ⁵⁷, J. Bracinek ²¹, N. Brahimi ⁴,
 G. Brandt ¹⁷⁴, O. Brandt ³³, F. Braren ⁴⁹, B. Brau ¹⁰⁵, J.E. Brau ¹²⁶, R. Brenner ¹⁷²,
 L. Brenner ¹¹⁷, R. Brenner ¹⁶⁴, S. Bressler ¹⁷², G. Brianti ^{79a,79b}, D. Britton ⁶⁰, D. Britzger ¹¹²,
 I. Brock ²⁵, R. Brock ¹⁰⁹, G. Brooijmans ⁴², E.M. Brooks ^{159b}, E. Brost ³⁰, L.M. Brown ¹⁶⁸,
 L.E. Bruce ⁶², T.L. Bruckler ¹²⁹, P.A. Bruckman de Renstrom ⁸⁸, B. Brüers ⁴⁹, A. Bruni ^{24b},
 G. Bruni ^{24b}, M. Bruschi ^{24b}, N. Brusino ^{76a,76b}, T. Buanes ¹⁷, Q. Buat ¹⁴², D. Buchin ¹¹²,
 A.G. Buckley ⁶⁰, O. Bulekov ³⁸, B.A. Bullard ¹⁴⁷, S. Burdin ⁹⁴, C.D. Burgard ⁵⁰,
 A.M. Burger ³⁷, B. Burghgrave ⁸, O. Burlayenko ⁵⁵, J. Burleson ¹⁶⁵, J.T.P. Burr ³³,
 J.C. Burzynski ¹⁴⁶, E.L. Busch ⁴², V. Büscher ¹⁰², P.J. Bussey ⁶⁰, J.M. Butler ²⁶, C.M. Buttar ⁶⁰,
 J.M. Butterworth ⁹⁸, W. Buttinger ¹³⁷, C.J. Buxo Vazquez ¹⁰⁹, A.R. Buzykaev ³⁸,
 S. Cabrera Urbán ¹⁶⁶, L. Cadamuro ⁶⁷, D. Caforio ⁵⁹, H. Cai ¹³², Y. Cai ^{14,114c}, Y. Cai ^{114a},
 V.M.M. Cairo ³⁷, O. Cakir ^{3a}, N. Calace ³⁷, P. Calafiura ^{18a}, G. Calderini ¹³⁰, P. Calfayan ⁶⁹,
 G. Callea ⁶⁰, L.P. Caloba ^{84b}, D. Calvet ⁴¹, S. Calvet ⁴¹, M. Calvetti ^{75a,75b}, R. Camacho Toro ¹³⁰,
 S. Camarda ³⁷, D. Camarero Munoz ²⁷, P. Camarri ^{77a,77b}, M.T. Camerlingo ^{73a,73b},
 D. Cameron ³⁷, C. Camincher ¹⁶⁸, M. Campanelli ⁹⁸, A. Camplani ⁴³, V. Canale ^{73a,73b},
 A.C. Canbay ^{3a}, E. Canonero ⁹⁷, J. Cantero ¹⁶⁶, Y. Cao ¹⁶⁵, F. Capocasa ²⁷, M. Capua ^{44b,44a},
 A. Carbone ^{72a,72b}, R. Cardarelli ^{77a}, J.C.J. Cardenas ⁸, G. Carducci ^{44b,44a}, T. Carli ³⁷,
 G. Carlino ^{73a}, J.I. Carlotto ¹³, B.T. Carlson ^{132,q}, E.M. Carlson ^{168,159a}, J. Carmignani ⁹⁴,
 L. Carminati ^{72a,72b}, A. Carnelli ¹³⁸, M. Carnesale ^{76a,76b}, S. Caron ¹¹⁶, E. Carquin ^{140f},
 S. Carrá ^{72a}, G. Carratta ^{24b,24a}, A.M. Carroll ¹²⁶, T.M. Carter ⁵³, M.P. Casado ^{13,i},
 M. Caspar ⁴⁹, F.L. Castillo ⁴, L. Castillo Garcia ¹³, V. Castillo Gimenez ¹⁶⁶, N.F. Castro ^{133a,133e},
 A. Catinaccio ³⁷, J.R. Catmore ¹²⁸, T. Cavaliere ⁴, V. Cavaliere ³⁰, N. Cavalli ^{24b,24a},
 L.J. Caviedes Betancourt ^{23b}, Y.C. Cekmecelioglu ⁴⁹, E. Celebi ⁸³, S. Cella ³⁷, F. Celli ¹²⁹,
 M.S. Centonze ^{71a,71b}, V. Cepaitis ⁵⁷, K. Cerny ¹²⁵, A.S. Cerqueira ^{84a}, A. Cerri ¹⁵⁰,
 L. Cerrito ^{77a,77b}, F. Cerutti ^{18a}, B. Cervato ¹⁴⁵, A. Cervelli ^{24b}, G. Cesarini ⁵⁴, S.A. Cetin ⁸³,
 D. Chakraborty ¹¹⁸, J. Chan ^{18a}, W.Y. Chan ¹⁵⁷, J.D. Chapman ³³, E. Chapon ¹³⁸,
 B. Chargeishvili ^{153b}, D.G. Charlton ²¹, M. Chatterjee ²⁰, C. Chauhan ¹³⁶, Y. Che ^{114a},
 S. Chekanov ⁶, S.V. Chekulaev ^{159a}, G.A. Chelkov ^{39,a}, A. Chen ¹⁰⁸, B. Chen ¹⁵⁵, B. Chen ¹⁶⁸,
 H. Chen ^{114a}, H. Chen ³⁰, J. Chen ^{63c}, J. Chen ¹⁴⁶, M. Chen ¹²⁹, S. Chen ¹⁵⁷, S.J. Chen ^{114a},
 X. Chen ^{63c,138}, X. Chen ^{15,ad}, Y. Chen ^{63a}, C.L. Cheng ¹⁷³, H.C. Cheng ^{65a}, S. Cheong ¹⁴⁷,
 A. Cheplakov ³⁹, E. Cheremushkina ⁴⁹, E. Cherepanova ¹¹⁷, R. Cherkaoui El Moursli ^{36e},
 E. Cheu ⁷, K. Cheung ⁶⁶, L. Chevalier ¹³⁸, V. Chiarella ⁵⁴, G. Chiarelli ^{75a}, N. Chiedde ¹⁰⁴,
 G. Chiodini ^{71a}, A.S. Chisholm ²¹, A. Chitan ^{28b}, M. Chitishvili ¹⁶⁶, M.V. Chizhov ^{39,r},

K. Choi ¹¹, Y. Chou ¹⁴², E.Y.S. Chow ¹¹⁶, K.L. Chu ¹⁷², M.C. Chu ^{65a}, X. Chu ^{14,114c},
 Z. Chubinidze ⁵⁴, J. Chudoba ¹³⁴, J.J. Chwastowski ⁸⁸, D. Cieri ¹¹², K.M. Ciesla ^{87a},
 V. Cindro ⁹⁵, A. Ciocio ^{18a}, F. Cirotto ^{73a,73b}, Z.H. Citron ¹⁷², M. Citterio ^{72a}, D.A. Ciubotaru ^{28b},
 A. Clark ⁵⁷, P.J. Clark ⁵³, N. Clarke Hall ⁹⁸, C. Clarry ¹⁵⁸, J.M. Clavijo Columbie ⁴⁹,
 S.E. Clawson ⁴⁹, C. Clement ^{48a,48b}, Y. Coadou ¹⁰⁴, M. Cobal ^{70a,70c}, A. Coccaro ^{58b},
 R.F. Coelho Barrue ^{133a}, R. Coelho Lopes De Sa ¹⁰⁵, S. Coelli ^{72a}, B. Cole ⁴², J. Collot ⁶¹,
 P. Conde Muiño ^{133a,133g}, M.P. Connell ^{34c}, S.H. Connell ^{34c}, E.I. Conroy ¹²⁹, F. Conventi ^{73a,af},
 H.G. Cooke ²¹, A.M. Cooper-Sarkar ¹²⁹, F.A. Corchia ^{24b,24a}, A. Cordeiro Oudot Choi ¹³⁰,
 L.D. Corpe ⁴¹, M. Corradi ^{76a,76b}, F. Corriveau ^{106,x}, A. Cortes-Gonzalez ¹⁹, M.J. Costa ¹⁶⁶,
 F. Costanza ⁴, D. Costanzo ¹⁴³, B.M. Cote ¹²², J. Couthures ⁴, G. Cowan ⁹⁷, K. Cranmer ¹⁷³,
 D. Cremonini ^{24b,24a}, S. Crépe-Renaudin ⁶¹, F. Crescioli ¹³⁰, M. Cristinziani ¹⁴⁵,
 M. Cristoforetti ^{79a,79b}, V. Croft ¹¹⁷, J.E. Crosby ¹²⁴, G. Crosetti ^{44b,44a}, A. Cueto ¹⁰¹, H. Cui ⁹⁸,
 Z. Cui ⁷, W.R. Cunningham ⁶⁰, F. Curcio ¹⁶⁶, J.R. Curran ⁵³, P. Czodrowski ³⁷,
 M.M. Czurylo ³⁷, M.J. Da Cunha Sargedas De Sousa ^{58b,58a}, J.V. Da Fonseca Pinto ^{84b},
 C. Da Via ¹⁰³, W. Dabrowski ^{87a}, T. Dado ⁵⁰, S. Dahbi ¹⁵², T. Dai ¹⁰⁸, D. Dal Santo ²⁰,
 C. Dallapiccola ¹⁰⁵, M. Dam ⁴³, G. D'amen ³⁰, V. D'Amico ¹¹¹, J. Damp ¹⁰², J.R. Dandoy ³⁵,
 D. Dannheim ³⁷, M. Danninger ¹⁴⁶, V. Dao ¹⁴⁹, G. Darbo ^{58b}, S.J. Das ^{30,ag}, F. Dattola ⁴⁹,
 S. D'Auria ^{72a,72b}, A. D'Avanzo ^{73a,73b}, C. David ^{34a}, T. Davidek ¹³⁶, I. Dawson ⁹⁶,
 H.A. Day-hall ¹³⁵, K. De ⁸, R. De Asmundis ^{73a}, N. De Biase ⁴⁹, S. De Castro ^{24b,24a},
 N. De Groot ¹¹⁶, P. de Jong ¹¹⁷, H. De la Torre ¹¹⁸, A. De Maria ^{114a}, A. De Salvo ^{76a},
 U. De Sanctis ^{77a,77b}, F. De Santis ^{71a,71b}, A. De Santo ¹⁵⁰, J.B. De Vivie De Regie ⁶¹,
 D.V. Dedovich ³⁹, J. Degens ⁹⁴, A.M. Deiana ⁴⁵, F. Del Corso ^{24b,24a}, J. Del Peso ¹⁰¹,
 F. Del Rio ^{64a}, L. Delagrange ¹³⁰, F. Deliot ¹³⁸, C.M. Delitzsch ⁵⁰, M. Della Pietra ^{73a,73b},
 D. Della Volpe ⁵⁷, A. Dell'Acqua ³⁷, L. Dell'Asta ^{72a,72b}, M. Delmastro ⁴, P.A. Delsart ⁶¹,
 S. Demers ¹⁷⁵, M. Demichev ³⁹, S.P. Denisov ³⁸, L. D'Eramo ⁴¹, D. Derendarz ⁸⁸, F. Derue ¹³⁰,
 P. Dervan ⁹⁴, K. Desch ²⁵, C. Deutsch ²⁵, F.A. Di Bello ^{58b,58a}, A. Di Ciaccio ^{77a,77b},
 L. Di Ciaccio ⁴, A. Di Domenico ^{76a,76b}, C. Di Donato ^{73a,73b}, A. Di Girolamo ³⁷,
 G. Di Gregorio ³⁷, A. Di Luca ^{79a,79b}, B. Di Micco ^{78a,78b}, R. Di Nardo ^{78a,78b}, K.F. Di Petrillo ⁴⁰,
 M. Diamantopoulou ³⁵, F.A. Dias ¹¹⁷, T. Dias Do Vale ¹⁴⁶, M.A. Diaz ^{140a,140b},
 F.G. Diaz Capriles ²⁵, A.R. Didenko ³⁹, M. Didenko ¹⁶⁶, E.B. Diehl ¹⁰⁸, S. Díez Cornell ⁴⁹,
 C. Díez Pardos ¹⁴⁵, C. Dimitriadi ¹⁶⁴, A. Dimitrievska ²¹, J. Dingfelder ²⁵, T. Dingley ¹²⁹,
 I-M. Dinu ^{28b}, S.J. Dittmeier ^{64b}, F. Dittus ³⁷, M. Divisek ¹³⁶, F. Djama ¹⁰⁴, T. Djobava ^{153b},
 C. Doglioni ^{103,100}, A. Dohnalova ^{29a}, J. Dolejsi ¹³⁶, Z. Dolezal ¹³⁶, K. Domijan ^{87a},
 K.M. Dona ⁴⁰, M. Donadelli ^{84d}, B. Dong ¹⁰⁹, J. Donini ⁴¹, A. D'Onofrio ^{73a,73b},
 M. D'Onofrio ⁹⁴, J. Dopke ¹³⁷, A. Doria ^{73a}, N. Dos Santos Fernandes ^{133a}, P. Dougan ¹⁰³,
 M.T. Dova ⁹², A.T. Doyle ⁶⁰, M.A. Dragnet ¹²⁹, E. Dreyer ¹⁷², I. Drivas-koulouris ¹⁰,
 M. Drnevich ¹²⁰, M. Drozdova ⁵⁷, D. Du ^{63a}, T.A. du Pree ¹¹⁷, F. Dubinin ³⁸, M. Dubovsky ^{29a},
 E. Duchovni ¹⁷², G. Duckeck ¹¹¹, O.A. Ducu ^{28b}, D. Duda ⁵³, A. Dudarev ³⁷, E.R. Duden ²⁷,
 M. D'uffizi ¹⁰³, L. Duflost ⁶⁷, M. Dührssen ³⁷, I. Duminica ^{28g}, A.E. Dumitriu ^{28b},
 M. Dunford ^{64a}, S. Dungs ⁵⁰, K. Dunne ^{48a,48b}, A. Duperrin ¹⁰⁴, H. Duran Yildiz ^{3a},
 M. Düren ⁵⁹, A. Durglishvili ^{153b}, B.L. Dwyer ¹¹⁸, G.I. Dyckes ^{18a}, M. Dyndal ^{87a},
 B.S. Dziedzic ³⁷, Z.O. Earnshaw ¹⁵⁰, G.H. Eberwein ¹²⁹, B. Eckerova ^{29a}, S. Eggebrecht ⁵⁶,
 E. Egidio Purcino De Souza ¹³⁰, L.F. Ehrke ⁵⁷, G. Eigen ¹⁷, K. Einsweiler ^{18a}, T. Ekelof ¹⁶⁴,
 P.A. Ekman ¹⁰⁰, S. El Farkh ^{36b}, Y. El Ghazali ^{36b}, H. El Jarrari ³⁷, A. El Moussaouy ^{36a},
 V. Ellajosyula ¹⁶⁴, M. Ellert ¹⁶⁴, F. Ellinghaus ¹⁷⁴, N. Ellis ³⁷, J. Elmsheuser ³⁰, M. Elsayy ^{119a},
 M. Elsing ³⁷, D. Emelianov ¹³⁷, Y. Enari ¹⁵⁷, I. Ene ^{18a}, S. Epari ¹³, P.A. Erland ⁸⁸,
 D. Ernani Martins Neto ⁸⁸, M. Errenst ¹⁷⁴, M. Escalier ⁶⁷, C. Escobar ¹⁶⁶, E. Etzion ¹⁵⁵,

G. Evans [ID133a](#), H. Evans [ID69](#), L.S. Evans [ID97](#), A. Ezhilov [ID38](#), S. Ezzarqtouni [ID36a](#), F. Fabbri [ID24b,24a](#), L. Fabbri [ID24b,24a](#), G. Facini [ID98](#), V. Fadeyev [ID139](#), R.M. Fakhrutdinov [ID38](#), D. Fakoudis [ID102](#), S. Falciano [ID76a](#), L.F. Falda Ulhoa Coelho [ID37](#), F. Fallavollita [ID112](#), G. Falsetti [ID44b,44a](#), J. Faltova [ID136](#), C. Fan [ID165](#), Y. Fan [ID14](#), Y. Fang [ID14,114c](#), M. Fanti [ID72a,72b](#), M. Faraj [ID70a,70b](#), Z. Farazpay [ID99](#), A. Farbin [ID8](#), A. Farilla [ID78a](#), T. Farooque [ID109](#), S.M. Farrington [ID53](#), F. Fassi [ID36e](#), D. Fassouliotis [ID9](#), M. Faucci Giannelli [ID77a,77b](#), W.J. Fawcett [ID33](#), L. Fayard [ID67](#), P. Federic [ID136](#), P. Federicova [ID134](#), O.L. Fedin [ID38,a](#), M. Feickert [ID173](#), L. Feligioni [ID104](#), D.E. Fellers [ID126](#), C. Feng [ID63b](#), M. Feng [ID15](#), Z. Feng [ID117](#), M.J. Fenton [ID162](#), L. Ferencz [ID49](#), R.A.M. Ferguson [ID93](#), S.I. Fernandez Luengo [ID140f](#), P. Fernandez Martinez [ID13](#), M.J.V. Fernoux [ID104](#), J. Ferrando [ID93](#), A. Ferrari [ID164](#), P. Ferrari [ID117,116](#), R. Ferrari [ID74a](#), D. Ferrere [ID57](#), C. Ferretti [ID108](#), D. Fiacco [ID76a,76b](#), F. Fiedler [ID102](#), P. Fiedler [ID135](#), A. Filipčič [ID95](#), E.K. Filmer [ID1](#), F. Filthaut [ID116](#), M.C.N. Fiolhais [ID133a,133c,c](#), L. Fiorini [ID166](#), W.C. Fisher [ID109](#), T. Fitschen [ID103](#), P.M. Fitzhugh [ID138](#), I. Fleck [ID145](#), P. Fleischmann [ID108](#), T. Flick [ID174](#), M. Flores [ID34d,ab](#), L.R. Flores Castillo [ID65a](#), L. Flores Sanz De Acedo [ID37](#), F.M. Follega [ID79a,79b](#), N. Fomin [ID33](#), J.H. Foo [ID158](#), A. Formica [ID138](#), A.C. Forti [ID103](#), E. Fortin [ID37](#), A.W. Fortman [ID18a](#), M.G. Foti [ID18a](#), L. Fountas [ID9,j](#), D. Fournier [ID67](#), H. Fox [ID93](#), P. Francavilla [ID75a,75b](#), S. Francescato [ID62](#), S. Franchellucci [ID57](#), M. Franchini [ID24b,24a](#), S. Franchino [ID64a](#), D. Francis [ID37](#), L. Franco [ID116](#), V. Franco Lima [ID37](#), L. Franconi [ID49](#), M. Franklin [ID62](#), G. Frattari [ID27](#), Y.Y. Frid [ID155](#), J. Friend [ID60](#), N. Fritzsche [ID51](#), A. Froch [ID55](#), D. Froidevaux [ID37](#), J.A. Frost [ID129](#), Y. Fu [ID63a](#), S. Fuenzalida Garrido [ID140f](#), M. Fujimoto [ID104](#), K.Y. Fung [ID65a](#), E. Furtado De Simas Filho [ID84e](#), M. Furukawa [ID157](#), J. Fuster [ID166](#), A. Gaa [ID56](#), A. Gabrielli [ID24b,24a](#), A. Gabrielli [ID158](#), P. Gadow [ID37](#), G. Gagliardi [ID58b,58a](#), L.G. Gagnon [ID18a](#), S. Gaid [ID163](#), S. Galantzan [ID155](#), E.J. Gallas [ID129](#), B.J. Gallop [ID137](#), K.K. Gan [ID122](#), S. Ganguly [ID157](#), Y. Gao [ID53](#), F.M. Garay Walls [ID140a,140b](#), B. Garcia [ID30](#), C. García [ID166](#), A. Garcia Alonso [ID117](#), A.G. Garcia Caffaro [ID175](#), J.E. García Navarro [ID166](#), M. Garcia-Sciveres [ID18a](#), G.L. Gardner [ID131](#), R.W. Gardner [ID40](#), N. Garelli [ID161](#), D. Garg [ID81](#), R.B. Garg [ID147](#), J.M. Gargan [ID53](#), C.A. Garner [ID158](#), C.M. Garvey [ID34a](#), V.K. Gassmann [ID161](#), G. Gaudio [ID74a](#), V. Gautam [ID13](#), P. Gauzzi [ID76a,76b](#), J. Gavranovic [ID95](#), I.L. Gavrilenko [ID38](#), A. Gavrilyuk [ID38](#), C. Gay [ID167](#), G. Gaycken [ID126](#), E.N. Gazis [ID10](#), A.A. Geanta [ID28b](#), C.M. Gee [ID139](#), A. Gekow [ID122](#), C. Gemme [ID58b](#), M.H. Genest [ID61](#), A.D. Gentry [ID115](#), S. George [ID97](#), W.F. George [ID21](#), T. Geralis [ID47](#), P. Gessinger-Befurt [ID37](#), M.E. Geyik [ID174](#), M. Ghani [ID170](#), K. Ghorbanian [ID96](#), A. Ghosal [ID145](#), A. Ghosh [ID162](#), A. Ghosh [ID7](#), B. Giacobbe [ID24b](#), S. Giagu [ID76a,76b](#), T. Giani [ID117](#), A. Giannini [ID63a](#), S.M. Gibson [ID97](#), M. Gignac [ID139](#), D.T. Gil [ID87b](#), A.K. Gilbert [ID87a](#), B.J. Gilbert [ID42](#), D. Gillberg [ID35](#), G. Gilles [ID117](#), L. Ginabat [ID130](#), D.M. Gingrich [ID2,ae](#), M.P. Giordani [ID70a,70c](#), P.F. Giraud [ID138](#), G. Giugliarelli [ID70a,70c](#), D. Giugni [ID72a](#), F. Giuli [ID37](#), I. Gkialas [ID9,j](#), L.K. Gladilin [ID38](#), C. Glasman [ID101](#), G.R. Gledhill [ID126](#), G. Glemža [ID49](#), M. Glisic [ID126](#), I. Gnesi [ID44b,e](#), Y. Go [ID30](#), M. Goblirsch-Kolb [ID37](#), B. Gocke [ID50](#), D. Godin [ID110](#), B. Gokturk [ID22a](#), S. Goldfarb [ID107](#), T. Golling [ID57](#), M.G.D. Gololo [ID34g](#), D. Golubkov [ID38](#), J.P. Gombas [ID109](#), A. Gomes [ID133a,133b](#), G. Gomes Da Silva [ID145](#), A.J. Gomez Delegido [ID166](#), R. Gonçalves [ID133a](#), L. Gonella [ID21](#), A. Gongadze [ID153c](#), F. Gonnella [ID21](#), J.L. Gonski [ID147](#), R.Y. González Andana [ID53](#), S. González de la Hoz [ID166](#), R. Gonzalez Lopez [ID94](#), C. Gonzalez Renteria [ID18a](#), M.V. Gonzalez Rodrigues [ID49](#), R. Gonzalez Suarez [ID164](#), S. Gonzalez-Sevilla [ID57](#), L. Goossens [ID37](#), B. Gorini [ID37](#), E. Gorini [ID71a,71b](#), A. Gorišek [ID95](#), T.C. Gosart [ID131](#), A.T. Goshaw [ID52](#), M.I. Gostkin [ID39](#), S. Goswami [ID124](#), C.A. Gottardo [ID37](#), S.A. Gotz [ID111](#), M. Gouighri [ID36b](#), V. Goumarre [ID49](#), A.G. Goussiou [ID142](#), N. Govender [ID34c](#), I. Grabowska-Bold [ID87a](#), K. Graham [ID35](#), E. Gramstad [ID128](#), S. Grancagnolo [ID71a,71b](#), C.M. Grant [ID1,138](#), P.M. Gravila [ID28f](#), F.G. Gravili [ID71a,71b](#), H.M. Gray [ID18a](#), M. Greco [ID71a,71b](#), M.J. Green [ID1](#), C. Grefe [ID25](#), A.S. Grefsrud [ID17](#), I.M. Gregor [ID49](#), K.T. Greif [ID162](#), P. Grenier [ID147](#), S.G. Grewe [ID112](#), A.A. Grillo [ID139](#), K. Grimm [ID32](#), S. Grinstein [ID13,t](#), J.-F. Grivaz [ID67](#), E. Gross [ID172](#), J. Grosse-Knetter [ID56](#), J.C. Grundy [ID129](#), L. Guan [ID108](#), J.G.R. Guerrero Rojas [ID166](#), G. Guerrieri [ID70a,70c](#), R. Gugel [ID102](#),

J.A.M. Guhit ¹⁰⁸, A. Guida ¹⁹, E. Guilloton ¹⁷⁰, S. Guindon ³⁷, F. Guo ^{14,114c}, J. Guo ^{63c}, L. Guo ⁴⁹, Y. Guo ¹⁰⁸, R. Gupta ¹³², S. Gurbuz ²⁵, S.S. Gurdasani ⁵⁵, G. Gustavino ^{76a,76b}, P. Gutierrez ¹²³, L.F. Gutierrez Zagazeta ¹³¹, M. Gutsche ⁵¹, C. Gutschow ⁹⁸, C. Gwenlan ¹²⁹, C.B. Gwilliam ⁹⁴, E.S. Haaland ¹²⁸, A. Haas ¹²⁰, M. Habedank ⁴⁹, C. Haber ^{18a}, H.K. Hadavand ⁸, A. Hadeef ⁵¹, S. Hadzic ¹¹², A.I. Hagan ⁹³, J.J. Hahn ¹⁴⁵, E.H. Haines ⁹⁸, M. Haleem ¹⁶⁹, J. Haley ¹²⁴, J.J. Hall ¹⁴³, G.D. Hallewell ¹⁰⁴, L. Halser ²⁰, K. Hamano ¹⁶⁸, M. Hamer ²⁵, G.N. Hamity ⁵³, E.J. Hampshire ⁹⁷, J. Han ^{63b}, K. Han ^{63a}, L. Han ^{114a}, L. Han ^{63a}, S. Han ^{18a}, Y.F. Han ¹⁵⁸, K. Hanagaki ⁸⁵, M. Hance ¹³⁹, D.A. Hangal ⁴², H. Hanif ¹⁴⁶, M.D. Hank ¹³¹, J.B. Hansen ⁴³, P.H. Hansen ⁴³, K. Hara ¹⁶⁰, D. Harada ⁵⁷, T. Harenberg ¹⁷⁴, S. Harkusha ³⁸, M.L. Harris ¹⁰⁵, Y.T. Harris ¹²⁹, J. Harrison ¹³, N.M. Harrison ¹²², P.F. Harrison ¹⁷⁰, N.M. Hartman ¹¹², N.M. Hartmann ¹¹¹, R.Z. Hasan ^{97,137}, Y. Hasegawa ¹⁴⁴, S. Hassan ¹⁷, R. Hauser ¹⁰⁹, C.M. Hawkes ²¹, R.J. Hawkings ³⁷, Y. Hayashi ¹⁵⁷, S. Hayashida ¹¹³, D. Hayden ¹⁰⁹, C. Hayes ¹⁰⁸, R.L. Hayes ¹¹⁷, C.P. Hays ¹²⁹, J.M. Hays ⁹⁶, H.S. Hayward ⁹⁴, F. He ^{63a}, M. He ^{14,114c}, Y. He ¹⁴¹, Y. He ⁴⁹, Y. He ⁹⁸, N.B. Heatley ⁹⁶, V. Hedberg ¹⁰⁰, A.L. Heggelund ¹²⁸, N.D. Hehir ^{96,*}, C. Heidegger ⁵⁵, K.K. Heidegger ⁵⁵, J. Heilman ³⁵, S. Heim ⁴⁹, T. Heim ^{18a}, J.G. Heinlein ¹³¹, J.J. Heinrich ¹²⁶, L. Heinrich ^{112,ac}, J. Hejbal ¹³⁴, A. Held ¹⁷³, S. Hellesund ¹⁷, C.M. Helling ¹⁶⁷, S. Hellman ^{48a,48b}, R.C.W. Henderson ⁹³, L. Henkelmann ³³, A.M. Henriques Correia ³⁷, H. Herde ¹⁰⁰, Y. Hernández Jiménez ¹⁴⁹, L.M. Herrmann ²⁵, T. Herrmann ⁵¹, G. Herten ⁵⁵, R. Hertenberger ¹¹¹, L. Hervas ³⁷, M.E. Hesping ¹⁰², N.P. Hessey ^{159a}, M. Hidaoui ^{36b}, N. Hidic ¹³⁶, E. Hill ¹⁵⁸, S.J. Hillier ²¹, J.R. Hinds ¹⁰⁹, F. Hinterkeuser ²⁵, M. Hirose ¹²⁷, S. Hirose ¹⁶⁰, D. Hirschbuehl ¹⁷⁴, T.G. Hitchings ¹⁰³, B. Hiti ⁹⁵, J. Hobbs ¹⁴⁹, R. Hobincu ^{28e}, N. Hod ¹⁷², M.C. Hodgkinson ¹⁴³, B.H. Hodgkinson ¹²⁹, A. Hoecker ³⁷, D.D. Hofer ¹⁰⁸, J. Hofer ⁴⁹, T. Holm ²⁵, M. Holzbock ¹¹², L.B.A.H. Hommels ³³, B.P. Honan ¹⁰³, J.J. Hong ⁶⁹, J. Hong ^{63c}, T.M. Hong ¹³², B.H. Hooberman ¹⁶⁵, W.H. Hopkins ⁶, M.C. Hoppesch ¹⁶⁵, Y. Horii ¹¹³, S. Hou ¹⁵², A.S. Howard ⁹⁵, J. Howarth ⁶⁰, J. Hoya ⁶, M. Hrabovsky ¹²⁵, A. Hrynevich ⁴⁹, T. Hryn'ova ⁴, P.J. Hsu ⁶⁶, S.-C. Hsu ¹⁴², T. Hsu ⁶⁷, M. Hu ^{18a}, Q. Hu ^{63a}, S. Huang ^{65b}, X. Huang ^{14,114c}, Y. Huang ¹⁴³, Y. Huang ¹⁰², Y. Huang ¹⁴, Z. Huang ¹⁰³, Z. Hubacek ¹³⁵, M. Huebner ²⁵, F. Huegging ²⁵, T.B. Huffman ¹²⁹, C.A. Hugli ⁴⁹, M. Huhtinen ³⁷, S.K. Huiberts ¹⁷, R. Hulsken ¹⁰⁶, N. Huseynov ^{12,g}, J. Huston ¹⁰⁹, J. Huth ⁶², R. Hyneman ¹⁴⁷, G. Iacobucci ⁵⁷, G. Iakovidis ³⁰, L. Iconomidou-Fayard ⁶⁷, J.P. Iddon ³⁷, P. Iengo ^{73a,73b}, R. Iguchi ¹⁵⁷, Y. Iiyama ¹⁵⁷, T. Iizawa ¹²⁹, Y. Ikegami ⁸⁵, N. Ilic ¹⁵⁸, H. Imam ^{36a}, M. Ince Lezki ⁵⁷, T. Ingebretsen Carlson ^{48a,48b}, J.M. Inglis ⁹⁶, G. Introzzi ^{74a,74b}, M. Iodice ^{78a}, V. Ippolito ^{76a,76b}, R.K. Irwin ⁹⁴, M. Ishino ¹⁵⁷, W. Islam ¹⁷³, C. Issever ^{19,49}, S. Istin ^{22a,ai}, H. Ito ¹⁷¹, R. Iuppa ^{79a,79b}, A. Ivina ¹⁷², J.M. Izen ⁴⁶, V. Izzo ^{73a}, P. Jacka ¹³⁴, P. Jackson ¹, C.S. Jagfeld ¹¹¹, G. Jain ^{159a}, P. Jain ⁴⁹, K. Jakobs ⁵⁵, T. Jakoubek ¹⁷², J. Jamieson ⁶⁰, W. Jang ¹⁵⁷, M. Javurkova ¹⁰⁵, P. Jawahar ¹⁰³, L. Jeanty ¹²⁶, J. Jejelava ^{153a,aa}, P. Jenni ^{55,f}, C.E. Jessiman ³⁵, C. Jia ^{63b}, J. Jia ¹⁴⁹, X. Jia ⁶², X. Jia ^{14,114c}, Z. Jia ^{114a}, C. Jiang ⁵³, S. Jiggins ⁴⁹, J. Jimenez Pena ¹³, S. Jin ^{114a}, A. Jinaru ^{28b}, O. Jinnouchi ¹⁴¹, P. Johansson ¹⁴³, K.A. Johns ⁷, J.W. Johnson ¹³⁹, D.M. Jones ¹⁵⁰, E. Jones ⁴⁹, P. Jones ³³, R.W.L. Jones ⁹³, T.J. Jones ⁹⁴, H.L. Joos ^{56,37}, R. Joshi ¹²², J. Jovicevic ¹⁶, X. Ju ^{18a}, J.J. Junggeburch ¹⁰⁵, T. Junkermann ^{64a}, A. Juste Rozas ^{13,t}, M.K. Juzek ⁸⁸, S. Kabana ^{140e}, A. Kaczmarska ⁸⁸, M. Kado ¹¹², H. Kagan ¹²², M. Kagan ¹⁴⁷, A. Kahn ¹³¹, C. Kahra ¹⁰², T. Kaji ¹⁵⁷, E. Kajomovitz ¹⁵⁴, N. Kakati ¹⁷², I. Kalaitzidou ⁵⁵, C.W. Kalderon ³⁰, N.J. Kang ¹³⁹, D. Kar ^{34g}, K. Karava ¹²⁹, M.J. Kareem ^{159b}, E. Karentzos ⁵⁵, O. Karkout ¹¹⁷, S.N. Karpov ³⁹, Z.M. Karpova ³⁹, V. Kartvelishvili ⁹³, A.N. Karyukhin ³⁸, E. Kasimi ¹⁵⁶, J. Katzy ⁴⁹, S. Kaur ³⁵, K. Kawade ¹⁴⁴, M.P. Kawale ¹²³, C. Kawamoto ⁸⁹, T. Kawamoto ^{63a}, E.F. Kay ³⁷, F.I. Kaya ¹⁶¹,







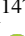

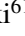
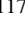
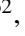






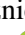
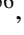




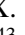

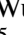




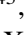





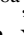



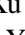




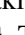
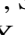
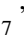



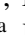





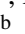

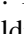
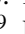








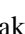

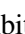










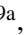

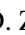


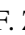

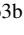




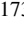
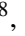

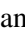

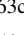

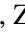

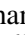

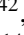
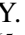
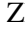
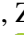

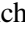
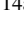
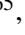
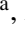

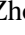
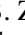
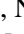
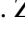
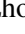


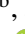
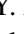
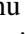
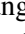
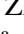




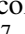
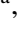


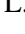











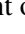

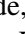
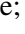


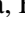
S. Kazakos ¹⁰⁹, V.F. Kazanin ³⁸, Y. Ke ¹⁴⁹, J.M. Keaveney ^{34a}, R. Keeler ¹⁶⁸, G.V. Kehris ⁶²,
 J.S. Keller ³⁵, A.S. Kelly ⁹⁸, J.J. Kempster ¹⁵⁰, P.D. Kennedy ¹⁰², O. Kepka ¹³⁴, B.P. Kerridge ¹³⁷,
 S. Kersten ¹⁷⁴, B.P. Kerševan ⁹⁵, L. Keszeghova ^{29a}, S. Ketabchi Haghighat ¹⁵⁸, R.A. Khan ¹³²,
 A. Khanov ¹²⁴, A.G. Kharlamov ³⁸, T. Kharlamova ³⁸, E.E. Khoda ¹⁴², M. Kholodenko ³⁸,
 T.J. Khoo ¹⁹, G. Khorialuli ¹⁶⁹, J. Khubua ^{153b,*}, Y.A.R. Khwaira ¹³⁰, B. Kibirige ^{34g}, D. Kim ⁶,
 D.W. Kim ^{48a,48b}, Y.K. Kim ⁴⁰, N. Kimura ⁹⁸, M.K. Kingston ⁵⁶, A. Kirchhoff ⁵⁶, C. Kirfel ²⁵,
 F. Kirfel ²⁵, J. Kirk ¹³⁷, A.E. Kiryunin ¹¹², C. Kitsaki ¹⁰, O. Kivernyk ²⁵, M. Klassen ¹⁶¹,
 C. Klein ³⁵, L. Klein ¹⁶⁹, M.H. Klein ⁴⁵, S.B. Klein ⁵⁷, U. Klein ⁹⁴, P. Klimek ³⁷,
 A. Klimentov ³⁰, T. Klioutchnikova ³⁷, P. Kluit ¹¹⁷, S. Kluth ¹¹², E. Kneringer ⁸⁰,
 T.M. Knight ¹⁵⁸, A. Knue ⁵⁰, R. Kobayashi ⁸⁹, D. Kobylanski ¹⁷², S.F. Koch ¹²⁹,
 M. Kocian ¹⁴⁷, P. Kodyš ¹³⁶, D.M. Koeck ¹²⁶, P.T. Koenig ²⁵, T. Koffas ³⁵, O. Kolay ⁵¹,
 I. Koletsou ⁴, T. Komarek ⁸⁸, K. Köneke ⁵⁵, A.X.Y. Kong ¹, T. Kono ¹²¹, N. Konstantinidis ⁹⁸,
 P. Kontaxakis ⁵⁷, B. Konya ¹⁰⁰, R. Kopeliansky ⁴², S. Koperny ^{87a}, K. Korcyl ⁸⁸,
 K. Kordas ^{156,d}, A. Korn ⁹⁸, S. Korn ⁵⁶, I. Korolkov ¹³, N. Korotkova ³⁸, B. Kortman ¹¹⁷,
 O. Kortner ¹¹², S. Kortner ¹¹², W.H. Kostecka ¹¹⁸, V.V. Kostyukhin ¹⁴⁵, A. Kotsokechagia ¹³⁸,
 A. Kotwal ⁵², A. Koulouris ³⁷, A. Kourkoumeli-Charalampidi ^{74a,74b}, C. Kourkoumelis ⁹,
 E. Kourlitis ^{112,ac}, O. Kovanda ¹²⁶, R. Kowalewski ¹⁶⁸, W. Kozanecki ¹³⁸, A.S. Kozhin ³⁸,
 V.A. Kramarenko ³⁸, G. Kramberger ⁹⁵, P. Kramer ¹⁰², M.W. Krasny ¹³⁰, A. Krasznahorkay ³⁷,
 A.C. Kraus ¹¹⁸, J.W. Kraus ¹⁷⁴, J.A. Kremer ⁴⁹, T. Kresse ⁵¹, L. Kretschmann ¹⁷⁴,
 J. Kretschmar ⁹⁴, K. Kreul ¹⁹, P. Krieger ¹⁵⁸, S. Krishnamurthy ¹⁰⁵, M. Krivos ¹³⁶,
 K. Krizka ²¹, K. Kroeninger ⁵⁰, H. Kroha ¹¹², J. Kroll ¹³⁴, J. Kroll ¹³¹, K.S. Krowpman ¹⁰⁹,
 U. Kruchonak ³⁹, H. Krüger ²⁵, N. Krumnack ⁸², M.C. Kruse ⁵², O. Kuchinskaia ³⁸, S. Kuday ^{3a},
 S. Kuehn ³⁷, R. Kuesters ⁵⁵, T. Kuhl ⁴⁹, V. Kukhtin ³⁹, Y. Kulchitsky ^{38,a}, S. Kuleshov ^{140d,140b},
 M. Kumar ^{34g}, N. Kumari ⁴⁹, P. Kumari ^{159b}, A. Kupco ¹³⁴, T. Kupfer ⁵⁰, A. Kupich ³⁸,
 O. Kuprash ⁵⁵, H. Kurashige ⁸⁶, L.L. Kurchaninov ^{159a}, O. Kurdysh ⁶⁷, Y.A. Kurochkin ³⁸,
 A. Kurova ³⁸, M. Kuze ¹⁴¹, A.K. Kvam ¹⁰⁵, J. Kvitá ¹²⁵, T. Kwan ¹⁰⁶, N.G. Kyriacou ¹⁰⁸,
 L.A.O. Laatu ¹⁰⁴, C. Lacasta ¹⁶⁶, F. Lacava ^{76a,76b}, H. Lacker ¹⁹, D. Lacour ¹³⁰, N.N. Lad ⁹⁸,
 E. Ladygin ³⁹, A. Lafarge ⁴¹, B. Laforge ¹³⁰, T. Lagouri ¹⁷⁵, F.Z. Lahbabi ^{36a}, S. Lai ⁵⁶,
 J.E. Lambert ¹⁶⁸, S. Lammers ⁶⁹, W. Lampl ⁷, C. Lampoudis ^{156,d}, G. Lamprinoudis ¹⁰²,
 A.N. Lancaster ¹¹⁸, E. Lançon ³⁰, U. Landgraf ⁵⁵, M.P.J. Landon ⁹⁶, V.S. Lang ⁵⁵,
 O.K.B. Langrekken ¹²⁸, A.J. Lankford ¹⁶², F. Lanni ³⁷, K. Lantzsch ²⁵, A. Lanza ^{74a},
 J.F. Laporte ¹³⁸, T. Lari ^{72a}, F. Lasagni Manghi ^{24b}, M. Lassnig ³⁷, V. Latonova ¹³⁴,
 A. Laurier ¹⁵⁴, S.D. Lawlor ¹⁴³, Z. Lawrence ¹⁰³, R. Lazaridou ¹⁷⁰, M. Lazzaroni ^{72a,72b}, B. Le ¹⁰³,
 E.M. Le Boulicaut ⁵², L.T. Le Pottier ^{18a}, B. Leban ^{24b,24a}, A. Lebedev ⁸², M. LeBlanc ¹⁰³,
 F. Ledroit-Guillon ⁶¹, S.C. Lee ¹⁵², S. Lee ^{48a,48b}, T.F. Lee ⁹⁴, L.L. Leeuw ^{34c}, H.P. Lefebvre ⁹⁷,
 M. Lefebvre ¹⁶⁸, C. Leggett ^{18a}, G. Lehmann Miotto ³⁷, M. Leigh ⁵⁷, W.A. Leight ¹⁰⁵,
 W. Leinonen ¹¹⁶, A. Leisos ^{156,s}, M.A.L. Leite ^{84c}, C.E. Leitgeb ¹⁹, R. Leitner ¹³⁶,
 K.J.C. Leney ⁴⁵, T. Lenz ²⁵, S. Leone ^{75a}, C. Leonidopoulos ⁵³, A. Leopold ¹⁴⁸, R. Les ¹⁰⁹,
 C.G. Lester ³³, M. Levchenko ³⁸, J. Levêque ⁴, L.J. Levinson ¹⁷², G. Levrini ^{24b,24a},
 M.P. Lewicki ⁸⁸, C. Lewis ¹⁴², D.J. Lewis ⁴, A. Li ⁵, B. Li ^{63b}, C. Li ^{63a}, C-Q. Li ¹¹², H. Li ^{63a},
 H. Li ^{63b}, H. Li ^{114a}, H. Li ¹⁵, H. Li ^{63b}, J. Li ^{63c}, K. Li ¹⁴², L. Li ^{63c}, M. Li ^{14,114c},
 S. Li ^{14,114c}, S. Li ^{63d,63c}, T. Li ⁵, X. Li ¹⁰⁶, Z. Li ¹²⁹, Z. Li ¹⁵⁷, Z. Li ^{14,114c}, S. Liang ^{14,114c},
 Z. Liang ¹⁴, M. Liberatore ¹³⁸, B. Liberti ^{77a}, K. Lie ^{65c}, J. Lieber Marin ^{84e}, H. Lien ⁶⁹,
 H. Lin ¹⁰⁸, K. Lin ¹⁰⁹, R.E. Lindley ⁷, J.H. Lindon ², J. Ling ⁶², E. Lipeles ¹³¹,
 A. Lipniacka ¹⁷, A. Lister ¹⁶⁷, J.D. Little ⁶⁹, B. Liu ¹⁴, B.X. Liu ^{114b}, D. Liu ^{63d,63c},
 E.H.L. Liu ²¹, J.B. Liu ^{63a}, J.K.K. Liu ³³, K. Liu ^{63d}, K. Liu ^{63d,63c}, M. Liu ^{63a}, M.Y. Liu ^{63a},
 P. Liu ¹⁴, Q. Liu ^{63d,142,63c}, X. Liu ^{63a}, X. Liu ^{63b}, Y. Liu ^{114b,114c}, Y.L. Liu ^{63b}, Y.W. Liu ^{63a},

J. Llorente Merino ¹⁴⁶, S.L. Lloyd ⁹⁶, E.M. Lobodzinska ⁴⁹, P. Loch ⁷, T. Lohse ¹⁹,
 K. Lohwasser ¹⁴³, E. Loiacono ⁴⁹, M. Lokajicek ^{134,*}, J.D. Lomas ²¹, J.D. Long ¹⁶⁵,
 I. Longarini ¹⁶², R. Longo ¹⁶⁵, I. Lopez Paz ⁶⁸, A. Lopez Solis ⁴⁹, N. Lorenzo Martinez ⁴,
 A.M. Lory ¹¹¹, M. Losada ^{119a}, G. Löschcke Centeno ¹⁵⁰, O. Loseva ³⁸, X. Lou ^{48a,48b},
 X. Lou ^{14,114c}, A. Lounis ⁶⁷, P.A. Love ⁹³, G. Lu ^{14,114c}, M. Lu ⁶⁷, S. Lu ¹³¹, Y.J. Lu ⁶⁶,
 H.J. Lubatti ¹⁴², C. Luci ^{76a,76b}, F.L. Lucio Alves ^{114a}, F. Luehring ⁶⁹, I. Luise ¹⁴⁹,
 O. Lukianchuk ⁶⁷, O. Lundberg ¹⁴⁸, B. Lund-Jensen ^{148,*}, N.A. Luongo ⁶, M.S. Lutz ³⁷,
 A.B. Lux ²⁶, D. Lynn ³⁰, R. Lysak ¹³⁴, E. Lytken ¹⁰⁰, V. Lyubushkin ³⁹, T. Lyubushkina ³⁹,
 M.M. Lyukova ¹⁴⁹, M.Firdaus M. Soberi ⁵³, H. Ma ³⁰, K. Ma ^{63a}, L.L. Ma ^{63b}, W. Ma ^{63a},
 Y. Ma ¹²⁴, J.C. MacDonald ¹⁰², P.C. Machado De Abreu Farias ^{84e}, R. Madar ⁴¹, T. Madula ⁹⁸,
 J. Maeda ⁸⁶, T. Maeno ³⁰, H. Maguire ¹⁴³, V. Maiboroda ¹³⁸, A. Maio ^{133a,133b,133d}, K. Maj ^{87a},
 O. Majersky ⁴⁹, S. Majewski ¹²⁶, N. Makovec ⁶⁷, V. Maksimovic ¹⁶, B. Malaescu ¹³⁰,
 Pa. Malecki ⁸⁸, V.P. Maleev ³⁸, F. Malek ^{61,n}, M. Mali ⁹⁵, D. Malito ⁹⁷, U. Mallik ^{81,*},
 S. Maltezos ¹⁰, S. Malyukov ³⁹, J. Mamuzic ¹³, G. Mancini ⁵⁴, M.N. Mancini ²⁷, G. Manco ^{74a,74b},
 J.P. Mandalia ⁹⁶, S.S. Mandarray ¹⁵⁰, I. Mandić ⁹⁵, L. Manhaes de Andrade Filho ^{84a},
 I.M. Maniatis ¹⁷², J. Manjarres Ramos ⁹¹, D.C. Mankad ¹⁷², A. Mann ¹¹¹, S. Manzoni ³⁷,
 L. Mao ^{63c}, X. Mapekula ^{34c}, A. Marantis ^{156,s}, G. Marchiori ⁵, M. Marcisovsky ¹³⁴,
 C. Marcon ^{72a}, M. Marinescu ²¹, S. Marium ⁴⁹, M. Marjanovic ¹²³, A. Markhoos ⁵⁵,
 M. Markovitch ⁶⁷, E.J. Marshall ⁹³, Z. Marshall ^{18a}, S. Marti-Garcia ¹⁶⁶, J. Martin ⁹⁸,
 T.A. Martin ¹³⁷, V.J. Martin ⁵³, B. Martin dit Latour ¹⁷, L. Martinelli ^{76a,76b}, M. Martinez ^{13,t},
 P. Martinez Agullo ¹⁶⁶, V.I. Martinez Outschoorn ¹⁰⁵, P. Martinez Suarez ¹³, S. Martin-Haugh ¹³⁷,
 G. Martinovicova ¹³⁶, V.S. Martoiu ^{28b}, A.C. Martyniuk ⁹⁸, A. Marzin ³⁷, D. Mascione ^{79a,79b},
 L. Masetti ¹⁰², T. Mashimo ¹⁵⁷, J. Masik ¹⁰³, A.L. Maslennikov ³⁸, P. Massarotti ^{73a,73b},
 P. Mastrandrea ^{75a,75b}, A. Mastroberardino ^{44b,44a}, T. Masubuchi ¹⁵⁷, T. Mathisen ¹⁶⁴,
 J. Matousek ¹³⁶, N. Matsuzawa ¹⁵⁷, J. Maurer ^{28b}, A.J. Maury ⁶⁷, B. Maček ⁹⁵, D.A. Maximov ³⁸,
 A.E. May ¹⁰³, R. Mazini ¹⁵², I. Maznas ¹¹⁸, M. Mazza ¹⁰⁹, S.M. Mazza ¹³⁹, E. Mazzeo ^{72a,72b},
 C. Mc Ginn ³⁰, J.P. Mc Gowan ¹⁶⁸, S.P. Mc Kee ¹⁰⁸, C.C. McCracken ¹⁶⁷, E.F. McDonald ¹⁰⁷,
 A.E. McDougall ¹¹⁷, J.A. Mcfayden ¹⁵⁰, R.P. McGovern ¹³¹, R.P. Mckenzie ^{34g},
 T.C. Mclachlan ⁴⁹, D.J. Mclaughlin ⁹⁸, S.J. McMahan ¹³⁷, C.M. Mcpartland ⁹⁴,
 R.A. McPherson ^{168,x}, S. Mehlhase ¹¹¹, A. Mehta ⁹⁴, D. Melini ¹⁶⁶, B.R. Mellado Garcia ^{34g},
 A.H. Melo ⁵⁶, F. Meloni ⁴⁹, A.M. Mendes Jacques Da Costa ¹⁰³, H.Y. Meng ¹⁵⁸, L. Meng ⁹³,
 S. Menke ¹¹², M. Mentink ³⁷, E. Meoni ^{44b,44a}, G. Mercado ¹¹⁸, S. Merianos ¹⁵⁶,
 C. Merlassino ^{70a,70c}, L. Merola ^{73a,73b}, C. Meroni ^{72a,72b}, J. Metcalfe ⁶, A.S. Mete ⁶,
 E. Meuser ¹⁰², C. Meyer ⁶⁹, J-P. Meyer ¹³⁸, R.P. Middleton ¹³⁷, L. Mijović ⁵³,
 G. Mikenberg ¹⁷², M. Migestikova ¹³⁴, M. Mikuž ⁹⁵, H. Mildner ¹⁰², A. Milic ³⁷,
 D.W. Miller ⁴⁰, E.H. Miller ¹⁴⁷, L.S. Miller ³⁵, A. Milov ¹⁷², D.A. Milstead ^{48a,48b}, T. Min ^{114a},
 A.A. Minaenko ³⁸, I.A. Minashvili ^{153b}, L. Mince ⁶⁰, A.I. Mincer ¹²⁰, B. Mindur ^{87a},
 M. Mineev ³⁹, Y. Mino ⁸⁹, L.M. Mir ¹³, M. Miralles Lopez ⁶⁰, M. Mironova ^{18a}, A. Mishima ¹⁵⁷,
 M.C. Missio ¹¹⁶, A. Mitra ¹⁷⁰, V.A. Mitsou ¹⁶⁶, Y. Mitsumori ¹¹³, O. Miu ¹⁵⁸,
 P.S. Miyagawa ⁹⁶, T. Mkrtychyan ^{64a}, M. Mlinarevic ⁹⁸, T. Mlinarevic ⁹⁸, M. Mlynarikova ³⁷,
 S. Mobius ²⁰, P. Mogg ¹¹¹, M.H. Mohamed Farook ¹¹⁵, A.F. Mohammed ^{14,114c}, S. Mohapatra ⁴²,
 G. Mokgatitwane ^{34g}, L. Moleri ¹⁷², B. Mondal ¹⁴⁵, S. Mondal ¹³⁵, K. Mönig ⁴⁹,
 E. Monnier ¹⁰⁴, L. Monsonis Romero ¹⁶⁶, J. Montejo Berlingen ¹³, M. Montella ¹²²,
 F. Montekali ^{78a,78b}, F. Monticelli ⁹², S. Monzani ^{70a,70c}, N. Morange ⁶⁷,
 A.L. Moreira De Carvalho ⁴⁹, M. Moreno Llácer ¹⁶⁶, C. Moreno Martinez ⁵⁷, P. Morettini ^{58b},
 S. Morgenstern ³⁷, M. Morii ⁶², M. Morinaga ¹⁵⁷, F. Morodei ^{76a,76b}, L. Morvaj ³⁷,
 P. Moschovakos ³⁷, B. Moser ³⁷, M. Mosidze ^{153b}, T. Moskalets ⁴⁵, P. Moskvitina ¹¹⁶,

J. Moss ^{32,k}, P. Moszkowicz ^{87a}, A. Moussa ^{36d}, E.J.W. Moyse ¹⁰⁵, O. Mtintsilana ^{34g}, S. Muanza ¹⁰⁴, J. Mueller ¹³², D. Muenstermann ⁹³, R. Müller ³⁷, G.A. Mullier ¹⁶⁴, A.J. Mullin ³³, J.J. Mullin ¹³¹, D.P. Mungo ¹⁵⁸, D. Munoz Perez ¹⁶⁶, F.J. Munoz Sanchez ¹⁰³, M. Murin ¹⁰³, W.J. Murray ^{170,137}, M. Muškinja ⁹⁵, C. Mwewa ³⁰, A.G. Myagkov ^{38,a}, A.J. Myers ⁸, G. Myers ¹⁰⁸, M. Myska ¹³⁵, B.P. Nachman ^{18a}, O. Nackenhorst ⁵⁰, K. Nagai ¹²⁹, K. Nagano ⁸⁵, J.L. Nagle ^{30,ag}, E. Nagy ¹⁰⁴, A.M. Nairz ³⁷, Y. Nakahama ⁸⁵, K. Nakamura ⁸⁵, K. Nakkalil ⁵, H. Nanjo ¹²⁷, E.A. Narayanan ¹¹⁵, I. Naryshkin ³⁸, L. Nasella ^{72a,72b}, M. Naseri ³⁵, S. Nasri ^{119b}, C. Nass ²⁵, G. Navarro ^{23a}, J. Navarro-Gonzalez ¹⁶⁶, R. Nayak ¹⁵⁵, A. Nayaz ¹⁹, P.Y. Nechaeva ³⁸, S. Nechaeva ^{24b,24a}, F. Nechansky ⁴⁹, L. Nedic ¹²⁹, T.J. Neep ²¹, A. Negri ^{74a,74b}, M. Negrini ^{24b}, C. Nellist ¹¹⁷, C. Nelson ¹⁰⁶, K. Nelson ¹⁰⁸, S. Nemecek ¹³⁴, M. Nessi ^{37,h}, M.S. Neubauer ¹⁶⁵, F. Neuhaus ¹⁰², J. Neundorf ⁴⁹, P.R. Newman ²¹, C.W. Ng ¹³², Y.W.Y. Ng ⁴⁹, B. Ngair ^{119a}, H.D.N. Nguyen ¹¹⁰, R.B. Nickerson ¹²⁹, R. Nicolaidou ¹³⁸, J. Nielsen ¹³⁹, M. Niemeyer ⁵⁶, J. Niermann ⁵⁶, N. Nikiforou ³⁷, V. Nikolaenko ^{38,a}, I. Nikolic-Audit ¹³⁰, K. Nikolopoulos ²¹, P. Nilsson ³⁰, I. Ninca ⁴⁹, G. Ninio ¹⁵⁵, A. Nisati ^{76a}, N. Nishu ², R. Nisius ¹¹², J-E. Nitschke ⁵¹, E.K. Nkadimeng ^{34g}, T. Nobe ¹⁵⁷, T. Nommensen ¹⁵¹, M.B. Norfolk ¹⁴³, B.J. Norman ³⁵, M. Noury ^{36a}, J. Novak ⁹⁵, T. Novak ⁹⁵, L. Novotny ¹³⁵, R. Novotny ¹¹⁵, L. Nozka ¹²⁵, K. Ntekas ¹⁶², N.M.J. Nunes De Moura Junior ^{84b}, J. Ocariz ¹³⁰, A. Ochi ⁸⁶, I. Ochoa ^{133a}, S. Oerdek ^{49,u}, J.T. Offermann ⁴⁰, A. Ogrodnik ¹³⁶, A. Oh ¹⁰³, C.C. Ohm ¹⁴⁸, H. Oide ⁸⁵, R. Oishi ¹⁵⁷, M.L. Ojeda ⁴⁹, Y. Okumura ¹⁵⁷, L.F. Oleiro Seabra ^{133a}, I. Oleksiyuk ⁵⁷, S.A. Olivares Pino ^{140d}, G. Oliveira Correa ¹³, D. Oliveira Damazio ³⁰, D. Oliveira Goncalves ^{84a}, J.L. Oliver ¹⁶², Ö.O. Öncel ⁵⁵, A.P. O'Neill ²⁰, A. Onofre ^{133a,133e}, P.U.E. Onyisi ¹¹, M.J. Oreglia ⁴⁰, G.E. Orellana ⁹², D. Orestano ^{78a,78b}, N. Orlando ¹³, R.S. Orr ¹⁵⁸, L.M. Osojnak ¹³¹, R. Ospanov ^{63a}, G. Otero y Garzon ³¹, H. Otono ⁹⁰, P.S. Ott ^{64a}, G.J. Ottino ^{18a}, M. Ouchrif ^{36d}, F. Ould-Saada ¹²⁸, T. Ovsiannikova ¹⁴², M. Owen ⁶⁰, R.E. Owen ¹³⁷, V.E. Ozcan ^{22a}, F. Ozturk ⁸⁸, N. Ozturk ⁸, S. Ozturk ⁸³, H.A. Pacey ¹²⁹, A. Pacheco Pages ¹³, C. Padilla Aranda ¹³, G. Padovano ^{76a,76b}, S. Pagan Griso ^{18a}, G. Palacino ⁶⁹, A. Palazzo ^{71a,71b}, J. Pampel ²⁵, J. Pan ¹⁷⁵, T. Pan ^{65a}, D.K. Panchal ¹¹, C.E. Pandini ¹¹⁷, J.G. Panduro Vazquez ¹³⁷, H.D. Pandya ¹, H. Pang ¹⁵, P. Pani ⁴⁹, G. Panizzo ^{70a,70c}, L. Panwar ¹³⁰, L. Paolozzi ⁵⁷, S. Parajuli ¹⁶⁵, A. Paramonov ⁶, C. Paraskevopoulos ⁵⁴, D. Paredes Hernandez ^{65b}, A. Pareti ^{74a,74b}, K.R. Park ⁴², T.H. Park ¹⁵⁸, M.A. Parker ³³, F. Parodi ^{58b,58a}, E.W. Parrish ¹¹⁸, V.A. Parrish ⁵³, J.A. Parsons ⁴², U. Parzefall ⁵⁵, B. Pascual Dias ¹¹⁰, L. Pascual Dominguez ¹⁰¹, E. Pasqualucci ^{76a}, S. Passaggio ^{58b}, F. Pastore ⁹⁷, P. Patel ⁸⁸, U.M. Patel ⁵², J.R. Pater ¹⁰³, T. Pauly ³⁷, C.I. Pazos ¹⁶¹, J. Pearkes ¹⁴⁷, M. Pedersen ¹²⁸, R. Pedro ^{133a}, S.V. Peleganchuk ³⁸, O. Penc ³⁷, E.A. Pender ⁵³, G.D. Penn ¹⁷⁵, K.E. Penski ¹¹¹, M. Penzin ³⁸, B.S. Peralva ^{84d}, A.P. Pereira Peixoto ¹⁴², L. Pereira Sanchez ¹⁴⁷, D.V. Perepelitsa ^{30,ag}, G. Perera ¹⁰⁵, E. Perez Codina ^{159a}, M. Perganti ¹⁰, H. Pernegger ³⁷, S. Perrella ^{76a,76b}, O. Perrin ⁴¹, K. Peters ⁴⁹, R.F.Y. Peters ¹⁰³, B.A. Petersen ³⁷, T.C. Petersen ⁴³, E. Petit ¹⁰⁴, V. Petousis ¹³⁵, C. Petridou ^{156,d}, T. Petru ¹³⁶, A. Petrukhin ¹⁴⁵, M. Pettee ^{18a}, A. Petukhov ³⁸, K. Petukhova ³⁷, R. Pezoa ^{140f}, L. Pezzotti ³⁷, G. Pezzullo ¹⁷⁵, T.M. Pham ¹⁷³, T. Pham ¹⁰⁷, P.W. Phillips ¹³⁷, G. Piacquadio ¹⁴⁹, E. Pianori ^{18a}, F. Piazza ¹²⁶, R. Piegai ³¹, D. Pietreanu ^{28b}, A.D. Pilkington ¹⁰³, M. Pinamonti ^{70a,70c}, J.L. Pinfeld ², B.C. Pinheiro Pereira ^{133a}, A.E. Pinto Pinoargote ^{138,138}, L. Pintucci ^{70a,70c}, K.M. Piper ¹⁵⁰, A. Pirttikoski ⁵⁷, D.A. Pizzi ³⁵, L. Pizzimento ^{65b}, A. Pizzini ¹¹⁷, M.-A. Pleier ³⁰, V. Pleskot ¹³⁶, E. Plotnikova ³⁹, G. Poddar ⁹⁶, R. Poettgen ¹⁰⁰, L. Poggioli ¹³⁰, I. Pokharel ⁵⁶, S. Polacek ¹³⁶, G. Polesello ^{74a}, A. Poley ^{146,159a}, A. Polini ^{24b}, C.S. Pollard ¹⁷⁰, Z.B. Pollock ¹²², E. Pompa Pacchi ^{76a,76b}, N.I. Pond ⁹⁸, D. Ponomarenko ¹¹⁶, L. Pontecorvo ³⁷, S. Popa ^{28a}, G.A. Popeneciu ^{28d},

A. Poreba ³⁷, D.M. Portillo Quintero ^{159a}, S. Pospisil ¹³⁵, M.A. Postill ¹⁴³, P. Postolache ^{28c},
 K. Potamianos ¹⁷⁰, P.A. Potepa ^{87a}, I.N. Potrap ³⁹, C.J. Potter ³³, H. Potti ¹⁵¹, J. Poveda ¹⁶⁶,
 M.E. Pozo Astigarraga ³⁷, A. Prades Ibanez ¹⁶⁶, J. Pretel ⁵⁵, D. Price ¹⁰³, M. Primavera ^{71a},
 M.A. Principe Martin ¹⁰¹, R. Privara ¹²⁵, T. Procter ⁶⁰, M.L. Proffitt ¹⁴², N. Proklova ¹³¹,
 K. Prokofiev ^{65c}, G. Proto ¹¹², J. Proudfoot ⁶, M. Przybycien ^{87a}, W.W. Przygoda ^{87b},
 A. Psallidas ⁴⁷, J.E. Puddefoot ¹⁴³, D. Pudzha ⁵⁵, D. Pyatiizbyantseva ³⁸, J. Qian ¹⁰⁸,
 D. Qichen ¹⁰³, Y. Qin ¹³, T. Qiu ⁵³, A. Quadt ⁵⁶, M. Queitsch-Maitland ¹⁰³, G. Quetant ⁵⁷,
 R.P. Quinn ¹⁶⁷, G. Rabanal Bolanos ⁶², D. Rafanoharana ⁵⁵, F. Raffaelli ^{77a,77b}, F. Ragusa ^{72a,72b},
 J.L. Rainbolt ⁴⁰, J.A. Raine ⁵⁷, S. Rajagopalan ³⁰, E. Ramakoti ³⁸, I.A. Ramirez-Berend ³⁵,
 K. Ran ^{49,114c}, D.S. Rankin ¹³¹, N.P. Rapheeha ^{34g}, H. Rasheed ^{28b}, V. Raskina ¹³⁰,
 D.F. Rassloff ^{64a}, A. Rastogi ^{18a}, S. Rave ¹⁰², S. Ravera ^{58b,58a}, B. Ravina ⁵⁶, I. Ravinovich ¹⁷²,
 M. Raymond ³⁷, A.L. Read ¹²⁸, N.P. Readioff ¹⁴³, D.M. Rebutzi ^{74a,74b}, G. Redlinger ³⁰,
 A.S. Reed ¹¹², K. Reeves ²⁷, J.A. Reidelsturz ¹⁷⁴, D. Reikher ¹⁵⁵, A. Rej ⁵⁰, C. Rembser ³⁷,
 M. Renda ^{28b}, F. Renner ⁴⁹, A.G. Rennie ¹⁶², A.L. Rescia ⁴⁹, S. Resconi ^{72a},
 M. Ressegotti ^{58b,58a}, S. Rettie ³⁷, J.G. Reyes Rivera ¹⁰⁹, E. Reynolds ^{18a}, O.L. Rezanova ³⁸,
 P. Reznicek ¹³⁶, H. Riani ^{36d}, N. Ribaric ⁹³, E. Ricci ^{79a,79b}, R. Richter ¹¹², S. Richter ^{48a,48b},
 E. Richter-Was ^{87b}, M. Ridel ¹³⁰, S. Ridouani ^{36d}, P. Rieck ¹²⁰, P. Riedler ³⁷, E.M. Riefel ^{48a,48b},
 J.O. Rieger ¹¹⁷, M. Rijssenbeek ¹⁴⁹, M. Rimoldi ³⁷, L. Rinaldi ^{24b,24a}, P. Rincke ^{56,164},
 T.T. Rinn ³⁰, M.P. Rinnagel ¹¹¹, G. Ripellino ¹⁶⁴, I. Riu ¹³, J.C. Rivera Vergara ¹⁶⁸,
 F. Rizatdinova ¹²⁴, E. Rizvi ⁹⁶, B.R. Roberts ^{18a}, S.H. Robertson ^{106,x}, D. Robinson ³³,
 C.M. Robles Gajardo ^{140f}, M. Robles Manzano ¹⁰², A. Robson ⁶⁰, A. Rocchi ^{77a,77b}, C. Roda ^{75a,75b},
 S. Rodriguez Bosca ³⁷, Y. Rodriguez Garcia ^{23a}, A. Rodriguez Rodriguez ⁵⁵,
 A.M. Rodríguez Vera ¹¹⁸, S. Roe ³⁷, J.T. Roemer ³⁷, A.R. Roepe-Gier ¹³⁹, O. Røhne ¹²⁸,
 R.A. Rojas ¹⁰⁵, C.P.A. Roland ¹³⁰, J. Roloff ³⁰, A. Romaniouk ³⁸, E. Romano ^{74a,74b},
 M. Romano ^{24b}, A.C. Romero Hernandez ¹⁶⁵, N. Rompotis ⁹⁴, L. Roos ¹³⁰, S. Rosati ^{76a},
 B.J. Rosser ⁴⁰, E. Rossi ¹²⁹, E. Rossi ^{73a,73b}, L.P. Rossi ⁶², L. Rossini ⁵⁵, R. Rosten ¹²²,
 M. Rotaru ^{28b}, B. Rottler ⁵⁵, C. Rougier ⁹¹, D. Rousseau ⁶⁷, D. Rousso ⁴⁹, A. Roy ¹⁶⁵,
 S. Roy-Garand ¹⁵⁸, A. Rozanov ¹⁰⁴, Z.M.A. Rozario ⁶⁰, Y. Rozen ¹⁵⁴, A. Rubio Jimenez ¹⁶⁶,
 A.J. Ruby ⁹⁴, V.H. Ruelas Rivera ¹⁹, T.A. Ruggeri ¹, A. Ruggiero ¹²⁹, A. Ruiz-Martinez ¹⁶⁶,
 A. Rummler ³⁷, Z. Rurikova ⁵⁵, N.A. Rusakovich ³⁹, H.L. Russell ¹⁶⁸, G. Russo ^{76a,76b},
 J.P. Rutherford ⁷, S. Rutherford Colmenares ³³, M. Rybar ¹³⁶, E.B. Rye ¹²⁸, A. Ryzhov ⁴⁵,
 J.A. Sabater Iglesias ⁵⁷, P. Sabatini ¹⁶⁶, H.F.W. Sadrozinski ¹³⁹, F. Safai Tehrani ^{76a},
 B. Safarzadeh Samani ¹³⁷, S. Saha ¹, M. Sahinsoy ¹¹², A. Saibel ¹⁶⁶, M. Saimpert ¹³⁸,
 M. Saito ¹⁵⁷, T. Saito ¹⁵⁷, A. Sala ^{72a,72b}, D. Salamani ³⁷, A. Salnikov ¹⁴⁷, J. Salt ¹⁶⁶,
 A. Salvador Salas ¹⁵⁵, D. Salvatore ^{44b,44a}, F. Salvatore ¹⁵⁰, A. Salzburger ³⁷, D. Sammel ⁵⁵,
 E. Sampson ⁹³, D. Sampsonidis ^{156,d}, D. Sampsonidou ¹²⁶, J. Sánchez ¹⁶⁶,
 V. Sanchez Sebastian ¹⁶⁶, H. Sandaker ¹²⁸, C.O. Sander ⁴⁹, J.A. Sandesara ¹⁰⁵, M. Sandhoff ¹⁷⁴,
 C. Sandoval ^{23b}, L. Sanfilippo ^{64a}, D.P.C. Sankey ¹³⁷, T. Sano ⁸⁹, A. Sansoni ⁵⁴, L. Santi ^{37,76b},
 C. Santoni ⁴¹, H. Santos ^{133a,133b}, A. Santra ¹⁷², E. Sanzani ^{24b,24a}, K.A. Saoucha ¹⁶³,
 J.G. Saraiva ^{133a,133d}, J. Sardain ⁷, O. Sasaki ⁸⁵, K. Sato ¹⁶⁰, C. Sauer ^{64b}, E. Sauvan ⁴,
 P. Savard ^{158,ae}, R. Sawada ¹⁵⁷, C. Sawyer ¹³⁷, L. Sawyer ⁹⁹, C. Sbarra ^{24b}, A. Sbrizzi ^{24b,24a},
 T. Scanlon ⁹⁸, J. Schaarschmidt ¹⁴², U. Schäfer ¹⁰², A.C. Schaffer ^{67,45}, D. Schaile ¹¹¹,
 R.D. Schamberger ¹⁴⁹, C. Scharf ¹⁹, M.M. Schefer ²⁰, V.A. Schegelsky ³⁸, D. Scheirich ¹³⁶,
 M. Schernau ¹⁶², C. Scheulen ⁵⁶, C. Schiavi ^{58b,58a}, M. Schioppa ^{44b,44a}, B. Schlag ¹⁴⁷,
 K.E. Schleicher ⁵⁵, S. Schlenker ³⁷, J. Schmeing ¹⁷⁴, M.A. Schmidt ¹⁷⁴, K. Schmieden ¹⁰²,
 C. Schmitt ¹⁰², N. Schmitt ¹⁰², S. Schmitt ⁴⁹, L. Schoeffel ¹³⁸, A. Schoening ^{64b},
 P.G. Scholer ³⁵, E. Schopf ¹²⁹, M. Schott ²⁵, J. Schovancova ³⁷, S. Schramm ⁵⁷, T. Schroer ⁵⁷,

H-C. Schultz-Coulon ^{64a}, M. Schumacher ⁵⁵, B.A. Schumm ¹³⁹, Ph. Schune ¹³⁸, A.J. Schuy ¹⁴²,
 H.R. Schwartz ¹³⁹, A. Schwartzman ¹⁴⁷, T.A. Schwarz ¹⁰⁸, Ph. Schwemling ¹³⁸,
 R. Schwienhorst ¹⁰⁹, F.G. Sciacca ²⁰, A. Sciandra ³⁰, G. Sciolla ²⁷, F. Scuri ^{75a},
 C.D. Sebastiani ⁹⁴, K. Sedlaczek ¹¹⁸, S.C. Seidel ¹¹⁵, A. Seiden ¹³⁹, B.D. Seidlitz ⁴², C. Seitz ⁴⁹,
 J.M. Seixas ^{84b}, G. Sekhniaidze ^{73a}, L. Selem ⁶¹, N. Semprini-Cesari ^{24b,24a}, D. Sengupta ⁵⁷,
 V. Senthilkumar ¹⁶⁶, L. Serin ⁶⁷, M. Sessa ^{77a,77b}, H. Severini ¹²³, F. Sforza ^{58b,58a}, A. Sfyrlla ⁵⁷,
 Q. Sha ¹⁴, E. Shabalina ⁵⁶, A.H. Shah ³³, R. Shaheen ¹⁴⁸, J.D. Shahinian ¹³¹,
 D. Shaked Renous ¹⁷², L.Y. Shan ¹⁴, M. Shapiro ^{18a}, A. Sharma ³⁷, A.S. Sharma ¹⁶⁷,
 P. Sharma ⁸¹, P.B. Shatalov ³⁸, K. Shaw ¹⁵⁰, S.M. Shaw ¹⁰³, Q. Shen ^{63c}, D.J. Sheppard ¹⁴⁶,
 P. Sherwood ⁹⁸, L. Shi ⁹⁸, X. Shi ¹⁴, C.O. Shimmmin ¹⁷⁵, J.D. Shinner ⁹⁷, I.P.J. Shipsey ^{129,*},
 S. Shirabe ⁹⁰, M. Shiyakova ^{39,v}, M.J. Shochet ⁴⁰, D.R. Shope ¹²⁸, B. Shrestha ¹²³,
 S. Shrestha ^{122,ah}, M.J. Shroff ¹⁶⁸, P. Sicho ¹³⁴, A.M. Sickles ¹⁶⁵, E. Sideras Haddad ^{34g},
 A.C. Sidley ¹¹⁷, A. Sidoti ^{24b}, F. Siegert ⁵¹, Dj. Sijacki ¹⁶, F. Sili ⁹², J.M. Silva ⁵³,
 I. Silva Ferreira ^{84b}, M.V. Silva Oliveira ³⁰, S.B. Silverstein ^{48a}, S. Simion ⁶⁷, R. Simoniello ³⁷,
 E.L. Simpson ¹⁰³, H. Simpson ¹⁵⁰, L.R. Simpson ¹⁰⁸, N.D. Simpson ¹⁰⁰, S. Simsek ⁸³,
 S. Sindhu ⁵⁶, P. Sinervo ¹⁵⁸, S. Singh ¹⁵⁸, S. Sinha ⁴⁹, S. Sinha ¹⁰³, M. Sioli ^{24b,24a}, I. Siral ³⁷,
 E. Sitnikova ⁴⁹, J. Sjölin ^{48a,48b}, A. Skaf ⁵⁶, E. Skorda ²¹, P. Skubic ¹²³, M. Slawinska ⁸⁸,
 V. Smakhtin ¹⁷², B.H. Smart ¹³⁷, S.Yu. Smirnov ³⁸, Y. Smirnov ³⁸, L.N. Smirnova ^{38,a},
 O. Smirnova ¹⁰⁰, A.C. Smith ⁴², D.R. Smith ¹⁶², E.A. Smith ⁴⁰, H.A. Smith ¹²⁹, J.L. Smith ¹⁰³,
 R. Smith ¹⁴⁷, M. Smizanska ⁹³, K. Smolek ¹³⁵, A.A. Snesarev ³⁸, S.R. Snider ¹⁵⁸, H.L. Snoek ¹¹⁷,
 S. Snyder ³⁰, R. Sobie ^{168,x}, A. Soffer ¹⁵⁵, C.A. Solans Sanchez ³⁷, E.Yu. Soldatov ³⁸,
 U. Soldevila ¹⁶⁶, A.A. Solodkov ³⁸, S. Solomon ²⁷, A. Soloshenko ³⁹, K. Solovieva ⁵⁵,
 O.V. Solovyanov ⁴¹, P. Sommer ³⁷, A. Sonay ¹³, W.Y. Song ^{159b}, A. Sopczak ¹³⁵, A.L. Sopio ⁹⁸,
 F. Sopkova ^{29b}, J.D. Sorenson ¹¹⁵, I.R. Sotarriva Alvarez ¹⁴¹, V. Sothilingam ^{64a},
 O.J. Soto Sandoval ^{140c,140b}, S. Sottocornola ⁶⁹, R. Soualah ¹⁶³, Z. Soumami ^{36e}, D. South ⁴⁹,
 N. Soybelman ¹⁷², S. Spagnolo ^{71a,71b}, M. Spalla ¹¹², D. Sperlich ⁵⁵, G. Spigo ³⁷, S. Spinali ⁹³,
 B. Spisso ^{73a,73b}, D.P. Spiteri ⁶⁰, M. Spousta ¹³⁶, E.J. Staats ³⁵, R. Stamen ^{64a}, A. Stampekis ²¹,
 M. Standke ²⁵, E. Stanecka ⁸⁸, W. Stanek-Maslouska ⁴⁹, M.V. Stange ⁵¹, B. Stanislaus ^{18a},
 M.M. Stanitzki ⁴⁹, B. Stapf ⁴⁹, E.A. Starchenko ³⁸, G.H. Stark ¹³⁹, J. Stark ⁹¹, P. Staroba ¹³⁴,
 P. Starovoitov ^{64a}, S. Stärz ¹⁰⁶, R. Staszewski ⁸⁸, G. Stavropoulos ⁴⁷, A. Stefl ³⁷, P. Steinberg ³⁰,
 B. Stelzer ^{146,159a}, H.J. Stelzer ¹³², O. Stelzer-Chilton ^{159a}, H. Stenzel ⁵⁹, T.J. Stevenson ¹⁵⁰,
 G.A. Stewart ³⁷, J.R. Stewart ¹²⁴, M.C. Stockton ³⁷, G. Stoicea ^{28b}, M. Stolarski ^{133a},
 S. Stonjek ¹¹², A. Straessner ⁵¹, J. Strandberg ¹⁴⁸, S. Strandberg ^{48a,48b}, M. Stratmann ¹⁷⁴,
 M. Strauss ¹²³, T. Streblner ¹⁰⁴, P. Strizenc ^{29b}, R. Ströhmer ¹⁶⁹, D.M. Strom ¹²⁶,
 R. Stroynowski ⁴⁵, A. Strubig ^{48a,48b}, S.A. Stucci ³⁰, B. Stugu ¹⁷, J. Stupak ¹²³, N.A. Styles ⁴⁹,
 D. Su ¹⁴⁷, S. Su ^{63a}, W. Su ^{63d}, X. Su ^{63a}, D. Suchy ^{29a}, K. Sugizaki ¹⁵⁷, V.V. Sulin ³⁸,
 M.J. Sullivan ⁹⁴, D.M.S. Sultan ¹²⁹, L. Sultanaliyeva ³⁸, S. Sultansoy ^{3b}, T. Sumida ⁸⁹,
 S. Sun ¹⁷³, O. Sunneborn Gudnadottir ¹⁶⁴, N. Sur ¹⁰⁴, M.R. Sutton ¹⁵⁰, H. Suzuki ¹⁶⁰,
 M. Svatos ¹³⁴, M. Swiatlowski ^{159a}, T. Swirski ¹⁶⁹, I. Sykora ^{29a}, M. Sykora ¹³⁶, T. Sykora ¹³⁶,
 D. Ta ¹⁰², K. Tackmann ^{49,u}, A. Taffard ¹⁶², R. Tafirout ^{159a}, J.S. Tafoya Vargas ⁶⁷,
 Y. Takubo ⁸⁵, M. Talby ¹⁰⁴, A.A. Talyshev ³⁸, K.C. Tam ^{65b}, N.M. Tamir ¹⁵⁵, A. Tanaka ¹⁵⁷,
 J. Tanaka ¹⁵⁷, R. Tanaka ⁶⁷, M. Tanasini ¹⁴⁹, Z. Tao ¹⁶⁷, S. Tapia Araya ^{140f}, S. Tapprogge ¹⁰²,
 A. Tarek Abouelfadl Mohamed ¹⁰⁹, S. Tarem ¹⁵⁴, K. Tariq ¹⁴, G. Tarna ^{28b}, G.F. Tartarelli ^{72a},
 M.J. Tartarin ⁹¹, P. Tas ¹³⁶, M. Tasevsky ¹³⁴, E. Tassi ^{44b,44a}, A.C. Tate ¹⁶⁵, G. Tateno ¹⁵⁷,
 Y. Tayalati ^{36e,w}, G.N. Taylor ¹⁰⁷, W. Taylor ^{159b}, R. Teixeira De Lima ¹⁴⁷, P. Teixeira-Dias ⁹⁷,
 J.J. Teoh ¹⁵⁸, K. Terashi ¹⁵⁷, J. Terron ¹⁰¹, S. Terzo ¹³, M. Testa ⁵⁴, R.J. Teuscher ^{158,x},
 A. Thaler ⁸⁰, O. Theiner ⁵⁷, N. Themistokleous ⁵³, T. Theveneaux-Pelzer ¹⁰⁴, O. Thielmann ¹⁷⁴,

B.J. Wilson , P.J. Windischhofer , F.I. Winkel , F. Winklmeier , B.T. Winter , J.K. Winter , M. Wittgen , M. Wobisch , T. Wojtkowski , Z. Wolffs , J. Wollrath , M.W. Wolter , H. Wolters , M.C. Wong , E.L. Woodward , S.D. Worm , B.K. Wosiek , K.W. Woźniak , S. Wozniowski , K. Wraight , C. Wu , M. Wu , M. Wu , S.L. Wu , X. Wu , Y. Wu , Z. Wu , J. Wuerzinger , T.R. Wyatt , B.M. Wynne , S. Xella , L. Xia , M. Xia , M. Xie , S. Xin , A. Xiong , J. Xiong , D. Xu , H. Xu , L. Xu , R. Xu , T. Xu , Y. Xu , Z. Xu , Z. Xu , B. Yabsley , S. Yacoob , Y. Yamaguchi , E. Yamashita , H. Yamauchi , T. Yamazaki , Y. Yamazaki , J. Yan , S. Yan , Z. Yan , H.J. Yang , H.T. Yang , S. Yang , T. Yang , X. Yang , X. Yang , Y. Yang , Y. Yang , Z. Yang , W.-M. Yao , H. Ye , H. Ye , J. Ye , S. Ye , X. Ye , Y. Yeh , I. Yeletsikh , B. Yeo , M.R. Yexley , T.P. Yildirim , P. Yin , K. Yorita , S. Younas , C.J.S. Young , C. Young , C. Yu , Y. Yu , J. Yuan , M. Yuan , R. Yuan , L. Yue , M. Zaazoua , B. Zabinski , E. Zaid , Z.K. Zak , T. Zakareishvili , S. Zambito , J.A. Zamora Saa , J. Zang , D. Zanzi , O. Zaplatilek , C. Zeitnitz , H. Zeng , J.C. Zeng , D.T. Zenger Jr , O. Zenin , T. Ženiš , S. Zenz , S. Zerradi , D. Zerwas , M. Zhai , D.F. Zhang , J. Zhang , J. Zhang , K. Zhang , L. Zhang , L. Zhang , P. Zhang , R. Zhang , S. Zhang , S. Zhang , T. Zhang , X. Zhang , X. Zhang , Y. Zhang , Y. Zhang , Y. Zhang , Z. Zhang , Z. Zhang , Z. Zhang , H. Zhao , T. Zhao , Y. Zhao , Z. Zhao , Z. Zhao , A. Zhemchugov , J. Zheng , K. Zheng , X. Zheng , Z. Zheng , D. Zhong , B. Zhou , H. Zhou , N. Zhou , Y. Zhou , Y. Zhou , Y. Zhou , C.G. Zhu , J. Zhu , X. Zhu , Y. Zhu , Y. Zhu , X. Zhuang , K. Zhukov , N.I. Zimine , J. Zinsser , M. Ziolkowski , L. Živković , A. Zoccoli , K. Zoch , T.G. Zorbas , O. Zormpa , W. Zou , L. Zwalinski 

¹Department of Physics, University of Adelaide, Adelaide; Australia.

²Department of Physics, University of Alberta, Edmonton AB; Canada.

³(^a)Department of Physics, Ankara University, Ankara; (^b)Division of Physics, TOBB University of Economics and Technology, Ankara; Türkiye.

⁴LAPP, Université Savoie Mont Blanc, CNRS/IN2P3, Annecy; France.

⁵APC, Université Paris Cité, CNRS/IN2P3, Paris; France.

⁶High Energy Physics Division, Argonne National Laboratory, Argonne IL; United States of America.

⁷Department of Physics, University of Arizona, Tucson AZ; United States of America.

⁸Department of Physics, University of Texas at Arlington, Arlington TX; United States of America.

⁹Physics Department, National and Kapodistrian University of Athens, Athens; Greece.

¹⁰Physics Department, National Technical University of Athens, Zografou; Greece.

¹¹Department of Physics, University of Texas at Austin, Austin TX; United States of America.

¹²Institute of Physics, Azerbaijan Academy of Sciences, Baku; Azerbaijan.

¹³Institut de Física d'Altes Energies (IFAE), Barcelona Institute of Science and Technology, Barcelona; Spain.

¹⁴Institute of High Energy Physics, Chinese Academy of Sciences, Beijing; China.

¹⁵Physics Department, Tsinghua University, Beijing; China.

¹⁶Institute of Physics, University of Belgrade, Belgrade; Serbia.

¹⁷Department for Physics and Technology, University of Bergen, Bergen; Norway.

¹⁸(^a)Physics Division, Lawrence Berkeley National Laboratory, Berkeley CA; (^b)University of California,

Berkeley CA; United States of America.

¹⁹Institut für Physik, Humboldt Universität zu Berlin, Berlin; Germany.

²⁰Albert Einstein Center for Fundamental Physics and Laboratory for High Energy Physics, University of Bern, Bern; Switzerland.

²¹School of Physics and Astronomy, University of Birmingham, Birmingham; United Kingdom.

²²(^a)Department of Physics, Bogazici University, Istanbul; (^b)Department of Physics Engineering, Gaziantep University, Gaziantep; (^c)Department of Physics, Istanbul University, Istanbul; Türkiye.

²³(^a)Facultad de Ciencias y Centro de Investigaciones, Universidad Antonio Nariño,

Bogotá; (^b)Departamento de Física, Universidad Nacional de Colombia, Bogotá; Colombia.

²⁴(^a)Dipartimento di Fisica e Astronomia A. Righi, Università di Bologna, Bologna; (^b)INFN Sezione di Bologna; Italy.

²⁵Physikalisches Institut, Universität Bonn, Bonn; Germany.

²⁶Department of Physics, Boston University, Boston MA; United States of America.

²⁷Department of Physics, Brandeis University, Waltham MA; United States of America.

²⁸(^a)Transilvania University of Brasov, Brasov; (^b)Horia Hulubei National Institute of Physics and Nuclear Engineering, Bucharest; (^c)Department of Physics, Alexandru Ioan Cuza University of Iasi, Iasi; (^d)National Institute for Research and Development of Isotopic and Molecular Technologies, Physics Department, Cluj-Napoca; (^e)National University of Science and Technology Politehnica, Bucharest; (^f)West University in Timisoara, Timisoara; (^g)Faculty of Physics, University of Bucharest, Bucharest; Romania.

²⁹(^a)Faculty of Mathematics, Physics and Informatics, Comenius University, Bratislava; (^b)Department of Subnuclear Physics, Institute of Experimental Physics of the Slovak Academy of Sciences, Kosice; Slovak Republic.

³⁰Physics Department, Brookhaven National Laboratory, Upton NY; United States of America.

³¹Universidad de Buenos Aires, Facultad de Ciencias Exactas y Naturales, Departamento de Física, y CONICET, Instituto de Física de Buenos Aires (IFIBA), Buenos Aires; Argentina.

³²California State University, CA; United States of America.

³³Cavendish Laboratory, University of Cambridge, Cambridge; United Kingdom.

³⁴(^a)Department of Physics, University of Cape Town, Cape Town; (^b)iThemba Labs, Western

Cape; (^c)Department of Mechanical Engineering Science, University of Johannesburg,

Johannesburg; (^d)National Institute of Physics, University of the Philippines Diliman

(Philippines); (^e)University of South Africa, Department of Physics, Pretoria; (^f)University of Zululand,

KwaDlangezwa; (^g)School of Physics, University of the Witwatersrand, Johannesburg; South Africa.

³⁵Department of Physics, Carleton University, Ottawa ON; Canada.

³⁶(^a)Faculté des Sciences Ain Chock, Université Hassan II de Casablanca; (^b)Faculté des Sciences, Université Ibn-Tofail, Kénitra; (^c)Faculté des Sciences Semlalia, Université Cadi Ayyad,

LPHEA-Marrakech; (^d)LPMR, Faculté des Sciences, Université Mohamed Premier, Oujda; (^e)Faculté des

sciences, Université Mohammed V, Rabat; (^f)Institute of Applied Physics, Mohammed VI Polytechnic

University, Ben Guerir; Morocco.

³⁷CERN, Geneva; Switzerland.

³⁸Affiliated with an institute covered by a cooperation agreement with CERN.

³⁹Affiliated with an international laboratory covered by a cooperation agreement with CERN.

⁴⁰Enrico Fermi Institute, University of Chicago, Chicago IL; United States of America.

⁴¹LPC, Université Clermont Auvergne, CNRS/IN2P3, Clermont-Ferrand; France.

⁴²Nevis Laboratory, Columbia University, Irvington NY; United States of America.

⁴³Niels Bohr Institute, University of Copenhagen, Copenhagen; Denmark.

⁴⁴(^a)Dipartimento di Fisica, Università della Calabria, Rende; (^b)INFN Gruppo Collegato di Cosenza, Laboratori Nazionali di Frascati; Italy.

- ⁴⁵Physics Department, Southern Methodist University, Dallas TX; United States of America.
- ⁴⁶Physics Department, University of Texas at Dallas, Richardson TX; United States of America.
- ⁴⁷National Centre for Scientific Research "Demokritos", Agia Paraskevi; Greece.
- ⁴⁸(^a)Department of Physics, Stockholm University; (^b)Oskar Klein Centre, Stockholm; Sweden.
- ⁴⁹Deutsches Elektronen-Synchrotron DESY, Hamburg and Zeuthen; Germany.
- ⁵⁰Fakultät Physik, Technische Universität Dortmund, Dortmund; Germany.
- ⁵¹Institut für Kern- und Teilchenphysik, Technische Universität Dresden, Dresden; Germany.
- ⁵²Department of Physics, Duke University, Durham NC; United States of America.
- ⁵³SUPA - School of Physics and Astronomy, University of Edinburgh, Edinburgh; United Kingdom.
- ⁵⁴INFN e Laboratori Nazionali di Frascati, Frascati; Italy.
- ⁵⁵Physikalisches Institut, Albert-Ludwigs-Universität Freiburg, Freiburg; Germany.
- ⁵⁶II. Physikalisches Institut, Georg-August-Universität Göttingen, Göttingen; Germany.
- ⁵⁷Département de Physique Nucléaire et Corpusculaire, Université de Genève, Genève; Switzerland.
- ⁵⁸(^a)Dipartimento di Fisica, Università di Genova, Genova; (^b)INFN Sezione di Genova; Italy.
- ⁵⁹II. Physikalisches Institut, Justus-Liebig-Universität Giessen, Giessen; Germany.
- ⁶⁰SUPA - School of Physics and Astronomy, University of Glasgow, Glasgow; United Kingdom.
- ⁶¹LPSC, Université Grenoble Alpes, CNRS/IN2P3, Grenoble INP, Grenoble; France.
- ⁶²Laboratory for Particle Physics and Cosmology, Harvard University, Cambridge MA; United States of America.
- ⁶³(^a)Department of Modern Physics and State Key Laboratory of Particle Detection and Electronics, University of Science and Technology of China, Hefei; (^b)Institute of Frontier and Interdisciplinary Science and Key Laboratory of Particle Physics and Particle Irradiation (MOE), Shandong University, Qingdao; (^c)School of Physics and Astronomy, Shanghai Jiao Tong University, Key Laboratory for Particle Astrophysics and Cosmology (MOE), SKLPPC, Shanghai; (^d)Tsung-Dao Lee Institute, Shanghai; (^e)School of Physics, Zhengzhou University; China.
- ⁶⁴(^a)Kirchhoff-Institut für Physik, Ruprecht-Karls-Universität Heidelberg, Heidelberg; (^b)Physikalisches Institut, Ruprecht-Karls-Universität Heidelberg, Heidelberg; Germany.
- ⁶⁵(^a)Department of Physics, Chinese University of Hong Kong, Shatin, N.T., Hong Kong; (^b)Department of Physics, University of Hong Kong, Hong Kong; (^c)Department of Physics and Institute for Advanced Study, Hong Kong University of Science and Technology, Clear Water Bay, Kowloon, Hong Kong; China.
- ⁶⁶Department of Physics, National Tsing Hua University, Hsinchu; Taiwan.
- ⁶⁷IJCLab, Université Paris-Saclay, CNRS/IN2P3, 91405, Orsay; France.
- ⁶⁸Centro Nacional de Microelectrónica (IMB-CNM-CSIC), Barcelona; Spain.
- ⁶⁹Department of Physics, Indiana University, Bloomington IN; United States of America.
- ⁷⁰(^a)INFN Gruppo Collegato di Udine, Sezione di Trieste, Udine; (^b)ICTP, Trieste; (^c)Dipartimento Politecnico di Ingegneria e Architettura, Università di Udine, Udine; Italy.
- ⁷¹(^a)INFN Sezione di Lecce; (^b)Dipartimento di Matematica e Fisica, Università del Salento, Lecce; Italy.
- ⁷²(^a)INFN Sezione di Milano; (^b)Dipartimento di Fisica, Università di Milano, Milano; Italy.
- ⁷³(^a)INFN Sezione di Napoli; (^b)Dipartimento di Fisica, Università di Napoli, Napoli; Italy.
- ⁷⁴(^a)INFN Sezione di Pavia; (^b)Dipartimento di Fisica, Università di Pavia, Pavia; Italy.
- ⁷⁵(^a)INFN Sezione di Pisa; (^b)Dipartimento di Fisica E. Fermi, Università di Pisa, Pisa; Italy.
- ⁷⁶(^a)INFN Sezione di Roma; (^b)Dipartimento di Fisica, Sapienza Università di Roma, Roma; Italy.
- ⁷⁷(^a)INFN Sezione di Roma Tor Vergata; (^b)Dipartimento di Fisica, Università di Roma Tor Vergata, Roma; Italy.
- ⁷⁸(^a)INFN Sezione di Roma Tre; (^b)Dipartimento di Matematica e Fisica, Università Roma Tre, Roma; Italy.
- ⁷⁹(^a)INFN-TIFPA; (^b)Università degli Studi di Trento, Trento; Italy.

- ⁸⁰Universität Innsbruck, Department of Astro and Particle Physics, Innsbruck; Austria.
- ⁸¹University of Iowa, Iowa City IA; United States of America.
- ⁸²Department of Physics and Astronomy, Iowa State University, Ames IA; United States of America.
- ⁸³Istinye University, Sariyer, Istanbul; Türkiye.
- ⁸⁴(^a) Departamento de Engenharia Elétrica, Universidade Federal de Juiz de Fora (UFJF), Juiz de Fora; (^b) Universidade Federal do Rio De Janeiro COPPE/EE/IF, Rio de Janeiro; (^c) Instituto de Física, Universidade de São Paulo, São Paulo; (^d) Rio de Janeiro State University, Rio de Janeiro; (^e) Federal University of Bahia, Bahia; Brazil.
- ⁸⁵KEK, High Energy Accelerator Research Organization, Tsukuba; Japan.
- ⁸⁶Graduate School of Science, Kobe University, Kobe; Japan.
- ⁸⁷(^a) AGH University of Krakow, Faculty of Physics and Applied Computer Science, Krakow; (^b) Marian Smoluchowski Institute of Physics, Jagiellonian University, Krakow; Poland.
- ⁸⁸Institute of Nuclear Physics Polish Academy of Sciences, Krakow; Poland.
- ⁸⁹Faculty of Science, Kyoto University, Kyoto; Japan.
- ⁹⁰Research Center for Advanced Particle Physics and Department of Physics, Kyushu University, Fukuoka ; Japan.
- ⁹¹L2IT, Université de Toulouse, CNRS/IN2P3, UPS, Toulouse; France.
- ⁹²Instituto de Física La Plata, Universidad Nacional de La Plata and CONICET, La Plata; Argentina.
- ⁹³Physics Department, Lancaster University, Lancaster; United Kingdom.
- ⁹⁴Oliver Lodge Laboratory, University of Liverpool, Liverpool; United Kingdom.
- ⁹⁵Department of Experimental Particle Physics, Jožef Stefan Institute and Department of Physics, University of Ljubljana, Ljubljana; Slovenia.
- ⁹⁶School of Physics and Astronomy, Queen Mary University of London, London; United Kingdom.
- ⁹⁷Department of Physics, Royal Holloway University of London, Egham; United Kingdom.
- ⁹⁸Department of Physics and Astronomy, University College London, London; United Kingdom.
- ⁹⁹Louisiana Tech University, Ruston LA; United States of America.
- ¹⁰⁰Fysiska institutionen, Lunds universitet, Lund; Sweden.
- ¹⁰¹Departamento de Física Teórica C-15 and CIAFF, Universidad Autónoma de Madrid, Madrid; Spain.
- ¹⁰²Institut für Physik, Universität Mainz, Mainz; Germany.
- ¹⁰³School of Physics and Astronomy, University of Manchester, Manchester; United Kingdom.
- ¹⁰⁴CPPM, Aix-Marseille Université, CNRS/IN2P3, Marseille; France.
- ¹⁰⁵Department of Physics, University of Massachusetts, Amherst MA; United States of America.
- ¹⁰⁶Department of Physics, McGill University, Montreal QC; Canada.
- ¹⁰⁷School of Physics, University of Melbourne, Victoria; Australia.
- ¹⁰⁸Department of Physics, University of Michigan, Ann Arbor MI; United States of America.
- ¹⁰⁹Department of Physics and Astronomy, Michigan State University, East Lansing MI; United States of America.
- ¹¹⁰Group of Particle Physics, University of Montreal, Montreal QC; Canada.
- ¹¹¹Fakultät für Physik, Ludwig-Maximilians-Universität München, München; Germany.
- ¹¹²Max-Planck-Institut für Physik (Werner-Heisenberg-Institut), München; Germany.
- ¹¹³Graduate School of Science and Kobayashi-Maskawa Institute, Nagoya University, Nagoya; Japan.
- ¹¹⁴(^a) Department of Physics, Nanjing University, Nanjing; (^b) School of Science, Shenzhen Campus of Sun Yat-sen University; (^c) University of Chinese Academy of Science (UCAS), Beijing; China.
- ¹¹⁵Department of Physics and Astronomy, University of New Mexico, Albuquerque NM; United States of America.
- ¹¹⁶Institute for Mathematics, Astrophysics and Particle Physics, Radboud University/Nikhef, Nijmegen; Netherlands.

- ¹¹⁷Nikhef National Institute for Subatomic Physics and University of Amsterdam, Amsterdam; Netherlands.
- ¹¹⁸Department of Physics, Northern Illinois University, DeKalb IL; United States of America.
- ¹¹⁹^(a)New York University Abu Dhabi, Abu Dhabi;^(b)United Arab Emirates University, Al Ain; United Arab Emirates.
- ¹²⁰Department of Physics, New York University, New York NY; United States of America.
- ¹²¹Ochanomizu University, Otsuka, Bunkyo-ku, Tokyo; Japan.
- ¹²²Ohio State University, Columbus OH; United States of America.
- ¹²³Homer L. Dodge Department of Physics and Astronomy, University of Oklahoma, Norman OK; United States of America.
- ¹²⁴Department of Physics, Oklahoma State University, Stillwater OK; United States of America.
- ¹²⁵Palacký University, Joint Laboratory of Optics, Olomouc; Czech Republic.
- ¹²⁶Institute for Fundamental Science, University of Oregon, Eugene, OR; United States of America.
- ¹²⁷Graduate School of Science, Osaka University, Osaka; Japan.
- ¹²⁸Department of Physics, University of Oslo, Oslo; Norway.
- ¹²⁹Department of Physics, Oxford University, Oxford; United Kingdom.
- ¹³⁰LPNHE, Sorbonne Université, Université Paris Cité, CNRS/IN2P3, Paris; France.
- ¹³¹Department of Physics, University of Pennsylvania, Philadelphia PA; United States of America.
- ¹³²Department of Physics and Astronomy, University of Pittsburgh, Pittsburgh PA; United States of America.
- ¹³³^(a)Laboratório de Instrumentação e Física Experimental de Partículas - LIP, Lisboa;^(b)Departamento de Física, Faculdade de Ciências, Universidade de Lisboa, Lisboa;^(c)Departamento de Física, Universidade de Coimbra, Coimbra;^(d)Centro de Física Nuclear da Universidade de Lisboa, Lisboa;^(e)Departamento de Física, Universidade do Minho, Braga;^(f)Departamento de Física Teórica y del Cosmos, Universidad de Granada, Granada (Spain);^(g)Departamento de Física, Instituto Superior Técnico, Universidade de Lisboa, Lisboa; Portugal.
- ¹³⁴Institute of Physics of the Czech Academy of Sciences, Prague; Czech Republic.
- ¹³⁵Czech Technical University in Prague, Prague; Czech Republic.
- ¹³⁶Charles University, Faculty of Mathematics and Physics, Prague; Czech Republic.
- ¹³⁷Particle Physics Department, Rutherford Appleton Laboratory, Didcot; United Kingdom.
- ¹³⁸IRFU, CEA, Université Paris-Saclay, Gif-sur-Yvette; France.
- ¹³⁹Santa Cruz Institute for Particle Physics, University of California Santa Cruz, Santa Cruz CA; United States of America.
- ¹⁴⁰^(a)Departamento de Física, Pontificia Universidad Católica de Chile, Santiago;^(b)Millennium Institute for Subatomic physics at high energy frontier (SAPHIR), Santiago;^(c)Instituto de Investigación Multidisciplinario en Ciencia y Tecnología, y Departamento de Física, Universidad de La Serena;^(d)Universidad Andres Bello, Department of Physics, Santiago;^(e)Instituto de Alta Investigación, Universidad de Tarapacá, Arica;^(f)Departamento de Física, Universidad Técnica Federico Santa María, Valparaíso; Chile.
- ¹⁴¹Department of Physics, Institute of Science, Tokyo; Japan.
- ¹⁴²Department of Physics, University of Washington, Seattle WA; United States of America.
- ¹⁴³Department of Physics and Astronomy, University of Sheffield, Sheffield; United Kingdom.
- ¹⁴⁴Department of Physics, Shinshu University, Nagano; Japan.
- ¹⁴⁵Department Physik, Universität Siegen, Siegen; Germany.
- ¹⁴⁶Department of Physics, Simon Fraser University, Burnaby BC; Canada.
- ¹⁴⁷SLAC National Accelerator Laboratory, Stanford CA; United States of America.
- ¹⁴⁸Department of Physics, Royal Institute of Technology, Stockholm; Sweden.

- ¹⁴⁹Departments of Physics and Astronomy, Stony Brook University, Stony Brook NY; United States of America.
- ¹⁵⁰Department of Physics and Astronomy, University of Sussex, Brighton; United Kingdom.
- ¹⁵¹School of Physics, University of Sydney, Sydney; Australia.
- ¹⁵²Institute of Physics, Academia Sinica, Taipei; Taiwan.
- ¹⁵³^(a)E. Andronikashvili Institute of Physics, Iv. Javakhishvili Tbilisi State University, Tbilisi;^(b)High Energy Physics Institute, Tbilisi State University, Tbilisi;^(c)University of Georgia, Tbilisi; Georgia.
- ¹⁵⁴Department of Physics, Technion, Israel Institute of Technology, Haifa; Israel.
- ¹⁵⁵Raymond and Beverly Sackler School of Physics and Astronomy, Tel Aviv University, Tel Aviv; Israel.
- ¹⁵⁶Department of Physics, Aristotle University of Thessaloniki, Thessaloniki; Greece.
- ¹⁵⁷International Center for Elementary Particle Physics and Department of Physics, University of Tokyo, Tokyo; Japan.
- ¹⁵⁸Department of Physics, University of Toronto, Toronto ON; Canada.
- ¹⁵⁹^(a)TRIUMF, Vancouver BC;^(b)Department of Physics and Astronomy, York University, Toronto ON; Canada.
- ¹⁶⁰Division of Physics and Tomonaga Center for the History of the Universe, Faculty of Pure and Applied Sciences, University of Tsukuba, Tsukuba; Japan.
- ¹⁶¹Department of Physics and Astronomy, Tufts University, Medford MA; United States of America.
- ¹⁶²Department of Physics and Astronomy, University of California Irvine, Irvine CA; United States of America.
- ¹⁶³University of Sharjah, Sharjah; United Arab Emirates.
- ¹⁶⁴Department of Physics and Astronomy, University of Uppsala, Uppsala; Sweden.
- ¹⁶⁵Department of Physics, University of Illinois, Urbana IL; United States of America.
- ¹⁶⁶Instituto de Física Corpuscular (IFIC), Centro Mixto Universidad de Valencia - CSIC, Valencia; Spain.
- ¹⁶⁷Department of Physics, University of British Columbia, Vancouver BC; Canada.
- ¹⁶⁸Department of Physics and Astronomy, University of Victoria, Victoria BC; Canada.
- ¹⁶⁹Fakultät für Physik und Astronomie, Julius-Maximilians-Universität Würzburg, Würzburg; Germany.
- ¹⁷⁰Department of Physics, University of Warwick, Coventry; United Kingdom.
- ¹⁷¹Waseda University, Tokyo; Japan.
- ¹⁷²Department of Particle Physics and Astrophysics, Weizmann Institute of Science, Rehovot; Israel.
- ¹⁷³Department of Physics, University of Wisconsin, Madison WI; United States of America.
- ¹⁷⁴Fakultät für Mathematik und Naturwissenschaften, Fachgruppe Physik, Bergische Universität Wuppertal, Wuppertal; Germany.
- ¹⁷⁵Department of Physics, Yale University, New Haven CT; United States of America.
- ^a Also Affiliated with an institute covered by a cooperation agreement with CERN.
- ^b Also at An-Najah National University, Nablus; Palestine.
- ^c Also at Borough of Manhattan Community College, City University of New York, New York NY; United States of America.
- ^d Also at Center for Interdisciplinary Research and Innovation (CIRI-AUTH), Thessaloniki; Greece.
- ^e Also at Centro Studi e Ricerche Enrico Fermi; Italy.
- ^f Also at CERN, Geneva; Switzerland.
- ^g Also at CMD-AC UNEC Research Center, Azerbaijan State University of Economics (UNEC); Azerbaijan.
- ^h Also at Département de Physique Nucléaire et Corpusculaire, Université de Genève, Genève; Switzerland.
- ⁱ Also at Departament de Física de la Universitat Autònoma de Barcelona, Barcelona; Spain.
- ^j Also at Department of Financial and Management Engineering, University of the Aegean, Chios; Greece.

- k* Also at Department of Physics, California State University, Sacramento; United States of America.
- l* Also at Department of Physics, King's College London, London; United Kingdom.
- m* Also at Department of Physics, Stanford University, Stanford CA; United States of America.
- n* Also at Department of Physics, Stellenbosch University; South Africa.
- o* Also at Department of Physics, University of Fribourg, Fribourg; Switzerland.
- p* Also at Department of Physics, University of Thessaly; Greece.
- q* Also at Department of Physics, Westmont College, Santa Barbara; United States of America.
- r* Also at Faculty of Physics, Sofia University, 'St. Kliment Ohridski', Sofia; Bulgaria.
- s* Also at Hellenic Open University, Patras; Greece.
- t* Also at Institutio Catalana de Recerca i Estudis Avancats, ICREA, Barcelona; Spain.
- u* Also at Institut für Experimentalphysik, Universität Hamburg, Hamburg; Germany.
- v* Also at Institute for Nuclear Research and Nuclear Energy (INRNE) of the Bulgarian Academy of Sciences, Sofia; Bulgaria.
- w* Also at Institute of Applied Physics, Mohammed VI Polytechnic University, Ben Guerir; Morocco.
- x* Also at Institute of Particle Physics (IPP); Canada.
- y* Also at Institute of Physics and Technology, Mongolian Academy of Sciences, Ulaanbaatar; Mongolia.
- z* Also at Institute of Physics, Azerbaijan Academy of Sciences, Baku; Azerbaijan.
- aa* Also at Institute of Theoretical Physics, Ilia State University, Tbilisi; Georgia.
- ab* Also at National Institute of Physics, University of the Philippines Diliman (Philippines); Philippines.
- ac* Also at Technical University of Munich, Munich; Germany.
- ad* Also at The Collaborative Innovation Center of Quantum Matter (CICQM), Beijing; China.
- ae* Also at TRIUMF, Vancouver BC; Canada.
- af* Also at Università di Napoli Parthenope, Napoli; Italy.
- ag* Also at University of Colorado Boulder, Department of Physics, Colorado; United States of America.
- ah* Also at Washington College, Chestertown, MD; United States of America.
- ai* Also at Yeditepe University, Physics Department, Istanbul; Türkiye.
- * Deceased